



Technical Letter Report
[TLR-RES/DE/REB-2026-06]

***Topics Related to Pyrochemical Reprocessing: Technical
Descriptions to Aid Regulatory Considerations***

Date:

February 2026

Prepared in response to Task 1 in User Need Request NMSS-2024-003 by:

**Guy L. Fredrickson
Stephanie H. Bruffey
Tae-Sic Yoo
Brennan C. Mohr**

**Ranon G. Fuller
Morgan T. Kropp
Kevin R. Tolman**

Idaho National Laboratory

Wendy Reed

US Nuclear Regulatory Commission

NRC Project Manager:

Wendy A. Reed

Reactor Engineering Branch

**Division of Engineering
Office of Nuclear Regulatory Research
U.S. Nuclear Regulatory Commission
Washington, DC 20555-0001**

DISCLAIMER: This report was prepared as an account of work sponsored by an agency of the U.S. Government. Neither the U.S. Government nor any agency thereof, nor any employee, makes any warranty, expressed or implied, or assumes any legal liability or responsibility for any third party's use, or the results of such use, of any information, apparatus, product, or process disclosed in this publication, or represents that its use by such third party complies with applicable law.

Topics Related to Pyrochemical Reprocessing

Technical Descriptions to Aid Regulatory
Considerations

FEBRUARY 2026

Guy L. Fredrickson
Stephanie H. Bruffey
Tae-Sic Yoo
Brennan C. Mohr
Ranon G. Fuller
Morgan T. Kropp
Kevin R. Tolman

Idaho National Laboratory

Wendy Reed

Nuclear Regulatory Commission



DISCLAIMER

This information was prepared as an account of work sponsored by an agency of the U.S. Government. Neither the U.S. Government nor any agency thereof, nor any of their employees, makes any warranty, expressed or implied, or assumes any legal liability or responsibility for the accuracy, completeness, or usefulness, of any information, apparatus, product, or process disclosed, or represents that its use would not infringe privately owned rights. References herein to any specific commercial product, process, or service by trade name, trade mark, manufacturer, or otherwise, does not necessarily constitute or imply its endorsement, recommendation, or favoring by the U.S. Government or any agency thereof. The views and opinions of authors expressed herein do not necessarily state or reflect those of the U.S. Government or any agency thereof.

Topics Related to Pyrochemical Reprocessing

Technical Descriptions to Aid Regulatory Considerations

**Guy L. Fredrickson
Stephanie H. Bruffey
Tae-Sic Yoo
Brennan C. Mohr
Ranon G. Fuller
Morgan T. Kropp
Kevin R. Tolman
Idaho National Laboratory
Wendy Reed
Nuclear Regulatory Commission**

February 2026

**Idaho National Laboratory
Idaho Falls, Idaho 83415**

<http://www.inl.gov>

**Prepared for the
U.S. Department of Energy
Office of Energy
Under DOE Idaho Operations Office
Contract DE-AC07-05ID14517**

Page intentionally left blank

EXECUTIVE SUMMARY

To prepare for potential license applications for commercial reprocessing facilities, the U.S. Nuclear Regulatory Commission (NRC) is conducting several activities to help the agency understand the state-of-knowledge on applicable aqueous and pyrochemical reprocessing technologies. The NRC staff need to understand potential safety considerations for the processes that will occur within reprocessing facilities, including those reprocessing technologies that have not previously been demonstrated on a commercial-scale. Examples of the latter include voloxidation and oxide reduction. This report identifies potential reprocessing technologies that could be deployed in the near and midterm with a particular focus on technologies related to pyrochemical reprocessing, and touches on some of the expected safety-related aspects of these technologies.

The opening sections discuss fuel cycles and the types of fuels and reactors that may be involved. The purpose of these sections is to emphasize that reprocessing technologies are selected based on the explicit requirements of the fuel cycle application. Some fuel cycles and fuel types may be more amenable to aqueous reprocessing routes, while others may be more amenable to pyrochemical reprocessing routes. In general, aqueous reprocessing recovers the actinides as oxides, while pyrochemical reprocessing recovers the actinides as metals. This difference alone will certainly influence the decision of an application of which technological path to pursue, but other factors must be considered as well. For example, actinides recovered as oxides or metals can be converted to any other chemical form by additional metallurgical processing. Consequently, the NRC will need to be prepared to review a variety of reprocessing technologies as part of a license application.

The report discusses reprocessing technologies which have not been demonstrated an engineering or a commercial-scale in the U.S. Voloxidation is an optional head-end process for oxide fuels in both aqueous reprocessing (before fuel dissolution) and pyrochemical reprocessing (before oxide reduction). Between decladding, voloxidation, and oxide reduction, the bulk of the volatile fission products are released into the off-gas systems. Voloxidation and oxide reduction have not been deployed at commercial scales, and the behaviors of volatile fission products during these operations are still under investigation.

Fluoride volatility is a separations process that exploits differences in vapor pressures between different metal fluorides. The process was developed for oxide fuels. Different fluorinating reagents can be applied to fluorinate different metals in the spent oxide fuel. Separations occur between metal fluorides of higher

vapor pressure (reporting to the vapor phase) and lower vapor pressure (remaining in the solid phase). The chemistry of fluorination is widely used during the conversion of uranium oxide to uranium hexafluoride for enrichment by diffusion or centrifugation techniques. Uranium oxide can be fluorinated by the action of fluorine gas and hydrogen fluoride gas. Whereas the fluorination of plutonium oxide requires more aggressive fluorinating reagents such as bromine trifluoride.

Pyrochemical reprocessing involves the use of molten chloride salts for oxide reduction and uranium electrorefining. These salts accumulate fission products and transuranics as metal chlorides. At some point the accumulation of fission products in the salts must be managed by treating the salts for waste disposal. One effect of this accumulation is to increase the liquidus temperature of the salt (i.e., the temperature below which solid precipitates form). As the increasing liquidus temperature approaches the operating temperature, salt must either be replaced or chemically treated. Methods have been proposed for manufacturing several different categories of waste forms that can accommodate fission products for storage and geologic disposition. Salt waste forms include different types of glasses, ceramics, and dehalogenated minerals. Optimal waste forms for these applications will depend on the transportation and acceptance requirements of the disposal facility. Sodium-bonded metal fuels represent a category of fuels that are the leading candidates for pyrochemical reprocessing for its metal-to-metal capability. Pyrochemical reprocessing can accept spent metal fuels and recover the actinides as metals to make new metal fuels. However, the bond-sodium contributes significantly to the production of salt waste by forming sodium chloride in the electrorefiner salt. The amount of sodium reporting to the electrorefiner salt can be reduced by a head-end process of sodium distillation, but this will generate a new waste stream in the form of distillate sodium metal with dissolved cesium, strontium, and iodine fission products.

Reprocessing of other fuel types is also discussed. Tristructural isotropic (TRISO) fuels poses challenges to both aqueous and pyrochemical reprocessing. The fuel kernel (e.g., uranium oxide or uranium carbide) is surrounded by alternating layers of refractory pyrolytic graphite and silicon carbide. These layers, the small size of the TRISO fuel particles, and the graphite matrix that contains the particles make it very difficult to expose the spent fuel kernels to the solutions used to extract the actinides in these reprocessing routes. TRISO fuels may also be very high burnup fuels, raising the question of the economic viability of reprocessing.

Many aluminum-clad research reactor spent fuels contain metallic high-enriched uranium, which is a potential source of high-assay low-enriched uranium (HALEU) for the development of new demonstration reactors. Various pyrochemical reprocessing routes have been proposed to recover the actinides as metals. However, the presence of aluminum renders the process of uranium electrorefining ineffectual. The aluminum must be removed before uranium electrorefining is applied. Methods such as chloride volatility have been proposed to remove the aluminum while converting the uranium metal to uranium trichloride. Aluminum-clad fuels are good candidates for aqueous reprocessing; however, the uranium would be recovered as uranium oxide.

The impact of age of spent fuel on reprocessing is addressed, most significantly in terms of the radiation levels, decay heat load, and potential

chemical alterations resulting from corrosion during storage (e.g., oxidation of metal fuels). Aqueous reprocessing is sensitive to radiation levels and requires spent fuels that have cooled for 5 years or more. Pyrochemical reprocessing is not sensitive to radiation levels; however, many of the fission products that are responsible for the decay heat will accumulate in the process salts. This accumulation will require consideration from a salt waste management perspective. Where metallic spent fuels are involved, significant amounts of corrosion would prevent direct pyrochemical reprocessing; pre-treatment would be needed since electrorefining can only be conducted using metals.

In summary, there are many process options available for both aqueous and pyrochemical reprocessing. Some of these processes have been demonstrated at an industrial scale, while others have not and are only speculated. This report describes some of the potential technologies being considered for reprocessing facilities. A potential applicant can develop a flowsheet for a desired outcome, taking into consideration the various process options and the related safety aspects.

Page intentionally left blank

FOREWORD

Three complementary reports were prepared for the Nuclear Regulatory Commission.

- *Aqueous and Pyrochemical Reprocessing Off-Gas and Ventilation Systems: Technical Descriptions to Aid Regulatory Considerations*, INL/RPT-25-85408
- *Topics Related to Pyrochemical Reprocessing: Technical Descriptions to Aid Regulatory Considerations*, INL/RPT-25-85431
- *Aqueous and Pyrochemical Reprocessing Chemical Safety: Technical Descriptions to Aid Regulatory Considerations*, INL/RPT-25-87767.

The first report describes key issues associated with volatile radionuclides during both aqueous and pyrochemical reprocessing and provides a technical basis for any future NRC guidance pertaining to off-gas and ventilation systems at a reprocessing facility. The key topics include the chemistry of release into off-gas ventilation systems, the capture from off-gas ventilation systems, Federal regulations governing the release to the atmosphere, technical descriptions of existing hot cell facilities, and an extensive bibliography on related publications.

The second report expands the technical descriptions of pyrochemical reprocessing into subjects beyond the reference case discussed in the first report. These subjects include the application of pyrochemical reprocessing to various fuel types, the unit operations of voloxidation and oxide reduction, the technology of fluoride volatility, salt waste management, and the consequences of aged fuels. The report identifies expected safety-related aspects of existing potential technologies to support potential near-term reprocessing applications.

The third report provides a deeper assessment of key chemical process safety issues associated with both aqueous and pyrochemical reprocessing. These key issues include chemical excursions, pyrophoric materials, and chemical safety.

Page intentionally left blank

CONTENTS

EXECUTIVE SUMMARY	v
FOREWORD	vi
ACRONYMS.....	xiii
1. INTRODUCTION.....	1
2. FUEL CYCLE BASICS.....	2
2.1. Types of Nuclear Fuels and Nuclear Reactors	2
2.2. Role of Reprocessing and Actinide Elements.....	3
2.3. Separation Factors.....	4
2.4. Open and Closed Fuel Cycles	4
2.5. Reprocessing Practical Considerations and Experience.....	6
3. VOLOXIDATION	9
3.1. Decladding	9
3.2. Volatile Fission Products	12
3.3. Off-Gas Capture.....	15
4. OXIDE REDUCTION	17
4.1. Processing Rate	17
4.2. Current Interruption	20
4.3. Anode Corrosion (Metal and Carbon).....	21
4.4. Anode Off-Gas.....	21
4.5. Americium Behavior.....	22
5. FLUORIDE VOLATILITY PROCESSES	24
5.1. Process Chemistry.....	25
5.2. Fluidized Bed Reactor Technology.....	27
5.3. Corrosivity of Fluorination Reagents.....	28
6. SALT WASTE MANAGEMENT	36
6.1. Waste Form Properties.....	36
6.2. Salt Partitioning Strategies.....	37
6.3. Ceramic Waste Form Development	38
6.4. Tellurite Glass Waste Forms.....	41
6.5. Dehalogenated Salt Waste Forms	42
6.6. Metal Waste Forms	45
6.7. Captured Volatile Fission Product Waste	46

6.8.	Sodium-Bonded Metal Fuel	48
7.	REPROCESSING OF OTHER SPENT FUEL TYPES	49
7.1.	TRISO Fuel	49
7.1.1.	Current Head-End Processing Options	51
7.2.	Aluminum-Clad Research Reactor Fuel	53
7.2.1.	Reprocessing Options	54
8.	SPENT FUEL AGE	57
8.1.	Decay Heat	57
8.2.	Spent Fuel Storage	58
8.3.	Corrosion.....	58
8.4.	Molten Salt Reactor Fuel Salts.....	59
9.	SUMMARY	60
10.	REFERENCES.....	61

FIGURES

Figure 1.	Open fuel cycle with no reprocessing.....	5
Figure 2.	Closed fuel cycle with reprocessing.	5
Figure 3.	Closed fuel cycle between Reactor 1, which uses a uranium fuel, and Reactor 2, which uses a transuranic-containing fuel.	6
Figure 4.	Closed fuel cycle of a breeder reactor operating with fuel and blanket.....	6
Figure 5.	Particle size fraction with respect to fuel burn up and operation temperature.	11
Figure 6.	Iodine and cesium release trend with respect to temperature.	14
Figure 7.	Tritium and carbon-14 release trend with respect to temperature.	15
Figure 8.	A shrinking core representation for the oxide reduction process.	18
Figure 9.	Extent of possible oxygen removal with respect to plate width.	19
Figure 10.	Simulation of the extent of reaction in 2D pellet model.....	19
Figure 11.	Oxide reduction process under high convection. (a) Concentration field of Li_2O at several time instances. (b) Extent of reaction and diffusion.....	20
Figure 12.	Ellingham diagram of select fluorination reagents.....	26
Figure 13.	Schematic diagram of a fluidized bed reactor.	28
Figure 14.	Predominance area diagram of the U-F-O system at 600°C.....	33
Figure 15.	Predominance area diagram of the Np-F-O system at 600°C.....	34
Figure 16.	Predominance area diagram of the Pu-F-O system at 600°C.	35
Figure 17.	Photographs of purified (solidified LiCl) OR salt on a chilled steel plate. The salt is transparent and colorless.....	38

Figure 18. Photographs of purified (solidified LiCl-KCl) ER salt on a chilled steel plate. The salt is opaque and white.	38
Figure 19. Schematic flowsheet of ceramic waste form processing.	40
Figure 20. Photographs of an ACWF containing radioactive fission products (left) and an optical image of the microstructure (right). The photomicrograph is approximately 250 μm wide.	41
Figure 21. Schematic showing the process flow for fabricating an iron phosphate waste form.....	43
Figure 22. Photograph of iron phosphate glass waste form containing used ER salt.	43
Figure 23. Photographs of SAP waste form containing pyrochemical reprocessing salt (left) and in the process of being mounted for imaging (right).	44
Figure 24. Photograph of LaBS glass containing 60 wt% surrogate ER fission products added as oxides.....	45
Figure 25. Photograph of ingot from the first production-scale metal waste form.....	45
Figure 26. Photographs of zirconium-alloy cladding waste containing spent fuel residuals (left) and the resulting cermet waste form (right).....	46
Figure 27. Photographs of used stainless-steel hardware containing spent fuel residual (left) and the resulting cermet waste form (right).	46
Figure 28. Magnified view of a TRISO fuel particle clearly showing each of the structural layers. Source: DOE photograph.....	49
Figure 29. Photographs of graphite cylinder containing a dispersion of TRISO fuel particles. The image on the left is a cross section of the cylinder. Source: DOE photographs.	50
Figure 30. Photographs of a graphite sphere (pebble) containing a dispersion of TRISO fuel particles. The image on the left is a partial cross section of a graphite sphere. Source: DOE photographs.	50
Figure 31. Schematic of INL Advanced Test Reactor fuel arrangement.	54
Figure 32. EBR-II driver fuel assembly decay heat as a function of time.	57

TABLES

Table 1. Summary of oxide fuel types.	2
Table 2. Summary of metal alloy fuel types.	2
Table 3. Summary of molten salt fuel types.	2
Table 4. Summary of cermet fuel types.	3
Table 5. Summary of the actinides.....	3
Table 6. Summary of transmutation reactions representing one possible route.....	4
Table 7. Particle size fractions of fuels at various burnups and oxidation temperatures.	10
Table 8. Fuel recovery performance comparison.....	12
Table 9. Fission product release at different fuel burnups and oxidation temperatures.....	13
Table 10. Removal rate of the semi-volatile elements from a voloxidation process.	15

Table 11. Feasible reactions at anodes of oxide reduction processes.	22
Table 12. Fluorination of actinides by the action of $\text{KrF}_2(\text{g})$ and ΔG° (kJ) at 600°C	29
Table 13. Fluorination of actinides by the action of $\text{O}_2\text{F}_2(\text{g})$ and ΔG° (kJ) at 600°C	29
Table 14. Fluorination of actinides by the action of $\text{F}_2(\text{g})$ and ΔG° (kJ) at 600°C	30
Table 15. Fluorination of actinides by the action of $\text{NF}_3(\text{g})$ and ΔG° (kJ) at 600°C	30
Table 16. Fluorination of actinides by the action of $\text{ClF}_3(\text{g})$ and ΔG° (kJ) at 600°C	31
Table 17. Fluorination of actinides by the action of $\text{BrF}_5(\text{g})$ and ΔG° (kJ) at 600°C	31
Table 18. Fluorination of actinides by the action of $\text{BrF}_3(\text{g})$ and ΔG° (kJ) at 600°C	32
Table 19. Fluorination of actinides by the action of $\text{HF}(\text{g})$ and ΔG° (kJ) at 600°C	32

Page intentionally left blank

ACRONYMS

ACWF	Advanced ceramic waste forms
AIROX	Atomics International Reduction Oxidation
ANL	Argonne National Laboratory
CWF	Ceramic waste form
DOE	Department of Energy
DU	Depleted Uranium
FCF	Fuel Conditioning Facility
HALEU	High-assay low-enriched uranium
HEU	High-enriched uranium
HF	Hydrogen fluoride
HFEF	Hot Fuel Examination Facility
HI	Hydrogen iodide
HTGR	High-temperature gas-cooled reactors
ICPP	Idaho Chemical Processing Plant
IFR	Integral Fast Reactor
INL	Idaho National Laboratory
JFCS	Joint Fuel Cycle Study
LEU	Low-enriched uranium
LLW	Low-level waste
LWR	Light-water reactor
MFC	Materials and Fuels Complex
MOF	Metal-organic framework
MRP	Melt refining process
MSBR	Molten Salt Breeder Reactor
MSR	Molten salt reactor
MSRE	Molten Salt Reactor Experiment
NRC	Nuclear Regulatory Commission
OR	Oxide reduction
ORNL	Oak Ridge National Laboratory
RERTR	Reduced Enrichment for Research and Test Reactors
RIAR	Research Institute of Atomic Reactors
RSWF	Radioactive Scrap and Waste Facility
SAP	Silica-alumina-phosphate

SFR	Sodium-cooled fast reactors
SOZ	Salt-occluded zeolite
STP	Standard temperature and pressure
TRISO	Tristructural isotropic
ZIRCEX	Zirconium extraction

Page intentionally left blank

Topics Related to Pyrochemical Reprocessing

Technical Descriptions to Aid Regulatory Considerations

1. INTRODUCTION

To prepare for potential license applications for commercial reprocessing facilities, the U.S. Nuclear Regulatory Commission is conducting several activities to help the agency understand the state-of-knowledge on applicable aqueous and pyrochemical reprocessing technologies. The NRC staff need to understand potential safety considerations for the processes that will occur within reprocessing facilities. This includes reprocessing technologies that have not previously been demonstrated on an engineering or commercial scale. Examples of the latter include voloxidation and oxide reduction. This report identifies potential reprocessing technologies that could be deployed in the near and midterm and the expected safety-related aspects of these technologies.

The requirements of the fuel cycle dictate the requirements of the reprocessing facility with respect to the type of fuel to be processed and the chemical separations and recovery efficiencies needed for successful operations. Both aqueous and pyrochemical reprocessing offer many process options that can be tailored to meet these requirements through various assemblages of unit operation flowsheets.

The United States has no recent experience with commercial-scale reprocessing facilities. Such endeavors have not been pursued and constructed since the 1970s. All the processes discussed here are undergoing continued technical development for process maturity and scale-up. The following sections cover topics related to fuel cycles, voloxidation, oxide reduction, fluoride volatility, salt waste management (unique to pyrochemical reprocessing), technical considerations for reprocessing tristructural isotropic (TRISO) fuels and aluminum-clad fuels, and consequences related to spent fuel age.

The aqueous reprocessing and pyrochemical reprocessing of oxide fuels and metallic fuels are discussed in greater detail in this document because most reprocessing experience is related to these fuel types. Reprocessing of molten salt fuels is discussed to a lesser extent because experience with these fuel types is entirely lacking. Other fuel types such as TRISO and aluminum-clad research reactor fuels are briefly mentioned.

2. FUEL CYCLE BASICS

The purpose of reprocessing nuclear fuel is to support a specific fuel cycle. Therefore, all engineering aspects of the fuel cycle must be considered in the development of the design specifications of the reprocessing facility. The reactor, fuel, fuel cycle, and requirements of the reprocessing facility will need to be considered because they are each highly integrated systems. For example, specific requirements of the reprocessing facility will include the ability to accept certain types of fuel and perform certain chemical separations, all while meeting certain recovery efficiencies and certain atmospheric emissions limits. There is a broad spectrum of potential design features for a reprocessing facility. This section discusses some of the basic concepts of an integrated fuel cycle, including reactor type.

2.1. Types of Nuclear Fuels and Nuclear Reactors

Within the United States, there are 94 commercial light-water reactors (LWRs) generating electricity and 31 research reactors for various purposes. The LWRs all use uranium oxide fuels, and the research reactors use different forms of enriched uranium fuels. In addition to these reactors, there is commercial interest in pursuing sodium-cooled fast reactors (SFRs), high-temperature gas-cooled reactors (HTGRs), and molten salt reactors (MSRs). These near-term applications include reactors that are thermal-spectrum and fast-spectrum, and fuels that are oxides, metals, cermet (e.g., carbides and nitrides), and molten salts. Examples of fuel types from these four categories (i.e., oxide, metal, salt, and cermet) are summarized in Table 1 to Table 4, respectively. The information presented in these tables represents typical compositions and applications; it is not a comprehensive list.

Table 1. Summary of oxide fuel types.

Fuel Form	Chemical Formula	Uranium Enrichment	Reactor Spectrum
Uranium Oxide	UO ₂	LEU	Thermal
Mixed Oxide	UO ₂ and PuO ₂	DU	Thermal and Fast
TRISO	UO ₂ , UC, UCO, others	LEU	Thermal

Table 2. Summary of metal alloy fuel types.

Fuel Form	Chemical Formula	Uranium Enrichment	Reactor Spectrum
U/Zr	U/Zr	HEU	Fast
U/Pu/Zr	U/Pu/Zr	DU	Fast
U/Al	Various Alloys	LEU and HEU	Thermal
U/Mo	Various Alloys	LEU	Thermal
U/Zr/H (TRIGA-type)	(U _y Zr)H _x	LEU and HEU	Thermal

Table 3. Summary of molten salt fuel types.

Fuel Form	Chemical Formula	Uranium Enrichment	Reactor Spectrum
Chloride Molten Salt	UCl ₃	HEU	Fast
Chloride Molten Salt	PuCl ₃	No Uranium	Fast
Fluoride Molten Salt	UF ₄	LEU	Thermal

Table 4. Summary of cermet fuel types.

Fuel Form	Chemical Formula	Uranium Enrichment	Reactor Spectrum
Uranium Carbide	UC	LEU and HEU	Fast
Mixed Carbide	UC/PuC	LEU	Fast
Uranium Nitride	UN	LEU and HEU	Fast

2.2. Role of Reprocessing and Actinide Elements

A fuel cycle includes every aspect of fuel management from mining to final waste disposition. Reprocessing flowsheets are tailored to support specific fuel cycle applications. The function of reprocessing is always chemical separations. During reprocessing, certain elements are retained in the fuel cycle, and certain elements are rejected from the fuel cycle. Typically, the elements retained in the fuel cycle are select actinides, while the elements rejected as waste from the fuel cycle include both fission products and, in some cases, select actinides. However, for future fuel cycles, this may not be the case. As summarized in Table 5, the actinides consist of actinium and all heavier elements, the transuranics consist of all elements heavier than uranium, and the minor actinides consist of all transuranics excluding plutonium. Actinium is included in the table for completeness, but actinium is not an important constituent in fuels. Likewise, the table ends with californium because elements heavier than californium are not important constituents in fuels.

Table 5. Summary of the actinides.

Actinides	Transuranics	Minor Actinides
Actinium	—	—
Thorium	—	—
Protactinium	—	—
Uranium	—	—
Neptunium	Neptunium	Neptunium
Plutonium	Plutonium	—
Americium	Americium	Americium
Curium	Curium	Curium
Berkelium	Berkelium	Berkelium
Californium	Californium	Californium

Among the actinides, only thorium and uranium are direct mining commodities, with all nuclear fuels derived from the mining of these two elements. Natural uranium has an isotopic distribution of 99.28% U-238 and 0.72% U-235, and natural thorium is nearly exclusively a single isotope with 99.98% Th-232. Natural uranium can be enriched with respect to U-235 to any level required. A byproduct of uranium enrichment is depleted uranium that often contains approximately 99.76% U-238 and 0.24% U-235. All other actinides are produced in nuclear reactors. In some applications, U-238 and Th-232 are fertile isotopes. U-238 can transmute to Pu-239, and Th-232 can transmute to U-233, as summarized in Table 6. U-233, U-235, and Pu-239 are the fissile isotopes that constitute fuels. Distinctions are made between fuel cycles that maximize the production of plutonium (i.e., breed plutonium), consume plutonium (i.e., burn plutonium), or reduce the production of plutonium. However, because of the

neutronic behavior in a reactor core, all spent fuels will contain some plutonium and minor actinides, just to a greater or lesser extent.

Table 6. Summary of transmutation reactions representing one possible route.

U to Pu Reactions	Half-Life	Th to U Reactions	Half-Life
${}^{238}_{92}\text{U} + {}^1_0\text{n} \rightarrow {}^{239}_{92}\text{U}$	—	${}^{232}_{90}\text{Th} + {}^1_0\text{n} \rightarrow {}^{233}_{90}\text{Th}$	—
${}^{239}_{92}\text{U} \rightarrow {}^{239}_{93}\text{Np} + \beta^-$	23.5 min	${}^{233}_{90}\text{Th} \rightarrow {}^{233}_{91}\text{Pa} + \beta^-$	22.3 min
${}^{239}_{93}\text{Np} \rightarrow {}^{239}_{94}\text{Pu} + \beta^-$	2.35 d	${}^{233}_{91}\text{Pa} \rightarrow {}^{233}_{92}\text{U} + \beta^-$	27 d
${}^{239}_{94}\text{Pu} \rightarrow {}^{235}_{92}\text{U} + {}^4_2\text{He}$	Slow Transition	${}^{233}_{92}\text{U} \rightarrow {}^{232}_{92}\text{U} + (n, 2n)$	Slow Transition

Plutonium is not mined; it is created in nuclear reactors.^a The United States has two distinct inventories of plutonium: (1) plutonium intentionally produced for military applications in dedicated plutonium production reactors and (2) plutonium that exists in spent fuels from civilian power generating reactors. Plutonium from the former source was largely recovered from the spent fuels and exists in various purified forms. Plutonium from the latter source largely remains in the spent fuels. Currently proposed reprocessing technologies would look to separate out plutonium with uranium or other actinides to mitigate proliferation risks.

2.3. Separation Factors

A separation factor is a measure of the effectiveness of a chemical separations process. In the context of reprocessing, it is used as a measure of the effectiveness of separating fission products from actinides. Or, in other words, it is a measure of the effectiveness of separating elements that are to be rejected from the fuel cycle from those elements that are to be retained in the fuel cycle.

A separation factor can be defined in several ways, but it is commonly the ratio of the *fraction of impurity removed* to the *fraction of impurity remaining* after the separation has been completed. Each impurity can have a unique separation factor. A high separation factor indicates that the separation process was effective at removing the impurity from the product. For example, if 99.9% of an impurity was removed and 0.1% of the impurity remained, the separation factor would be the ratio 99.9:0.1, which is equal to 999. In principle, product purity can be increased even further by applying a series of sequential separations stages. However, a negative consequence of this approach is often an increase in flowsheet complexity and a decrease in overall product recovery. In other words, product purity is gained but at the expense of decreasing product recovery as a higher fraction of the product follows the impurities to the waste streams.

2.4. Open and Closed Fuel Cycles

An *open fuel cycle* is one that does not involve reprocessing. A *closed fuel cycle* is one that does involve reprocessing. Any number of fuel cycle concepts can be found in the vast body of technical literature. Four basic fuel cycle concepts are presented here in Figure 1 to Figure 4.

An open fuel cycle is shown in Figure 1, which is also called the *once through fuel cycle*. This fuel cycle does not use reprocessing. Because the spent fuel from this reactor is disposed of directly, it is considered an open fuel cycle. However, at some point in the future, spent fuel from an open fuel cycle could be reprocessed as part of a different closed fuel cycle.

a. Plutonium can be found in uranium ores from the adsorption of neutrons by ${}^{238}\text{U}$. In addition, there are rare examples of geologic evidence of uranium deposits undergoing fission events. In these occurrences, plutonium exists in geologic deposits in trace-level concentrations

A closed fuel cycle with reprocessing is shown in Figure 2. For example, this type of fuel cycle could retain only the uranium fraction, or it could retain some combination of the uranium and transuranic fractions, in the fuel cycle. The non-fissile fission products would be segregated to the waste streams.

A fuel cycle with reprocessing supporting two different types of reactors is shown in Figure 3. For example, Reactor 1 could be a thermal neutron spectrum reactor using a uranium-based fuel, and Reactor 2 could be a fast neutron spectrum reactor using a uranium-plutonium-based fuel.

A breeder fuel cycle with reprocessing supporting both fuel and blanket is shown in Figure 4. For example, the fuel and blanket may require two different reprocessing flowsheets. This fuel cycle produces excess fissile inventory that can be used to make fuel for a different type of reactor.

There are many variations of each of these fuel cycles that may support a uranium/plutonium fuel cycle, thorium/uranium fuel cycle, the consumption of plutonium, the consumption of minor actinides, the denaturing of weapons grade plutonium, etc. Regardless of the fuel cycle application, the reprocessing flowsheet is tailored to that application.

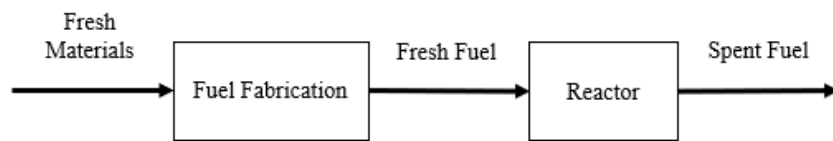


Figure 1. Open fuel cycle with no reprocessing.

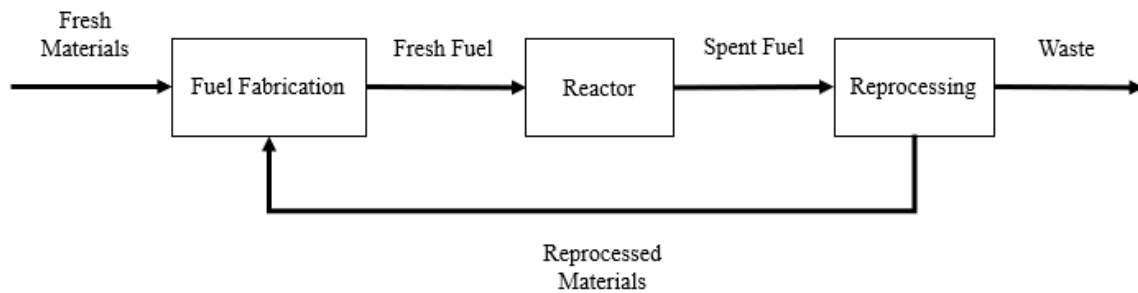


Figure 2. Closed fuel cycle with reprocessing.

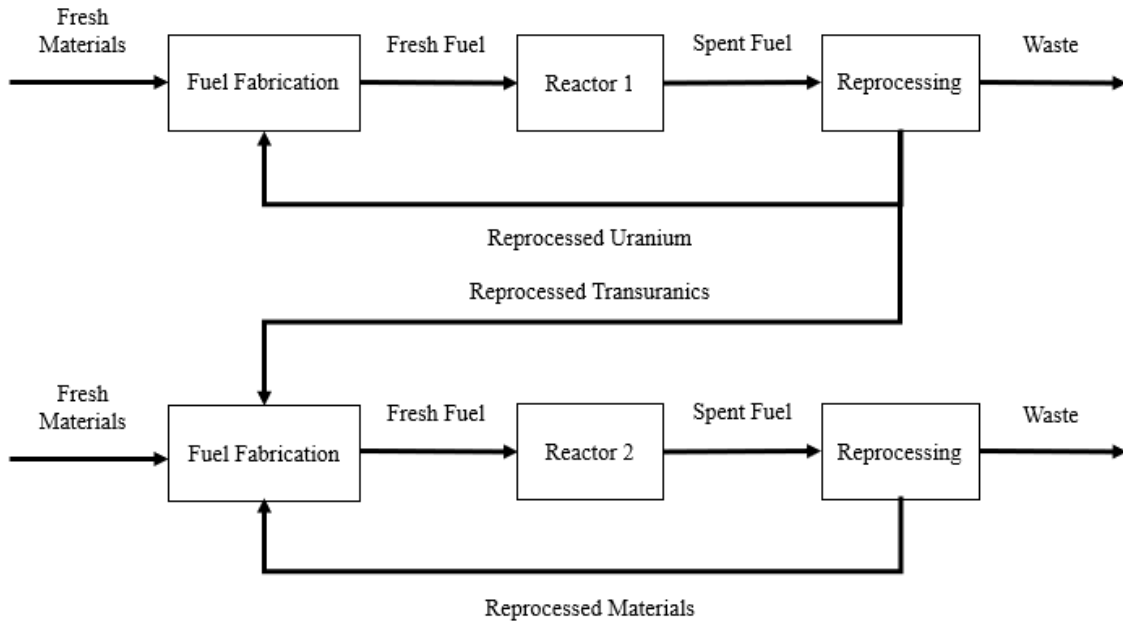


Figure 3. Closed fuel cycle between Reactor 1, which uses a uranium fuel, and Reactor 2, which uses a transuranic-containing fuel.

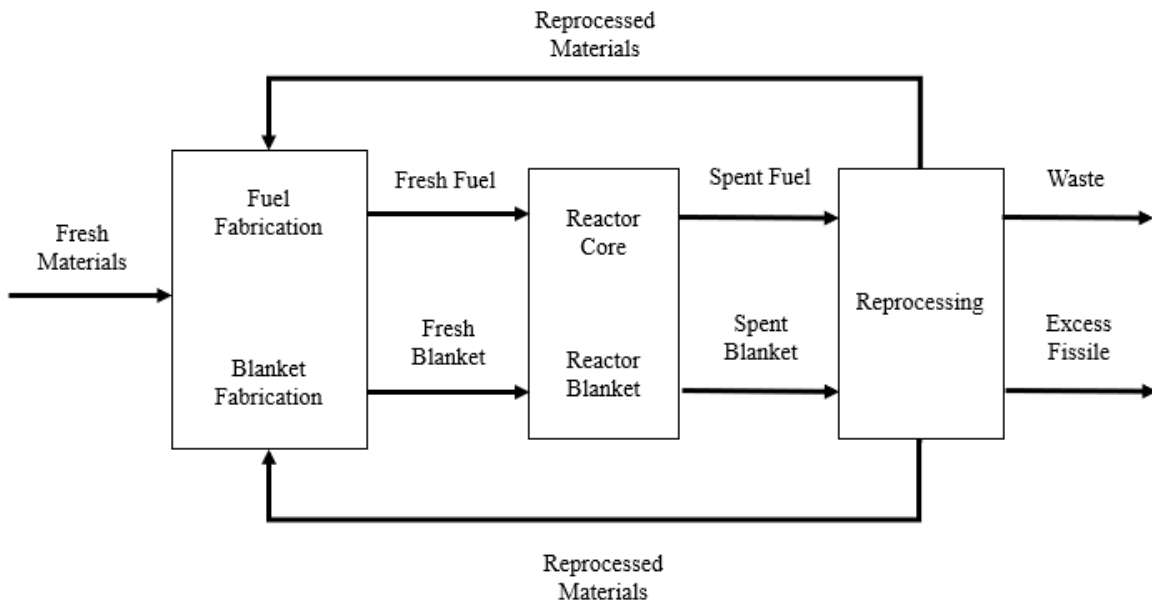


Figure 4. Closed fuel cycle of a breeder reactor operating with fuel and blanket.

2.5. Reprocessing Practical Considerations and Experience

In the U.S. experience, pyrochemical reprocessing has been most closely associated with the Argonne National Laboratory (ANL) Integral Fast Reactor (IFR) Program^b and the Oak Ridge National Laboratory

b. The IFR Program is the progenitor of what is now the Idaho National Laboratory (INL) Spent Fuel Treatment Program and the Joint Fuel Cycle Study (JFCS) Program.

(ORNL) Molten Salt Breeder Reactor (MSBR) Program. The IFR Program envisioned pyrochemical reprocessing and fuel fabrication facilities that are co-located with several SFRs as to avoid the transportation of spent nuclear fuels over long distances that would otherwise separate reprocessing facilities and reactors. The ORNL MSBR Program envisioned the pyrochemical treatment of a continuous slipstream of salt from the reactor taking place in a co-located reprocessing facility. However, demonstrations of these applications never came to fruition. This history explains why remote fuel fabrication is often associated with pyrochemical reprocessing.

In contrast, aqueous reprocessing has a long history of recovering and purifying actinides for both military and civilian applications. The separations processes are performed in shielded facilities. However, the materials recovered for fuel fabrication do not necessarily require shielding. These aqueous reprocessing flowsheets are designed to achieve high separations factors such that the residual radiation levels of the purified products may be sufficiently low as not to require shielded facilities for subsequent handling and fuel fabrication. In other words, in some instances, the same fuel fabrication facility that accepts virgin materials from uranium mining and enrichment operations, may also accept materials from aqueous reprocessing operations. Regardless of which reprocessing route is used, the actinide-bearing materials that are recovered will be used to make new fuel. Both aqueous and pyrochemical reprocessing flowsheets can be designed to yield high separation factors and refined materials. Depending on the flowsheet, the refined product may not require shielding. If the radiation levels of these materials are low enough, then the materials can be contact-handled, otherwise the materials must be remote-handled [1].

Selection of the reprocessing performance is only one aspect to consider. Fuel cycles are derived from considerations of economics and complex selections of technologies related to reactors, reprocessing, fuel fabrication, and waste management.

There is an ever-changing landscape of existing and emerging variants of reprocessing technologies that influence fuel cycle selection; therefore, definitive statements regarding the applicability of aqueous and pyrochemical reprocessing applications to different fuel cycles cannot be made. Certain comparisons can be made, however. Regardless of the spent fuel type, aqueous reprocessing does not recover actinides as metals. Generally, the actinides are recovered as oxides, and if metals are desired, these oxides must be converted to metals using metallurgical operations that are downstream of the reprocessing operations. Regardless of the spent fuel type, pyrochemical reprocessing can recover actinides as metals. Therefore, if an oxide product is desired, then aqueous reprocessing may have inherent advantages over pyrochemical reprocessing; and if a metal product is desired, then pyrochemical reprocessing may have inherent advantages over aqueous reprocessing. However, the selection of the optimal reprocessing route remains highly application specific. Examples are provided below:

- *LWR spent fuels containing low-enriched uranium (LEU) oxide.* If the purpose of reprocessing is to recover only the LEU for use in making fresh LWR fuels, then aqueous reprocessing would be a logical choice because the desired product is uranium oxide.
- *SFR spent fuels containing high-enriched uranium (HEU) metal.* If the purpose of reprocessing is to recover only the HEU for use in making fresh SFR fuels, then pyrochemical reprocessing would be a logical choice because the desired product is uranium metal.
- *Fluid-fueled MSRs (i.e., reactors that use fuel salts).* If the purpose of reprocessing is to condition the fuel salt for continued use in the reactor, then pyrochemical reprocessing would be a logical choice because the desired product is a fluoride or chloride salt. If aqueous reprocessing were applied, the actinides would be recovered as oxides, and these oxides would require conversion back to fluoride or chloride salts using downstream metallurgical operations.

There are exceptions to the above arguments. The Research Institute of Atomic Reactors (RIAR) Process used in Russia is an example where pyrochemical reprocessing is used to reprocess mixed oxide (MOX) fuel from an SFR. In this scenario, pyrochemical reprocessing is applied to a spent oxide fuel to

recover a purified oxide product [2]. The Joint Fuel Cycle Study (JFCS) Program is an example where pyrochemical reprocessing is used to recover a uranium/plutonium metal alloy for making SFR metal fuel from LWR spent oxide fuel. That is, pyrochemical reprocessing is applied to a spent oxide fuel to recover a metal product. A process known as oxide reduction, which is described in this report, can be used to convert the spent oxide fuel to a metal form suitable for electrorefining. Other technologies are being developed to facilitate separation processes in the head-end (e.g. voloxidation) and to manage salt waste generated in pyroprocessing operations. These are discussed in subsequent chapters.

3. VOLOXIDATION

In the 1960s, oxidation technologies were being developed by Atomics International, e.g., the Atomics International Reduction Oxidation (AIROX) Process [3, 4], and the Japanese Atomic Energy Research Institute (JAERI) [5]. Building on these earlier efforts, ORNL introduced the term “voloxidation” to describe the process of oxidizing UO_2 to U_3O_8 , as a head-end method for decladding oxide fuels and removing some of the volatile fission products [6].

Within the suite of technology options in pyrochemical reprocessing, gaseous species can evolve from various unit processes. Among these processes, voloxidation deserves attention for its off-gas behavior. Voloxidation is a high-temperature roasting process. During voloxidation, the uranium oxide (UO_2) fuel pellets are exposed to an oxygen-containing atmosphere at high temperature to further oxidize the UO_2 to a higher valence state compound, U_3O_8 . This results in the decrepitation of the fuel pellets into a high surface area powder and the emission into the off-gas stream of various volatile and semi-volatile gaseous species. These effects are highly dependent on operational conditions such as the oxygen partial pressure, process time, and process temperature.

Voloxidation may be employed in both aqueous and pyrochemical reprocessing flowsheets as a head-end process usually applied to oxide fuels. Voloxidation is used for three primary reasons: (1) to improve the effectiveness of fuel decladding, (2) to remove some of the volatile fission products, and (3) to convert the high-density fuel into a high surface area powder [7].

Noble fission gases, such as xenon (Xe) and krypton (Kr), can be released from various unit processes in pyrochemical reprocessing, regardless of the specific processing options. Front-end unit processes such as chopping and voloxidation are likely to release these noble gases, but potential release points exist throughout all unit processes. Due to their chemical inertness, these gases do not react chemically and will transition to the gas phase once they are no longer trapped within the fuel matrix. Consequently, these noble fission gas species will not be addressed as gaseous species in the subsequent discussions on the downstream individual unit processes.

In reprocessing, krypton-85 (Kr-85) needs to be managed due to its radioactive properties and environmental impact. Kr-85 has a half-life of 10.76 years and emits beta and gamma radiation. Additionally, xenon isotopes, including Xe-133 and Xe-135, do not pose the same concerns. Xe-133 has a half-life of 5.25 days, and Xe-135 has a half-life of 9.14 hours. These xenon isotopes, while having shorter half-lives, can affect reactor performance as neutron poisons (e.g., Xe-135), but are not a concern to off-gas emissions during reprocessing. Other xenon and krypton isotopes are non-radioactive and chemically inert and, therefore, do not pose the same level of concern.

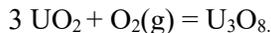
3.1. Decladding

The two conflicting objectives of the use of voloxidation as a decladding process are to: (1) minimize particle size to increase decladding efficiency and provide a higher surface area feed material to the oxide reduction cell and (2) regulate particle size to minimize the dispersion of fines or powder into the hot cell atmosphere. The first objective allows for higher current density and minimizing diffusion length, thereby enhancing reaction kinetics during oxide reduction [8, 9, 10]. Another important factor to consider is finding the lowest operational temperature to enable a greater selection of structural materials for the process equipment and achieve higher throughputs with reduced thermal cycle times.

Understanding the size distribution resulting from specific operational conditions has been a subject of research throughout the development of this process [5, 6, 11, 12, 13, 14]. Depending on these conditions, off-gas species from the feed materials and the degree of their escape from the feed materials will vary. Consequently, literature results are available that detail particle size and associated off-gas species under various operational conditions [5, 6, 11, 12, 13, 14]. Particle size is an important parameter

that directly affects the exposed surface area of the oxide particles, thereby affecting the reaction kinetics during oxide reduction.

Voloxidation results in a higher oxidation state of oxides, as represented by the following reaction:



Uranium dioxide (UO_2) is a black crystalline material that serves as the primary fuel in nuclear reactors. Triuranium octoxide (U_3O_8) is a dark green or black crystalline material. Similar oxidation reactions are applied to all spent fuel constituents.

Upon oxidation, the U_3O_8 product becomes a powder due to a density differential, a process known as spalling or decrepitation. This phenomenon is driven by the density differential between the original UO_2 and the final U_3O_8 product. As UO_2 oxidizes, the volume expansion and the formation of less dense U_3O_8 lead to internal stresses that cause the material to crack and spall [15].

For particle size distributions at temperatures ranging from 400 to 900°C, relevant data from six studies are shown in Table 7. Interpolation of values from plotted data was performed, and averaging was done to derive a single value at a given burnup or temperature. Burnup was chosen as an additional variable to highlight its significant effect. A particle size of 45 μm was chosen as the transition point for material that can be easily contained in a hot cell environment, corresponding to a 325 mesh sieve (U.S. Sieve Series). Not all of the studies listed in Table 7 utilized the 45 μm criteria; therefore, reasonable estimates were made for the data at 45 μm .

Another variable in the six studies was the oxidation temperature. In some cases, oxidations were performed isothermally at the temperatures shown in Table 7, and vacuum or inert conditions were applied following oxidation at those temperatures. The oxidative gas supplied in most studies was air with varying degrees of oxygen concentrations.^c Data were only collected for the complete or nearly complete oxidation of UO_2 to U_3O_8 , as determined by gravimetric monitoring. As temperature increases, or when the restraint of cladding limits fuel expansion, sintering or agglomeration effects are also expected to interfere with particle size distributions. In addition to differences between unclad and clad starting material, relative humidities, annealing times, and sieving or particle separation procedures varied from study to study. Therefore, comparisons made between studies may not be absolute and rigorous, but the data are expected to yield general trends for temperature and burnup.

Table 7. Particle size fractions of fuels at various burnups and oxidation temperatures.

Study	Fuel Burnup (GWd/MTU)	Temperature (°C)	Particle Size Fraction <45 μm (%)
[5] Iwasaki	Unirradiated	400	97
—	Unirradiated	500	97
—	Unirradiated	600	80
—	Unirradiated	700	56
[12] Liu	19	500	99.6
—	19	700	35.8
—	19	900	1.6
[4] Brand	20	600	65
[6] Goode	32	450	85

c. Air is assumed to be synthetic air, which is a mixture of high purity oxygen with high purity nitrogen. No moisture is present.

Study	Fuel Burnup (GWd/MTU)	Temperature (°C)	Particle Size Fraction <45 μm (%)
[14] Westphal	37	500	95
—	37	600	75
—	37	700	44
[11] Kosaka	50	480	90
—	50	700	5

Figure 5 presents the data from Table 7, illustrating the trend of increasing particle size with rising temperature. This trend is likely due to the re-sintering effect at higher temperatures. If particles larger than 45 μm are desirable for process control, a temperature of at least 900°C should be applied for the oxidation and re-sintering of used LWR fuel.

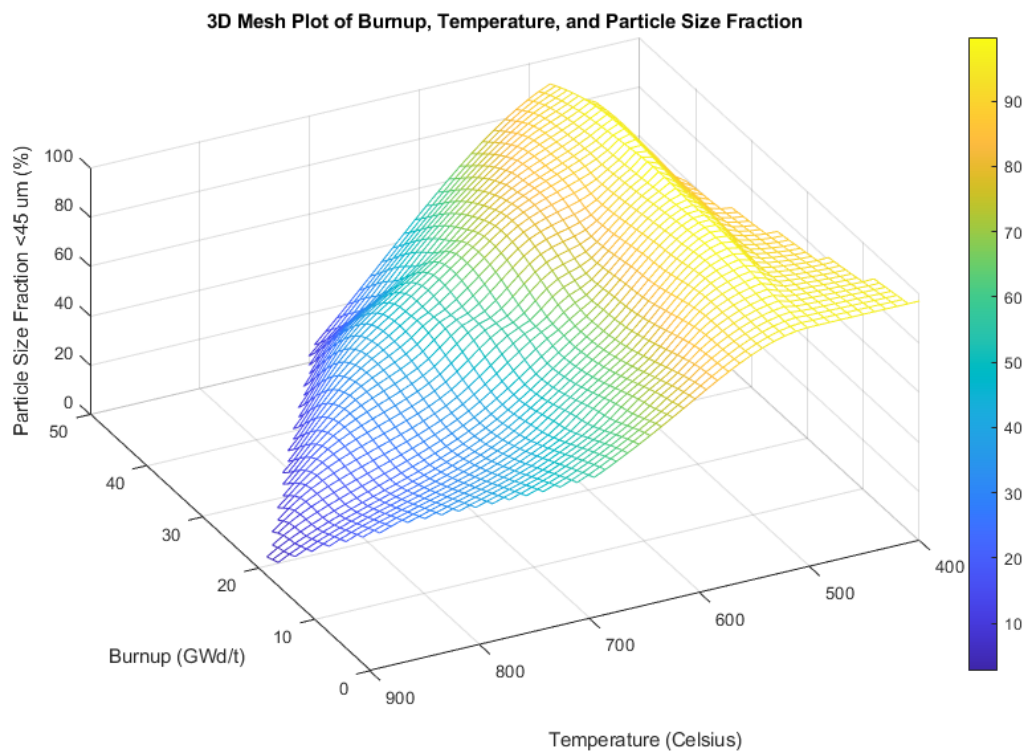


Figure 5. Particle size fraction with respect to fuel burn up and operation temperature.

Data on fuel recovery performance with voloxidation is available in Park [16] and is reproduced below in Table 8. The fuel recovery performance comparison shows that while oxidation aids the process, effective mechanical decladding, such as slitting to physically release the fuel from the cladding, is crucial for achieving higher recovery rates. Without mechanical agitation, recovery rates with voloxidation typically fall below 90%. The key takeaway is that over 99% recovery of fuel appears feasible when combining mechanical separation and voloxidation techniques.

Table 8. Fuel recovery performance comparison.

Fuel Burnup (GWd/MTU)	Mechanical Decladding Only	Mechanical Decladding Post-Voloxidation
65	94.9	99.6
58	99.1	99.7

3.2. Volatile Fission Products

From the perspective of off-gas species management and regulation, understanding the potential off-gas streams from this process is crucial. For this purpose, fission product release data from the literature for iodine, cesium, tritium, and carbon-14 during the oxidation of UO₂ have been compiled, with varying fuel burnups and temperatures.

Assumptions in place were the complete oxidation of the feed and the complete capture of gaseous species. Data handling techniques, including averaging, were employed to arrive at meaningful values. Data were analyzed from a wide variety of independent studies. Additionally, the effects arising from differences in experimental systems, procedures, materials, and thermal cycles were not taken into account in the analytical results presented here. The key point of this section is not to achieve the best quantification and estimates of the release but to identify the species being released during voloxidation. Nonetheless, given sufficient data, trends in the data should be evident despite the outliers.

High-temperature oxidation conditions induce the release of volatile fission products from spent oxide fuels. These include gaseous species at room temperature as well as species that become volatile at high temperatures, often through oxidation. Specifically, iodine, cesium, tritium, and carbon are of primary interest due to their radioactivity and the regulations governing the release limits of radioactive isotopes into the environment. Other volatile species include noble metal oxides, such as those of Tc, Ru, Rh, Te, Mo, and Rb, which typically form highly volatile oxides. The list below details each element and isotope. The following points provide useful insights and information into the gaseous products released during the voloxidation operation.

Iodine: Iodine-131 (I-131) has a half-life of approximately 8 days and emits both beta and gamma radiation. However, with sufficient cooling time, this isotope will decay into xenon-131 (Xe-131), which is a stable and non-radioactive isotope. Thus, unless there is a very short cooling period, such as during inline separations being considered for some MSR concepts [17], I-131 is not likely to be found in spent fuel because it typically decays prior to reprocessing.

Iodine-129 (I-129) has a much longer half-life of about 15.7 million years, which makes it a long-term radiological concern due to its persistence in the environment. Thus, the volatilization of I-129 needs to be considered in off-gas management in both aqueous and pyrochemical reprocessing. During the voloxidation process, iodine can be released as a volatile species, including molecular iodine (I₂), which has a slight vapor pressure at room temperature considering that its melting point is 113.7°C. Therefore, iodine needs to be captured in the off-gas handling system.

Cesium: The isotope of primary significance is cesium-137 (Cs-137), which has a half-life of approximately 30 years and emits both beta and gamma radiation. Cs-137 is of particular interest due to its relatively long half-life and its potential to cause significant environmental contamination and health hazards if released. Another isotope, cesium-134 (Cs-134), also contributes to radiological concerns. Cs-134 has a shorter half-life of approximately 2 years but remains relevant due to its beta and gamma emissions, especially when shorter fuel cooling times are applied.

During the voloxidation process, cesium can be released as a volatile species at high temperatures. Possible chemical forms include metallic cesium, cesium oxide (Cs₂O), and cesium iodide (CsI). These

forms do not exhibit high vapor pressure at room temperature and, therefore, they are likely to condense on cooler surfaces within or near exiting the high-temperature process equipment.

Tritium: Tritium (H-3) is a radioactive isotope of hydrogen with a half-life of approximately 12.3 years and decays into the non-radioactive noble gas helium-3 (He-3). It is produced in nuclear reactors through several mechanisms, including neutron activation of lithium-6 (Li-6) impurities in the fuel or reactor materials. Tritium is a beta-emitter, and its radiological properties make it a consideration for both environmental and health impacts if released during nuclear fuel reprocessing. While the decay of tritium into non-radioactive He-3 is beneficial in terms of radioactive materials management, the extended decay times require management prior to disposal.

Tritium can be released as hydrogen gas if released directly from the fuel matrix without reacting with other elements. Tritium can also react with oxygen in the fuel or impurity oxygen in the surrounding environment to form water vapor. Both forms exhibit high vapor pressure at room temperature, so gaseous phase formation should be expected.

In U.S. aqueous applications, the term “tritium pretreatment” was sometimes substituted for “voloxidation.” Depending on process conditions, voloxidation can release almost all the tritium to the gas phase, which prevents its subsequent distribution into aqueous or pyrochemical media.

Carbon-14: Carbon-14 (C-14) is a radioactive isotope with a half-life of approximately 5,730 years. Carbon-14 is a beta-emitter and can pose a health risk if ingested or inhaled. The most common form of carbon-14 release during voloxidation is carbon dioxide (CO₂). Under certain conditions, particularly in a reducing atmosphere, carbon-14 can be released as carbon monoxide (CO). However, the latter is less common given the oxidizing conditions of the voloxidation process. In general, carbon-14 is the volatile of least concern and may not require sequestration depending on specifics of the reprocessing application.

Table 9 summarizes the gaseous species release data compiled from six different sources in the literature. Figure 6 and Figure 7 give graphical representations of the data in Table 9.

Table 9. Fission product release at different fuel burnups and oxidation temperatures.

Study	Fuel Burnup (GWd/MTU)	Temperature (°C)	Iodine Release (%)	Cesium Release (%)	Tritium Release (%)	Carbon-14 Release (%)
[6] Goode	32	450	41	—	99	—
[18] Stone	11	490	3.5	—	99.9	18.4
—	28	490	0.3	—	99.9	21.3
[14] Westphal	37	500	—	23	—	—
[19] Song	42	500	—	—	—	11.5
—	65	500	—	0	—	—
[14] Westphal	37	700	—	20	—	—
[19] Song	42	700	—	—	—	80
[11] Kosaka	50	700	70	1.5	90	25
[6] Goode	32	750	—	—	—	—
[14] Westphal	37	900	—	25	—	—
—	37	963	—	51	—	—

Study	Fuel Burnup (GWd/MTU)	Temperature (°C)	Iodine Release (%)	Cesium Release (%)	Tritium Release (%)	Carbon-14 Release (%)
[20] Shcherbina	40	1000	—	55	—	—
[11] Kosaka	50	1000	90	68	100	67
[19] Song	65	1000	—	15	—	—
[14] Westphal	37	1045	—	69	—	—
[21] Westphal	37	1200	—	70	—	—
[14] Westphal	37	1250	—	75	—	—
[19] Song	65	1250	—	90	—	—
[20] Shcherbina	40	1500	—	90	—	—
[19] Song	65	1500	—	95	—	—
[20] Shcherbina	40	2000	—	98	—	—

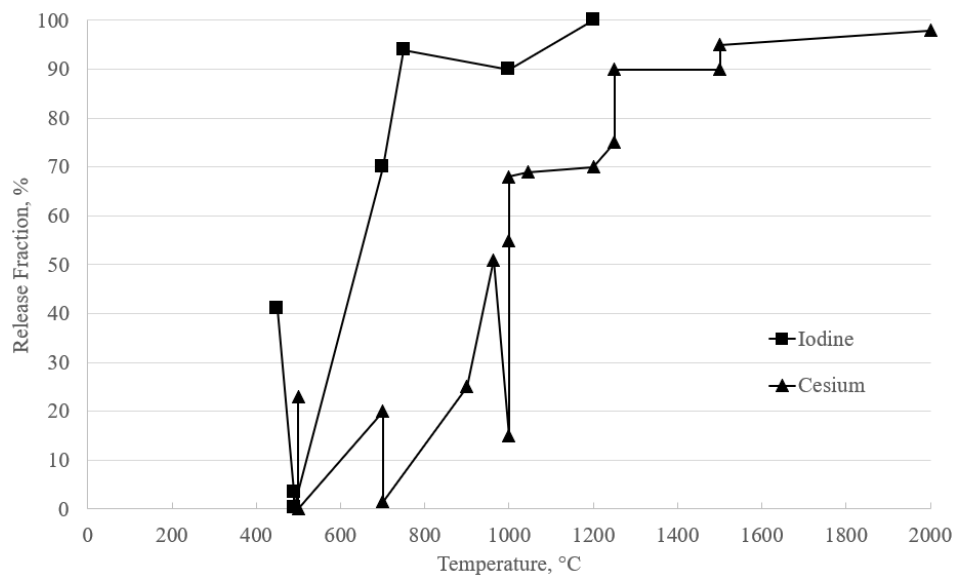


Figure 6. Iodine and cesium release trend with respect to temperature.

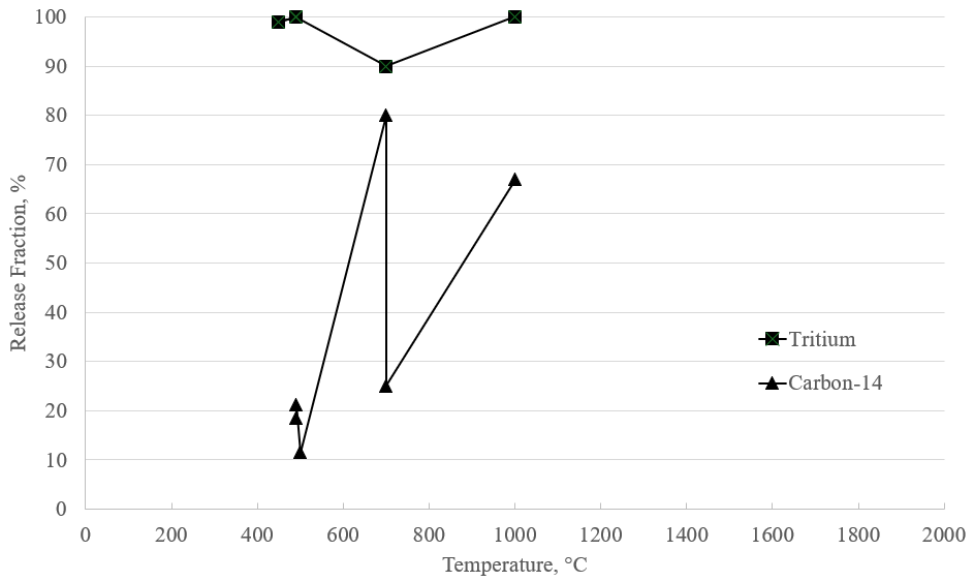


Figure 7. Tritium and carbon-14 release trend with respect to temperature.

Also of interest are semi-volatile species such as Tc, Ru, Rh, Te, Mo, and Rb, which typically form high volatility oxides. Data are scarce; a literature search found only one instance involving these species [20]. Table 10 was regenerated from the information presented in this source.

Table 10. Removal rate of the semi-volatile elements from a voloxidation process.

Elements	Tc	Ru	Rh	Te	Mo	Rb
Removal Rate (%)	92.3	97.6	82.7	53.3	61.7	96

3.3. Off-Gas Capture

Effective off-gas capture technology is critical for managing the volatile and potentially hazardous fission products released during voloxidation. The local gas purification system developed for this purpose comprises several key components, each designed to target specific contaminants. The filtration system typically consists of a series of filter materials and reaction devices. The following capture technologies have been typically used at spent fuel reprocessing facilities.

Iodine: Silver-containing zeolite and silver columns are used to capture iodine, as documented in [21, 22, 23, 24, 25]. Silver zeolite (AgZ) and Ag-functionalized aerogel are particularly effective, forming water-insoluble silver iodide (AgI).

Cesium: Metal ceramic filters [21, 22], pressed fly ash [23], and metal fabric filters [24] are employed to capture cesium.

Tritium: Molecular sieves are used to capture tritiated water vapor (i.e., formula of HTO) formed through the oxidation of exhaust gases on CuO [21]. Catalysts with deposited copper facilitate the oxidation of hydrogen [22]. Additional oxidation units can also capture hydrogen [24]. Essentially, the process involves the oxidation of tritium to water, followed by adsorption using moisture trapping chemicals such as zeolite to capture H-3.

Carbon-14: Carbon-14, predominantly in the form of CO₂, is captured using 13X molecular sieves [21] and a scrubber with a water solution of sodium hydroxide (NaOH) for catching CO₂ [22, 24]. The

spent alkaline solution is regenerated with calcium hydroxide, producing calcium carbonate containing the captured C-14, which is then cemented for long-term storage.

High volatility oxides (Tc, Ru, Rh, Te, Mo, and Rb): These species are captured assuming their solid nature using filters [21], metal ceramic filters [22], and columns with calcium-based packing [23]. Further reductive chemical treatment can be done to reduce volatility such as columns with 0.5 to 5 mm granules of γ -aluminum oxide for catching volatile ruthenium tetroxide by sorption and decomposition to non-volatile ruthenium dioxide [24].

Xenon and Krypton: Separating Xenon (Xe) and Krypton (Kr) is crucial in nuclear processing, particularly for managing radioactive waste such as Kr-85, which has a half-life of 10.76 years. Traditionally, cryogenic distillation is used for this separation. However, more energy-efficient methods, such as metal-organic frameworks (MOFs) and zeolite membranes, are being explored. Selected MOF materials have been successfully demonstrated to capture Kr and Xe without the need for separations at cryogenic temperatures, as documented in Reference [25].

Without voloxidation, iodine is likely to partition into the salt, and active investigations are ongoing to confirm the state of iodine in a chloride salt [26]. However, with voloxidation, the majority of iodine will be released as a gaseous species. Therefore, non-water-soluble species, such as silver iodides, are considered for retaining and disposal of iodine. Later, iodides may be incorporated into a ceramic waste form as consolidated waste. This approach may simplify waste stream management. However, since release fractions of iodine are so varied, even with voloxidation, there may still be iodine reporting to the salt and aqueous media. The U.S. implementation of voloxidation has historically focused on lower temperatures than other international work, which tends to limit iodine release.

The fate of captured fission products during voloxidation involves their transformation into gaseous forms, subsequent capture using various materials, and stabilization into less mobile and more manageable compounds for safe disposal. This process is crucial for reducing environmental impact and enhancing the safety of nuclear waste management.

Although voloxidation is a valuable tool for multiple purposes, it introduces complexities to pyrochemical reprocessing systems. It is essential to weigh the benefits against these added complexities. Advancements in mechanical decladding methods, as reported in References [27, 28, 29], highlight potential improvements in the decladding process and may allow acceptable spent fuel separation from cladding without the need for high-temperature oxidation processes. A careful analysis is required to justify the inclusion of voloxidation, balancing performance improvements against the desire to minimize the complexity of a reprocessing flowsheet.

Voloxidation can enhance decladding performance and improve reaction kinetics through size reduction and increased surface area of the oxide fuel. However, voloxidation also creates metal oxides with higher oxidation states, which often increases volatility of the metal oxides. This places an additional burden on the off-gas system to handle these species. Without voloxidation, the oxide reduction process is not likely to incur additional off-gas beyond trapped noble gases and carbon dioxide. Therefore, off-gas handling remains more straightforward in flowsheets that do not involve voloxidation.

Nevertheless, the presence or absence of voloxidation in a reprocessing flowsheet would appear to affect the quantity of species reporting to the off-gas system, more than it does the types of species reporting to the off-gas system. For example, voloxidation tends to release iodine and cesium into the off-gas, whereas oxide reduction tends to sequester iodine and cesium into the salt. However, some iodine and cesium remain in the product from voloxidation, and some iodine and cesium are released into the off-gas during oxide reduction. Therefore, it is advisable to design an off-gas system capable of handling gas, fume, and dust, regardless of the expected ideal behaviors of the volatile fission products during voloxidation and/or oxide reduction.

4. OXIDE REDUCTION

Pyrochemical reprocessing gained attention in the 1960s as a promising alternative to aqueous reprocessing, particularly for recycling metal fuel in SFRs. Pyrochemical reprocessing uses molten salts and electrochemical methods to separate and purify actinides and other valuable elements from spent nuclear fuel. Originally optimized for metal fuel, efforts were also made to adapt pyrochemical reprocessing for the reprocessing of oxide fuels, leading to the development of the oxide reduction process described in this section.

Oxide reduction is a high-temperature electrochemical process. During oxide reduction, the metal oxides comprising the spent fuel are converted to metals. The feed to oxide reduction is oxide fuel that may or may not have been treated by voloxidation. During oxide reduction, oxygen is liberated from the oxide fuel at the cathode and reports to the electrolyte as dissolved lithium oxide (Li_2O). The lithium oxide migrates through the electrolyte from the cathode to the anode where the oxygen is liberated from the electrolyte as oxygen gas ($\text{O}_2(\text{g})$). The selection of anode materials and operating conditions determines the off-gas species produced at the anode during the oxide reduction process.

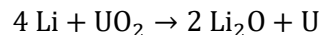
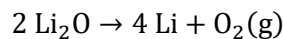
There is a precedent for electrochemical oxide reduction. A mature commercial-scale industrial application includes the Hall-Héroult process for converting aluminum oxide (Al_2O_3) to aluminum metal. The Hall-Héroult process has been the dominant industrial method since its invention in the late 19th century [30] and has contributed to the widespread availability of inexpensive aluminum metal. In this process, the Al_2O_3 is dissolved in a molten salt comprised of aluminum fluoride (AlF_3) and sodium fluoride (NaF) at 960°C . The reduction of aluminum occurs at a molten aluminum cathode, and oxygen is liberated as carbon dioxide (CO_2) at a carbon anode. A more recent example is the FFC Cambridge Process, reported in 1999, which is used for the conversion of titanium oxide (TiO_2) to titanium metal [31]. In this process, TiO_2 is reduced to titanium metal at a solid oxide cathode in molten salt comprised of calcium chloride (CaCl_2) with dissolved calcium oxide (CaO) at 900°C . Oxygen is liberated as carbon dioxide (CO_2) at a carbon anode.

Adapting the technology to an oxide-to-metal fuel cycle, the oxide reduction process must be applied to spent oxide fuels prior to the electrorefining process. An early version of the oxide reduction process used lithium metal as the reductant and lithium chloride solvent [32]. Later, an electrochemistry-based method was introduced for oxide fuels, following the precedent set by earlier electrochemistry-based metal oxide reduction processes for non-nuclear industrial applications [33].

Presently, the reference oxide reduction process employs the $\text{LiCl-Li}_2\text{O}$ molten salt system due to its high electrolytic conductivity and relatively low-melting point near 600°C . This salt system has been extensively studied for its effectiveness in facilitating the reduction of uranium oxide and other actinide oxides [34, 35, 36, 37, 38, 39, 40, 41, 42].

4.1. Processing Rate

A common feature of electrochemical oxide reduction processes is the oxidation of oxygen ions from dissolved carrier oxide species such as Li_2O in the molten LiCl salt. This results in the production of gaseous species at the anode, including oxygen gas ($\text{O}_2(\text{g})$) when an inert anode is used and carbon dioxide gas (CO_2) when carbon anode is used. The simplified overall electrochemical reaction involves the production of lithium metal to reduce uranium oxide to uranium metal at the cathode, and the evolution of oxygen gas at the anode as described below.



The first reaction requires a sufficient supply of lithium oxide to sustain the production of lithium metal at the cathode and the evolution of oxygen gas at the anode. This process remains sustainable and

does not become a kinetic limitation as long as there is a sufficient concentration of lithium oxide available and sufficient anode surface area available.

Meanwhile, the lithium oxide formed at the cathode by stripping oxygen ions from uranium oxide needs to migrate away from the reaction site. This migration involves passing through the metal layer resulting from the reactions that have occurred so far. As the reaction progresses, the length of diffusion increases, as depicted in a shrinking core model shown in Figure 8. In this figure, conversion from oxide-to-metal occurs from the outside toward the inside. Here, W is the thickness of the cathode basket loaded with oxide fuel, and $2X_c$ is the thickness of the remaining oxide material.

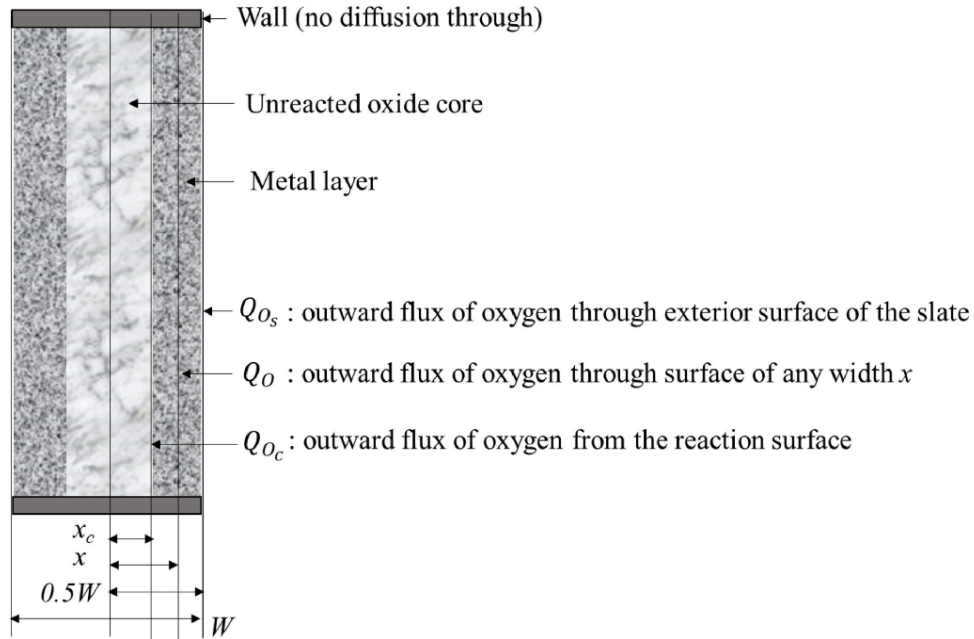


Figure 8. A shrinking core representation for the oxide reduction process.

Under present cell designs, the rate of processing will likely be controlled by the outward diffusion of product oxygen ions, in the form of Li_2O , from the cathode reaction interface. A study reported by Yoo [8] models the expected time for the completion of cathodic reactions based on available reaction data. The expression found in this study indicates that the time required for the oxide fuel to convert into metal was proportional to the square of the smallest dimension of the cathode geometry. Given the established parameters, Figure 9 illustrates the extent of oxygen removal from the cathode with respect to varying cathode thickness, assuming the bed of oxide fuel has a rectangular plate shape.

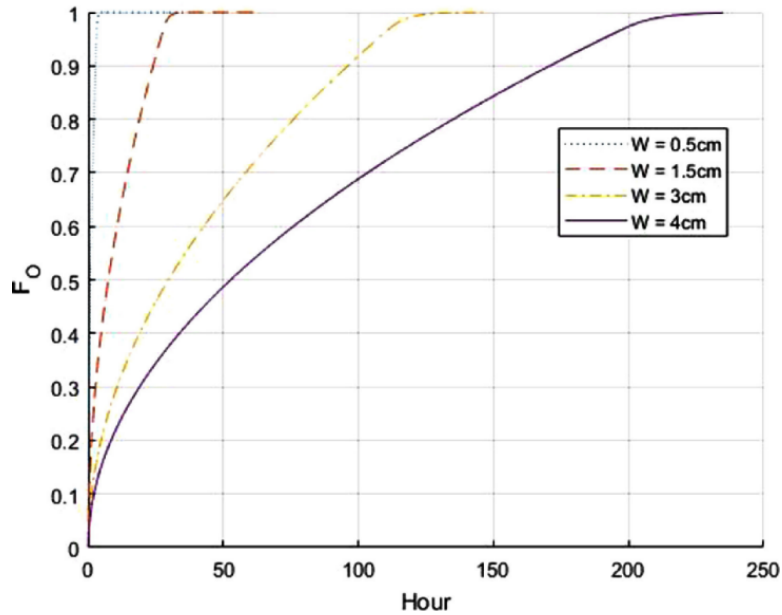


Figure 9. Extent of possible oxygen removal with respect to plate width.

Interpreting Figure 9, it was clear that scaling up should consider the cathode structure to avoid excessive reaction time, which would hinder high-throughput operations. Efforts such as pelletizing the oxide materials and minimizing diffusion length to improve reaction kinetics have been suggested and simulated by Kim [9] to assess their impact, as shown in Figure 10.

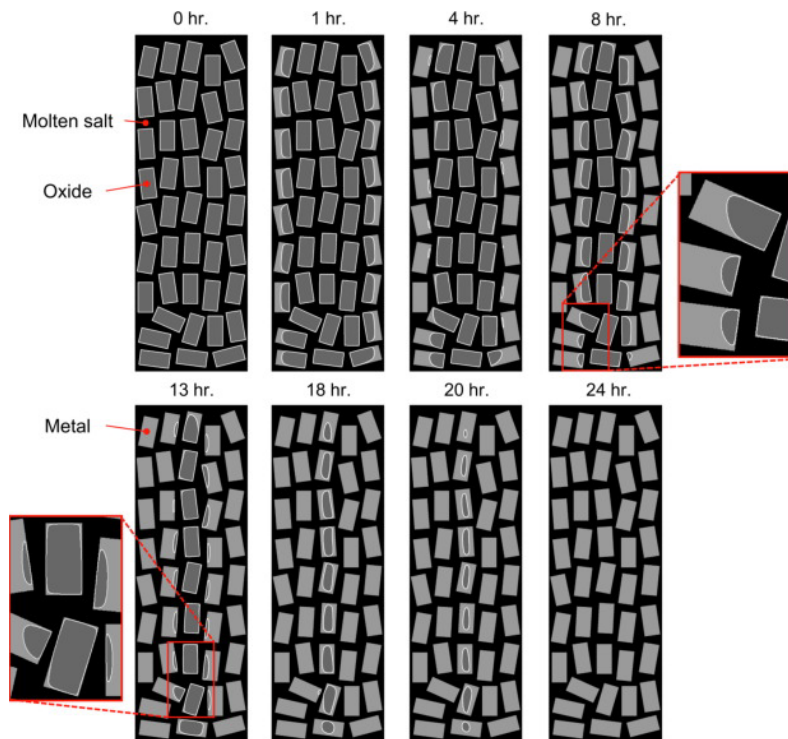


Figure 10. Simulation of the extent of reaction in 2D pellet model.

Additionally, vigorous electrolyte flow through controlled oxide-bed geometry helps improve reaction kinetics, as simulated Kim [10] and reproduced in Figure 11.

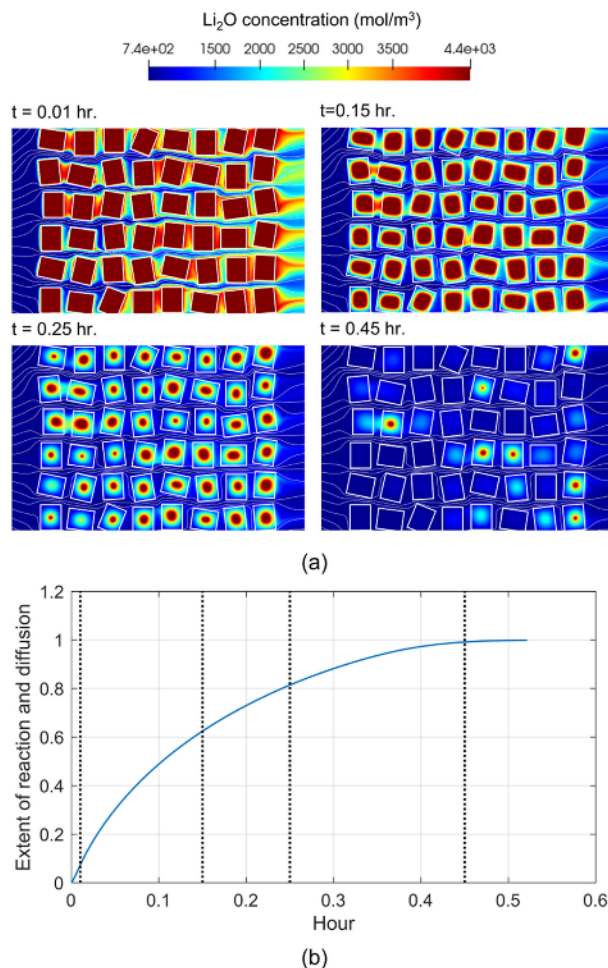


Figure 11. Oxide reduction process under high convection. (a) Concentration field of Li_2O at several time instances. (b) Extent of reaction and diffusion.

4.2. Current Interruption

Current interruption is a momentary pause in the current, provided by an external power supply, between the anode and cathode in the oxide reduction cell. Current interruption was considered as a means of relieving the accumulation of oxygen ions at the reaction interface between the cathode and the salt. This can be effective in scenarios where ionic species need to migrate toward the reaction interface, such as in operations, creating metal electrode deposits where ionic species must move to the reaction interface. Primarily, this type of operation aims to improve deposit quality [43, 44] rather than throughput improvement. In the context of oxide reduction process, the idea of current interruption was adopted to provide time for the concentration gradients within the electrolyte to relax and dissipate [45].

However, oxide reduction does not require ionic species migration toward the cathodic reaction interface, as the oxygen ions entering the salt are created at the cathode itself. Instead, it requires the movement of the oxygen ions away from the cathode reaction interface toward the anodic reaction interface to facilitate the oxidation of oxygen ions to form oxygen gas. Therefore, provided the anode side has sufficient surface area and the bulk salt is adequately agitated to make oxygen ions available at the anode reaction interface, current interruption is not expected to improve product quality or increase throughput. It is noteworthy that the buildup of oxygen is not problematic in the cathodic reaction, as the cathode reductive reaction can be completed without properly relieving ionic species beyond the saturation of oxygen species in the deposit. In Reference [42], experimental examination found that the

Li₂O concentration in the vicinity of the reduced uranium metal in the cathode compartment ranged from 26 to 46 wt%. This concentration range is much higher than the solubility limit of Li₂O in LiCl at 650°C, which is reported to be approximately 8.8 wt% [46, 47]. This implies that the cathode reaction kinetics can produce Li₂O even when Li₂O is saturated in LiCl. It is unlikely that the current interruption operation would significantly expedite oxygen diffusion, though this may need to be investigated further.

4.3. Anode Corrosion (Metal and Carbon)

In the oxide reduction process, oxygen gas is formed at the anode at temperatures of approximately 650°C. An ideal inert anode material would be a material that functions as an anodic electrode but is otherwise chemically inert to the process. An ideal inert anode material would not be consumed or corroded or change its shape. No ideal inert anode materials have been discovered for this application to date.

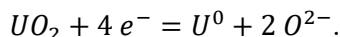
Noble metals such as platinum have been considered as an inert anode material in the LiCl-Li₂O molten salt system [33, 34]. However, noble metals are not completely inert in this salt system. For instance, the formation of lithium platinate (Li₂PtO₃) has been observed to corrode the anodic platinum electrode [34]. Therefore, many efforts have been made to develop alternative anode materials that are less prone to corrosive attack [35, 36, 37, 38].

One option is to use consumable anodes following the precedent established by the Hall-Héroult aluminum smelting process. In this context, the adoption of a carbon anode for the reduction of uranium oxide to uranium metal has been explored [35, 36, 37]. For this option, lithium carbonate (Li₂CO₃) management is required to assure the expected functionality of the cell [48, 36, 49].

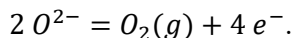
Another path is to identify alternative inert anode materials such as ruthenium and iridium [45, 50]. Recent innovations include the use of nickel ferrite as an anode material [38]. This is an active research area focused on finding the most economical options that provide suitable survivability over extended operation.

4.4. Anode Off-Gas

During the oxide reduction process, the uranium in uranium oxide is electrochemically reduced from U(IV) to U(0) according to the following reaction:



In this reaction, the reduced uranium metal remains in the cathode basket, and the oxygen anions are liberated into the salt and become associated with dissolved lithium oxide. The oxygen anions must transport through the salt from the cathode to the anode. When the anode material is inert to the electrode reaction, the oxygen anions are electrochemically oxidized to form oxygen gas according to the following reaction:



The overall reaction is the conversion of uranium oxide to uranium metal and oxygen gas. When a consumable anode material is used, such as carbon, the dissociated oxygen anions emerge as a mixture of carbon dioxide gas (CO₂(g)) and carbon monoxide gas (CO(g)). Table 11 elucidates the possible anode reactions depending on the applied electrode potentials. Higher potential reactions require more electrode activation and, therefore, inducing all lower potential reactions. For instance, chlorine evolution at 3.459V induces all other reactions listed in Table 11.

Table 11. Feasible reactions at anodes of oxide reduction processes.

Oxidation Reaction	Electrode Potential versus the Lithium Reduction Potential, V
$C + 3 O^{2-} \rightarrow CO_3^{2-} + 4 e^-$	1.226
$C + 2 O^{2-} \rightarrow CO_2(g) + 4 e^-$	1.440
$C + O^{2-} \rightarrow CO(g) + 2 e^-$	1.463
$C + 2 CO_3^{2-} \rightarrow 3 CO_2(g) + 4 e^-$	1.867
$C + 2 CO_3^{2-} \rightarrow CO_2(g) + CO(g) + 2 e^-$	1.890
$O^{2-} \rightarrow \frac{1}{2} O_2(g) + 2 e^-$	2.465
$Cl^- \rightarrow \frac{1}{2} Cl_2(g) + e^-$	3.459

Significant quantities of off-gas, such as oxygen or oxygen-associated gaseous species, will be released during the process. Based on 100 kg of UO₂, the molar mass of associated oxygen can be calculated as follows:

- The molecular mass of UO₂ is approximately 270 g per mole
- The mass fraction of oxygen in UO₂ is 0.12
- Therefore, the mass of oxygen in 100 kg of UO₂ is 11.85 kg.

The volume of oxygen gas at standard temperature and pressure (STP) can be calculated as follows:

- At STP of 0°C and 1 bar, 1 mole of an ideal gas occupies 22.711 L
- The number of moles of oxygen in 11.85 kg of O₂ is approximately 370 moles
- The volume of oxygen gas at STP is approximately 8,403 L.

Oxygen or chlorine gases cannot be released into the inert argon atmosphere of a hot cell, due to the reactive nature of these gases. Therefore, an off-gas system capable of handling high concentrations of oxygen and chlorine is necessary. The quantity of oxygen evolved depends on the oxidation state and quantity of oxide fuel feed material. Proper handling of high-temperature oxygen gas is essential to prevent corrosion of process equipment and ensure safe operation. Structural materials must be carefully selected to withstand the corrosive nature of high-temperature oxygen and other off-gases [51]. In this context, the application of a consumable anode such as carbon may be advantageous for reactive gas handling due to the superior chemical stability of carbon dioxide and carbon monoxide gases.

4.5. Americium Behavior

There have been some concerns about americium volatility during high-temperature casting operations. For example, in the IFR Program, counter gravity injection casting was used to fabricate a minor actinide-bearing fuel experiment for EBR-II, resulting in approximately 40% americium loss from

the original charge. Further investigations [52, 53] revealed that a significant portion of this loss was due to the plutonium-ameridium alloy (Pu-Am) feedstock being contaminated with magnesium and calcium, which boil below the casting temperature. When the Pu-Am alloy was added to the melt, magnesium and calcium boiled, causing ameridium to be ejected as droplets. Therefore, ameridium vaporization in a pyrochemical reprocessing facility is not likely to be a concern. However, not much is known about the behavior of ameridium and other minor actinides during oxide reduction.

5. FLUORIDE VOLATILITY PROCESSES

Fluorination of uranium is common in the nuclear industry, where conventional uranium enrichment processes such as diffusion and centrifugation utilize uranium as uranium hexafluoride (UF_6), which is produced through the fluorination of uranium oxides. In this application, the uranium oxide feed (UO_2 , U_3O_8 , and mixed UO_x) originates from uranium mining and extraction operations and, in the case of re-enrichment, spent fuels. UO_2 is converted to uranium tetrafluoride (UF_4) by the action of hydrogen fluoride (HF), and UF_4 is converted to UF_6 by the action of fluorine (F_2). There are both aqueous-based and dry-based variants of chemical routes and process flowsheets to perform these fluorination reactions [54]. At the back end of the process, the enriched UF_6 may be de-converted back to UF_4 or back to UO_2 . The enriched UO_2 can be used to make oxide fuel, and the enriched UF_4 can be reduced to metallic uranium or used as fuel salt in molten fluoride salt reactors.

Fluoride volatility processes have been proposed for different reprocessing applications. Fluoride volatility processes exploit differences in vapor pressures between select metal fluorides to affect chemical separations. Metal fluorides with high vapor pressures report to the vapor phase and are separated from the metal fluorides with low vapor pressures. The chemical separations strategies are based on partitioning between a gas phase and a condensed phase (solid or liquid). A select fluoride may be partitioned from the condensed phase to the gas phase, or from the gas phase to the condensed phase. Control variables include temperature, pressure, and the selection of the fluorination reagent (i.e., mild to aggressive). Only select applications are described here.

The *Aquafluor* process was developed by General Electric for its Midwest Fuel Recovery Plant in Morris, Illinois. However, the plant never came to fruition. The Aquafluor process was predominantly a PUREX-based separations process designed to separate, recover, and purify uranium, neptunium, and plutonium from spent LWR fuels. A unique feature of this process was the conversion of uranium oxide (the calcined product of uranyl nitrate hexahydrate) to uranium hexafluoride in a fluidized bed reactor. Additional processing steps purified the uranium hexafluoride, which was intended to be packaged and transported to enrichment facilities for re-enrichment [55, 56, 57].

The *FLUOREX* process was proposed by GE-Hitachi as a means of reprocessing a variety of oxide fuels, over an extended period, as the reactor fleet transitions from LWRs to fast breeder reactors utilizing mixed oxide (MOX) fuels. Like the Aquafluor process, the FLUOREX process is a hybrid process using both aqueous and non-aqueous technologies. The Aquafluor process included fluoride volatility of uranium, at the back end, to produce uranium hexafluoride for re-enrichment. The FLUOREX process includes fluoride volatility at the head-end for two purposes: (1) to control the Pu:U ratio of the materials entering the PUREX process and (2) to produce purified uranium hexafluoride for re-enrichment or other disposition paths [58, 59, 60, 61, 62].

The *Nitrofluor* process was an entirely non-aqueous reprocessing technology proposed by Brookhaven National Laboratory. The process was claimed to be applicable to a variety of fuel types. The fuel was dissolved in a mixture of anhydrous nitrogen dioxide (NO_2) and HF at moderate temperatures between 100 and 200°C. The primary separation stage is based on which metals form soluble fluorides in the solvent and which form insoluble oxides and oxy-nitrides. Subsequently, the solvent is decanted from the solids. Uranium and plutonium form soluble species and report with the solvent. Selective fluorination of the solvent will volatilize uranium as uranium hexafluoride (by the action of bromine trifluoride) and plutonium as plutonium hexafluoride (by the action of fluorine gas). These two product streams would be purified further [56, 58, 63, 64, 65].

The ORNL Th-232/U-233 fuel cycle MSBR concepts required processing of the fuel salts to manage the Pa-233 inventories and remove fission products. In the fuel salt processing flowsheets proposed by ORNL, fluorination and hydro-fluorination were major unit operations used primarily to volatilize uranium from the salts. There were two applications for this operation. First, to remove the bulk of the uranium from the salt stream entering the chemical process ahead of Pa-233 extraction, and second, to

recover U-233 from the process salt kept in storage while Pa-233 decayed to U-233 [66]. During operations of the ORNL Molten Salt Reactor Experiment (MSRE), fluoride volatility was used to defuel the fuel salt of U-235 (by conversion of UF_4 to UF_6) prior to the introduction of U-233 as UF_4 .

During a six-day period in August 1968 the MSRE fuel salt was fluorinated to remove U-235 before beginning operation with U-233. This processing also removed all those fission products having stable volatile fluorides and any Np present in the salt. In addition, the remaining noble gases and the halogens, Br and I, would also be expected to leave the salt. Accordingly, 100% of the elements H, He, Se, Br, Kr, Nb, Mo, Tc, Ru, Te, I, Xe, U and Np were removed from the salt 157 days after the end of power operation with U-235 [67].

Fluoride volatility has been proposed for several other fuel reprocessing schemes. For metal fuel processing there is a significant distinction between fluoride volatility and chloride volatility routes. In metal dispersion fuels, chloride volatility is proposed to volatilize the zirconium or aluminum matrix away from the uranium and plutonium. By contrast, fluoride volatility is proposed to volatilize the uranium and plutonium away from the matrix metals [68, 69, 70, 71]. Similar fluoride volatility concepts have been proposed for graphite matrix fuels [72].

Fluoride volatility processes have also been proposed for reprocessing LWR and fast reactor oxide fuels with the absence of aqueous separations. In one approach [73], the Zircaloy cladding is removed from the LWR fuel by action of hydrogen chloride (HCl) gas to form volatile zirconium chloride ($ZrCl_4$) and tin chloride ($SnCl_2$).^d The clad oxide fuel is subject to voloxidation to convert the uranium (IV) oxide (UO_2) fuel pellets to uranium (V, VI) oxide (U_3O_8) powder, which is then converted to volatile UF_6 by the action of bromine pentafluoride (BrF_5). During this process, the plutonium oxide (PuO_2) is converted to non-volatile plutonium tetrafluoride (PuF_4) and the UF_6 is collected and purified. With the uranium separated, the PuF_4 is converted to volatile plutonium hexafluoride (PuF_6) by the action of fluorine gas. The PuF_6 is collected and purified.

Another approach is proposed for advanced oxide fuels containing high concentrations of plutonium, such as MOX and plutonium-bearing inert-matrix fuels, as well as high-burnup short-cooled fuels [74, 75, 76]. Following decladding and voloxidation, the fuel is aggressively fluorinated with fluorine gas. Non-volatile actinides (e.g., Am and Cm) and fission products are discharged as waste solids. Volatile actinides (e.g., U, Np, and Pu) and fission products are discharged as gases. Subsequent chemical separations from the gas phase involve “condensation at different temperatures, sorption, and distillation processes.” The first condensation process eliminates the most volatile species such as O_2 , F_2 , Se, Te, Xe, Kr, and N_2 as waste gas. After this separation, the condensate contains the remaining fission products and the select actinides UF_6 , NpF_6 , and PuF_6 . Further separations exploit the relative stability of these actinide fluorides. UF_6 is the most stable, and PuF_6 is the least stable. The next separation allows the PuF_6 gas to decompose to PuF_4 solid. The next separation allows the NpF_6 gas to decompose to NpF_4 solid and adsorb onto a magnesia (MgO) substrate. The next separation allows the UF_6 gas to decompose to UF_4 solid. The I, Tc, Sb, and Mo fission products remain in the gas phase and report to waste gas processing.

The fluorination behaviors of actinides are still being investigated. It was reported that $NF_3(g)$ was incapable of fluorinating PuO_2 or PuF_4 , to PuF_6 [77]. It was reported that $KrF_2(g)$ and $O_2F_2(g)$ are capable of fluorinating UO_2 , NpO_2 , and PuO_2 to their hexafluorides [78]. This type of process chemistry is important for developing separations strategies.

5.1. Process Chemistry

Fluorine is the most electronegative element, making it also the most chemically reactive element. Fluorination reagents can be ranked based on their abilities to react with the different metal oxides in

d. Zircalloy is an alloy primarily of zirconium and tin, with the tin as a minor constituent (< 2.5 wt.%).

spent oxide fuels. Figure 12 is an Ellingham diagram showing the standard state Gibbs free energy of formation—normalized to one mole of $F_2(g)$ —of select fluorination reagents. In this figure, $HF(g)$ is the most stable, and $KrF_2(g)$ is the least stable. The information in Figure 12 gives some insight into the comparative effectiveness of different fluorination reagents, but the chemical form of the oxide reactants and the stoichiometry of the fluorination reactions are also important.

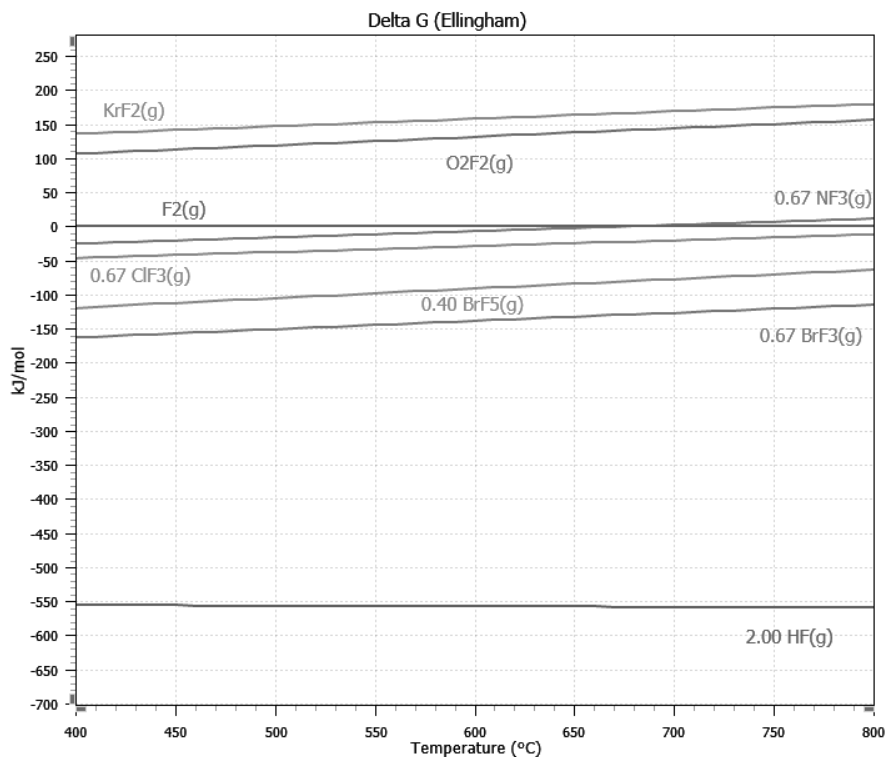


Figure 12. Ellingham diagram of select fluorination reagents.

The stoichiometries of fluorination reagents reacting with uranium, neptunium, and plutonium oxides to form fluorides are presented in Table 12 to Table 19 for fluorination reagents krypton difluoride ($KrF_2(g)$), dioxygen difluoride ($O_2F_2(g)$), fluorine ($F_2(g)$), nitrogen trifluoride ($NF_3(g)$), chlorine trifluoride ($ClF_3(g)$), bromine pentafluoride ($BrF_5(g)$), bromine trifluoride ($BrF_3(g)$), and hydrogen fluoride ($HF(g)$), respectively. For each reaction stoichiometry shown, the standard state Gibbs free energy change (ΔG°) at $600^\circ C$ is given in the accompanying column [79].

The reactions shown in the tables become more favorable as the values of ΔG° become more negative. However, in practice, the extent to which these reactions are driven is influenced by the chemical activities of the reactants and products. Chemical activities are strongly influenced by concentration. For example, continuously sweeping the reaction zone with the gaseous fluorination reagent decreases the concentrations of the gaseous reaction products, thereby driving the reaction more toward completion.

Predominance area diagrams for the U-F-O, Np-F-O, and Pu-F-O systems at $600^\circ C$ are shown in Figure 14 to Figure 16, respectively [79]. To simplify the discussion, the contents of the predominance area diagrams are intentionally limited to only the fluoride and oxide species listed in Table 12 to Table 19. A key takeaway from these diagrams is that the formation of PuF_6 requires a significantly higher $F_2(g)$ partial pressure (i.e., fluorine chemical potential) than both NpF_6 and UF_6 . In this simple sense, UF_6 is more stable than NpF_6 , which is more stable than PuF_6 , and it is easier to form UF_6 and NpF_6 than PuF_6 .

Efforts to synthesize and identify hexafluorides of americium (AmF_6) and curium (CmF_6) have not yielded definitive results [80, 81]. Even under very aggressive fluorination conditions, americium and curium do not form volatile hexafluorides like uranium, neptunium, and plutonium. Consequently, americium and curium can only be fluorinated to tetrafluorides.

5.2. Fluidized Bed Reactor Technology

Fluidized bed reactors have been selected for fluorinating oxides in many of the proposed processes for conversion and reprocessing. ANL issued a series of reports for the Engineering Development of Fluid-Bed Fluoride Volatility Process [82, 83, 84, 85, 86, 87, 88, 89, 90, 91, 92, 93, 94] and an accompanying series of reports for the Laboratory Investigations in Support of Fluid-Bed Fluoride Volatility Process [95, 96, 97, 98, 99, 100, 101, 102, 103, 104, 105, 106, 107, 108, 109, 110, 111, 112, 113, 114]. This version of the fluoride volatility process was intended to recover uranium and plutonium from oxide fuels. This body of work from ANL spans between 1963 and 1967. Anastasia summarized some of the ANL work in 1969 [115, 116]. Schmets published a comprehensive review article on fluoride volatility processes in 1970 [117].

Fluidized bed reactors can provide excellent mixing and contact between solids and gases. Fluidized bed reactors can support chemical reactions between solids and gases when the solids are reactive or between gases only when the solids are inert. Fluidization occurs when a gas stream is passed through a bed of solid particles. The particles become suspended in the gas stream and themselves behave as a fluid. The ability to fluidize is a material property of the particles. For successful fluidization, the particles need certain properties that include size distribution, density distribution, surface tackiness, and shape.

A schematic diagram of a fluidized bed reactor is shown in Figure 13. The process gas is introduced at the bottom and flows through a distribution plate. There are different styles of distribution plates; however, all are designed to allow gas to flow upward and prevent particles from flowing downward. Solids are introduced at a point above the distribution plate.^e The fluidized bed is maintained in the lower section of the reactor. As gas passes into the expansion section, the gas velocity decreases causing the solids carrying capacity of the gas to decrease. Coarse particles fall back into the lower section, while only fine particles are carried through the expansion section. A gas/solids separator is located at the top of the reactor that returns solids to the reactor. The gas/solids separator can be a combination of filtration and centrifugation. Solids are discharged from the reactor at a location below the expansion section. Heat is supplied from external heating and/or the enthalpy of the reactions inside the reactor. There are many different designs of fluidized bed reactors, but many designs share these basic features.

e. Feed streams can be dry solids, slurries (mixtures of solids and liquids), liquids, or gases. The solid particles need to remain free flowing. Agglomeration of the particles from tackiness will result in de-fluidization of the bed and plugging of the reactor.

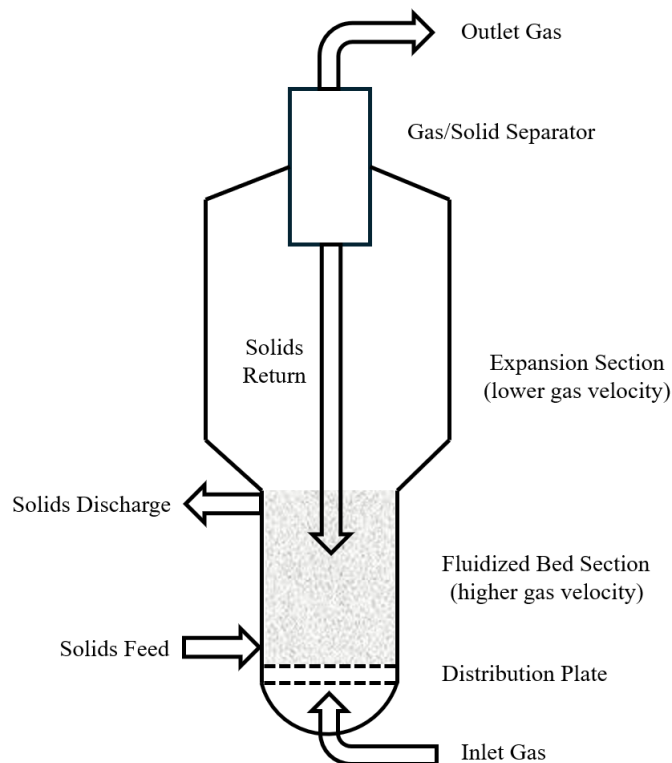


Figure 13. Schematic diagram of a fluidized bed reactor.

In the present application of fluorinating oxide fuels, the fluidized bed in Figure 13 would be maintained with alumina, which enhances mixing and heat distribution. Volatile fluorides exit the reactor with the outlet gas, and non-volatile fluorides and residuals exit the reactor with the solids discharge. Much research has focused on the recovery and purification of volatile hexafluorides of uranium, neptunium, and plutonium. Other fission products and minor actinides are relegated to waste streams.

5.3. Corrosivity of Fluorination Reagents

An obvious technical consideration regarding fluorination-based separations is the pursuit of materials of construction that are chemically compatible with the aggressive fluorination chemistries. In the process of uranium conversion, HF and F₂ are used successfully at industrial scales to make UF₄ and UF₆. During the ORNL MSRE, HF and F₂ were successfully used to make and purify fluoride salts and defuel the salt of U-235 as UF₆ to prepare for refueling with U-233 as UF₄.

According to the data in Table 19, HF(g) is not a very effective fluorination reagent for NpO₂ and PuO₂. Therefore, in the case of nuclear fuel reprocessing, where the separation chemistries rely on selective fluorination of actinide and fission product oxides, fluorination reagents more effective than HF(g) are required. In this respect, the data in Table 12 and Table 13 indicate that KrF₂(g) and O₂F₂(g) are much more aggressive fluorination reagents than HF(g). However, fluorination reagents more aggressive than HF and F₂ will require extremely corrosion resistant materials of construction. Separations schemes that work in theory may in practice be found to be impossible due to corrosion issues. Nickel and nickel alloys are the materials of choice for reactors supporting fluorination chemistries. However, these materials are also subject to different mechanisms of corrosion. For example, the action of the fluidized bed in a fluidized bed reactors has been shown to accelerate the corrosion of the nickel walls of the reactor [88, 108].

As mentioned previously, a potential alternative to HF is fluorination by NF_3 . Compared to hydrogen fluoride, nitrogen fluoride has a relatively lower toxicity, so it is easier to manage from a hazard's standpoint [118]. Additionally, it is non-corrosive, non-reactive at room temperature, and is believed to be a stronger fluorinating agent than HF at high temperatures. However, when working with NF_3 precautions must be taken to prevent adiabatic compression and unplanned thermal decomposition.

Table 12. Fluorination of actinides by the action of $\text{KrF}_2(\text{g})$ and ΔG° (kJ) at 600°C .

$\text{UO}_2 + 2 \text{KrF}_2(\text{g}) = \text{UF}_4 + \text{O}_2(\text{g}) + 2 \text{Kr}(\text{g})$	-1039.525
$\text{NpO}_2 + 2 \text{KrF}_2(\text{g}) = \text{NpF}_4 + \text{O}_2(\text{g}) + 2 \text{Kr}(\text{g})$	-910.969
$\text{PuO}_2 + 2 \text{KrF}_2(\text{g}) = \text{PuF}_4 + \text{O}_2(\text{g}) + 2 \text{Kr}(\text{g})$	-883.191
$\text{UO}_2 + 3 \text{KrF}_2(\text{g}) = \text{UF}_6 + \text{O}_2(\text{g}) + 3 \text{Kr}(\text{g})$	-1418.278
$\text{NpO}_2 + 3 \text{KrF}_2(\text{g}) = \text{NpF}_6 + \text{O}_2(\text{g}) + 3 \text{Kr}(\text{g})$	-1189.042
$\text{PuO}_2 + 3 \text{KrF}_2(\text{g}) = \text{PuF}_6 + \text{O}_2(\text{g}) + 3 \text{Kr}(\text{g})$	-1108.324
$\text{UF}_4 + \text{KrF}_2(\text{g}) = \text{UF}_6 + \text{Kr}(\text{g})$	-387.753
$\text{NpF}_4 + \text{KrF}_2(\text{g}) = \text{NpF}_6 + \text{Kr}(\text{g})$	-278.073
$\text{PuF}_4 + \text{KrF}_2(\text{g}) = \text{PuF}_6 + \text{Kr}(\text{g})$	-99.066

Table 13. Fluorination of actinides by the action of $\text{O}_2\text{F}_2(\text{g})$ and ΔG° (kJ) at 600°C .

$\text{UO}_2 + 2 \text{O}_2\text{F}_2(\text{g}) = \text{UF}_4 + 3 \text{O}_2(\text{g})$	-986.508
$\text{NpO}_2 + 2 \text{O}_2\text{F}_2(\text{g}) = \text{NpF}_4 + 3 \text{O}_2(\text{g})$	-857.952
$\text{PuO}_2 + 2 \text{O}_2\text{F}_2(\text{g}) = \text{PuF}_4 + 3 \text{O}_2(\text{g})$	-956.241
$\text{UO}_2 + 3 \text{O}_2\text{F}_2(\text{g}) = \text{UF}_6 + 4 \text{O}_2(\text{g})$	-1338.753
$\text{NpO}_2 + 3 \text{O}_2\text{F}_2(\text{g}) = \text{NpF}_6 + 4 \text{O}_2(\text{g})$	-1109.517
$\text{PuO}_2 + 3 \text{O}_2\text{F}_2(\text{g}) = \text{PuF}_6 + 4 \text{O}_2(\text{g})$	-1028.799
$\text{UF}_4 + \text{O}_2\text{F}_2(\text{g}) = \text{UF}_6 + \text{O}_2(\text{g})$	-352.244
$\text{NpF}_4 + \text{O}_2\text{F}_2(\text{g}) = \text{NpF}_6 + \text{O}_2(\text{g})$	-251.565
$\text{PuF}_4 + \text{O}_2\text{F}_2(\text{g}) = \text{PuF}_6 + \text{O}_2(\text{g})$	-72.558

Table 14. Fluorination of actinides by the action of F₂(g) and ΔG° (kJ) at 600°C.

UO ₂ + 2 F ₂ (g) = UF ₄ + O ₂ (g)	-723.765
NpO ₂ + 2 F ₂ (g) = NpF ₄ + O ₂ (g)	-595.208
PuO ₂ + 2 F ₂ (g) = PuF ₄ + O ₂ (g)	-693.497
UO ₂ + 3 F ₂ (g) = UF ₆ + O ₂ (g)	-944.637
NpO ₂ + 3 F ₂ (g) = NpF ₆ + O ₂ (g)	-715.401
PuO ₂ + 3 F ₂ (g) = PuF ₆ + O ₂ (g)	-634.683
UF ₄ + F ₂ (g) = UF ₆	-220.873
NpF ₄ + F ₂ (g) = NpF ₆	-120.193
PuF ₄ + F ₂ (g) = PuF ₆	+58.814

Table 15. Fluorination of actinides by the action of NF₃(g) and ΔG° (kJ) at 600°C.

UO ₂ + 1.33 NF ₃ (g) = UF ₄ + O ₂ (g) + 0.67 N ₂ (g)	-710.730
NpO ₂ + 1.33 NF ₃ (g) = NpF ₄ + O ₂ (g) + 0.67 N ₂ (g)	-582.278
PuO ₂ + 1.33 NF ₃ (g) = PuF ₄ + O ₂ (g) + 0.67 N ₂ (g)	-680.616
UO ₂ + 2 NF ₃ (g) = UF ₆ + O ₂ (g) + N ₂ (g)	-924.804
NpO ₂ + 2 NF ₃ (g) = NpF ₆ + O ₂ (g) + N ₂ (g)	-695.568
PuO ₂ + 2 NF ₃ (g) = PuF ₆ + O ₂ (g) + N ₂ (g)	-614.850
UF ₄ + 0.67 NF ₃ (g) = UF ₆ + 0.33 N ₂ (g)	-214.075
NpF ₄ + 0.67 NF ₃ (g) = NpF ₆ + 0.33 N ₂ (g)	-113.395
PuF ₄ + 0.67 NF ₃ (g) = PuF ₆ + 0.33 N ₂ (g)	+65.612

Table 16. Fluorination of actinides by the action of ClF₃(g) and ΔG° (kJ) at 600°C.

UO ₂ + 1.33 ClF ₃ (g) = UF ₄ + 0.67 Cl ₂ (g) + O ₂ (g)	-665.661
NpO ₂ + 1.33 ClF ₃ (g) = NpF ₄ + 0.67 Cl ₂ (g) + O ₂ (g)	-537.340
PuO ₂ + 1.33 ClF ₃ (g) = PuF ₄ + 0.67 Cl ₂ (g) + O ₂ (g)	-635.394
UO ₂ + 2 ClF ₃ (g) = UF ₆ + Cl ₂ (g) + O ₂ (g)	-857.514
NpO ₂ + 2 ClF ₃ (g) = NpF ₆ + Cl ₂ (g) + O ₂ (g)	-628.278
PuO ₂ + 2 ClF ₃ (g) = PuF ₆ + Cl ₂ (g) + O ₂ (g)	-547.560
UF ₄ + 0.67 ClF ₃ (g) = UF ₆ + 0.33 Cl ₂ (g)	-191.619
NpF ₄ + 0.67 ClF ₃ (g) = NpF ₆ + 0.33 Cl ₂ (g)	-90.939
PuF ₄ + 0.67 ClF ₃ (g) = PuF ₆ + 0.33 Cl ₂ (g)	+88.068

Table 17. Fluorination of actinides by the action of BrF₅(g) and ΔG° (kJ) at 600°C.

UO ₂ + 0.8 BrF ₅ (g) = UF ₄ + 0.4 Br ₂ (g) + O ₂ (g)	-581.903
NpO ₂ + 0.8 BrF ₅ (g) = NpF ₄ + 0.4 Br ₂ (g) + O ₂ (g)	-452.533
PuO ₂ + 0.8 BrF ₅ (g) = PuF ₄ + 0.4 Br ₂ (g) + O ₂ (g)	-550.822
UO ₂ + 1.2 BrF ₅ (g) = UF ₆ + 0.6 Br ₂ (g) + O ₂ (g)	-730.624
NpO ₂ + 1.2 BrF ₅ (g) = NpF ₆ + 0.6 Br ₂ (g) + O ₂ (g)	-501.388
PuO ₂ + 1.2 BrF ₅ (g) = PuF ₆ + 0.6 Br ₂ (g) + O ₂ (g)	-420.670
UF ₄ + 0.4 BrF ₅ (g) = UF ₆ + 0.2 Br ₂ (g)	-149.535
NpF ₄ + 0.4 BrF ₅ (g) = NpF ₆ + 0.2 Br ₂ (g)	-48.855
PuF ₄ + 0.4 BrF ₅ (g) = PuF ₆ + 0.2 Br ₂ (g)	+130.152

Table 18. Fluorination of actinides by the action of BrF₃(g) and ΔG° (kJ) at 600°C.

UO ₂ + 1.33 BrF ₃ (g) = UF ₄ + 0.67 Br ₂ (g) + O ₂ (g)	-512.852
NpO ₂ + 1.33 BrF ₃ (g) = NpF ₄ + 0.67 Br ₂ (g) + O ₂ (g)	-384.296
PuO ₂ + 1.33 BrF ₃ (g) = PuF ₄ + 0.67 Br ₂ (g) + O ₂ (g)	-482.585
UO ₂ + 2 BrF ₃ (g) = UF ₆ + Br ₂ (g) + O ₂ (g)	-628.313
NpO ₂ + 2 BrF ₃ (g) = NpF ₆ + Br ₂ (g) + O ₂ (g)	-399.077
PuO ₂ + 2 BrF ₃ (g) = PuF ₆ + Br ₂ (g) + O ₂ (g)	-318.359
UF ₄ + 0.67 BrF ₃ (g) = UF ₆ + 0.33 Br ₂ (g)	-115.316
NpF ₄ + 0.67 BrF ₃ (g) = NpF ₆ + 0.33 Br ₂ (g)	-14.736
PuF ₄ + 0.67 BrF ₃ (g) = PuF ₆ + 0.33 Br ₂ (g)	+164.122

Table 19. Fluorination of actinides by the action of HF(g) and ΔG° (kJ) at 600°C.

UO ₂ + 4 HF(g) = UF ₄ + 2 H ₂ O(g)	-8.247
NpO ₂ + 4 HF(g) = NpF ₄ + 2 H ₂ O(g)	+120.309
PuO ₂ + 4 HF(g) = PuF ₄ + 2 H ₂ O(g)	+22.020
UO ₂ + 6 HF(g) = UF ₆ + 2 H ₂ O(g) + H ₂ (g)	+328.188
NpO ₂ + 6 HF(g) = NpF ₆ + 2 H ₂ O(g) + H ₂ (g)	+557.424
PuO ₂ + 6 HF(g) = PuF ₆ + 2 H ₂ O(g) + H ₂ (g)	+638.142
UF ₄ + 2 HF(g) = UF ₆ + H ₂ (g)	+336.435
NpF ₄ + 2 HF(g) = NpF ₆ + H ₂ (g)	+437.115
PuF ₄ + 2 HF(g) = PuF ₆ + H ₂ (g)	+616.122

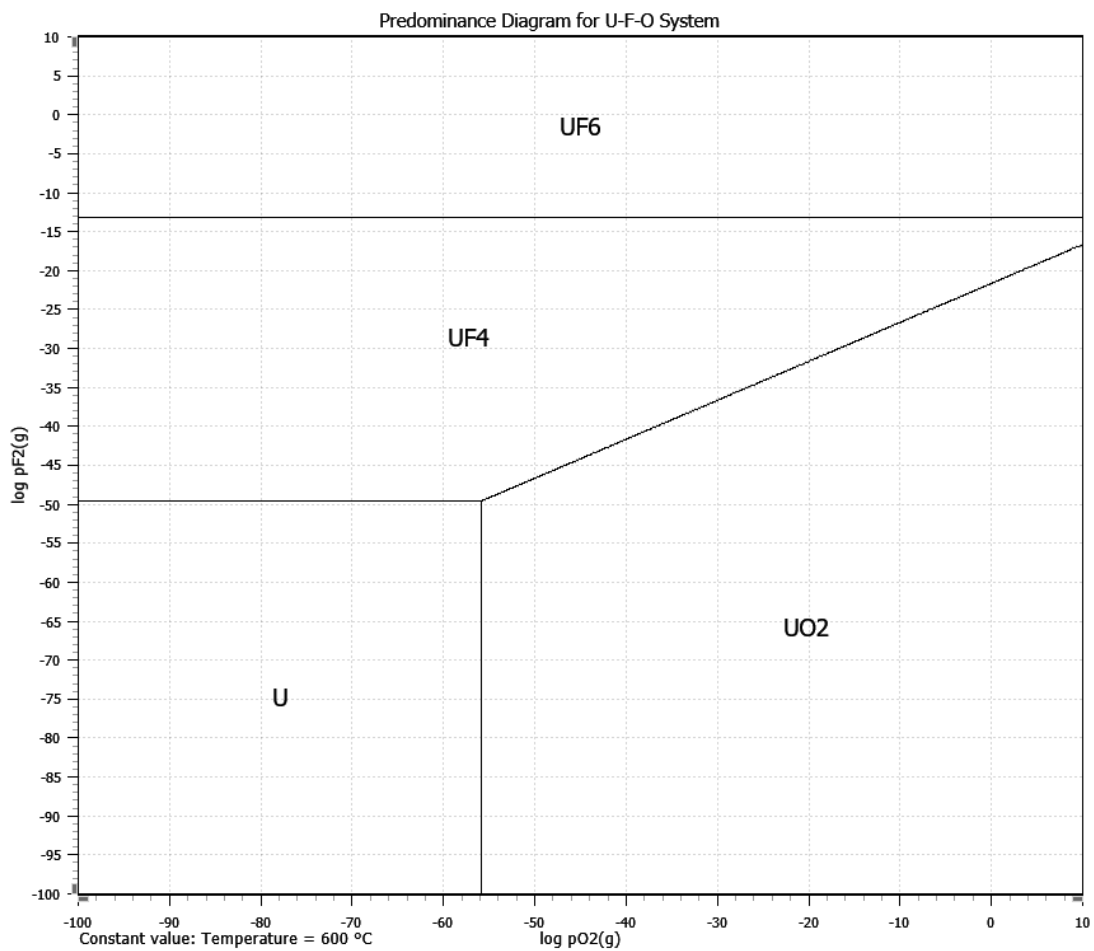


Figure 14. Predominance area diagram of the U-F-O system at 600°C.

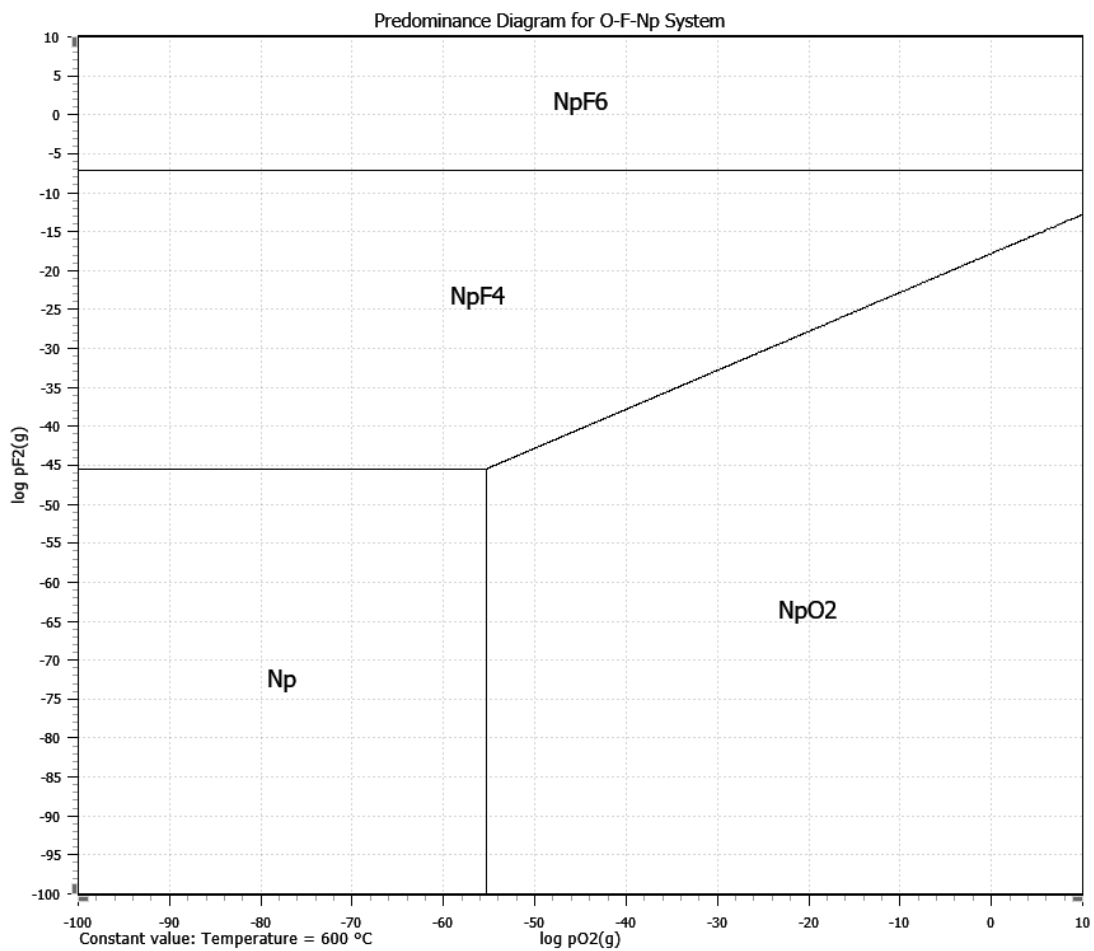


Figure 15. Predominance area diagram of the Np-F-O system at 600°C.

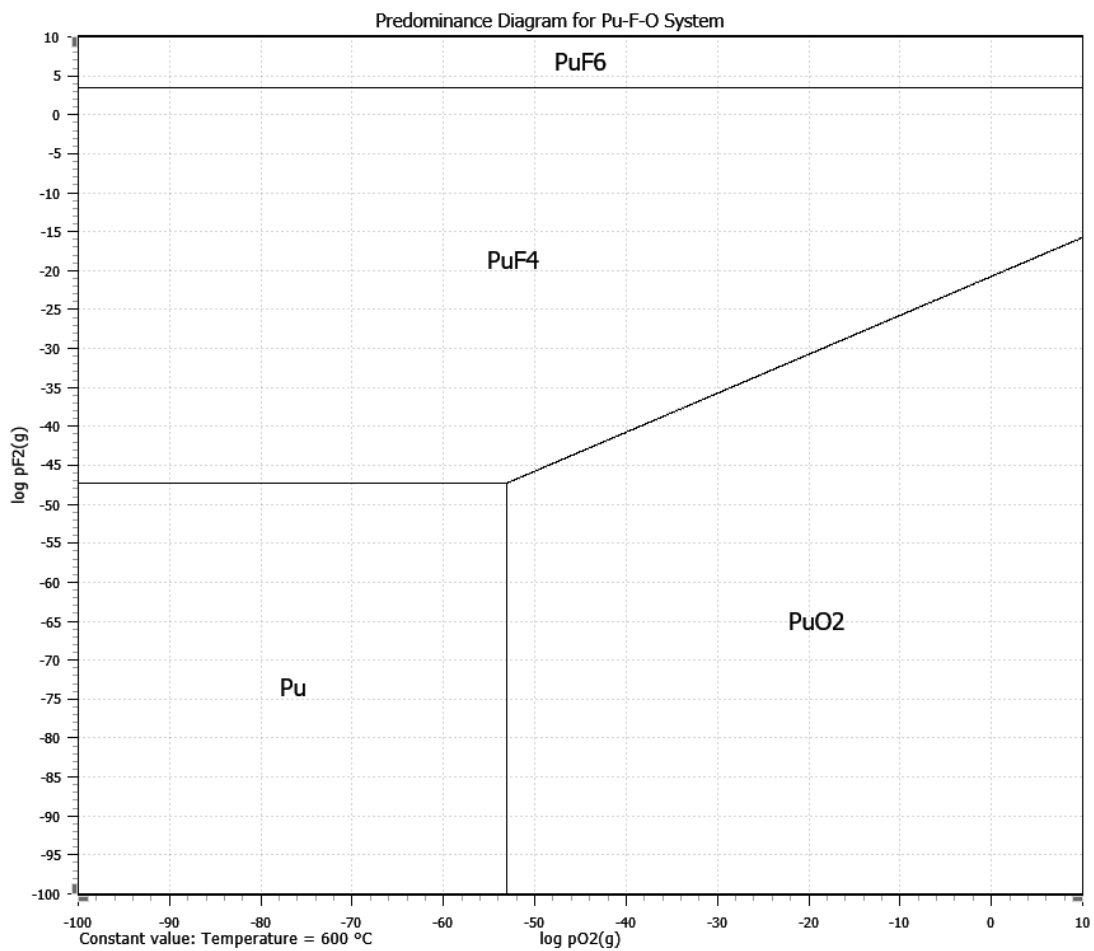


Figure 16. Predominance area diagram of the Pu-F-O system at 600°C.

6. SALT WASTE MANAGEMENT

During pyrochemical reprocessing, both the oxide reduction (OR) and electrorefiner (ER) processes generate waste in the forms of radioactive salts, cladding hulls, residual fuel, and fission product gases. As batches of used fuel are processed through these molten salt unit operations, fission products continue to accumulate in the salts until eventually the salts must be dealt with as waste. Generally, in the OR salt, fission product chlorides that are more stable than lithium chloride (LiCl) can displace the lithium chloride and accumulate in the salt. These fission products include alkali metals such as cesium, and alkali earth metals such as strontium, and barium. In the ER salt, fission product chlorides that are more stable than uranium trichloride (UCl₃) can displace the uranium trichloride and accumulate in the salt. These fission products include alkali, alkali earth, lanthanides, and transuranics.

Salts may reach the end of their service life due to, among other reasons, changes in thermophysical properties, decay heat loading, or excess salt generation. Similarly, cladding hulls, residual fuel, and fission product gases must be contained and disposed of. Engineered waste forms immobilize radioisotopes for safe transportation and disposal in geological repositories. Ultimately, from a repository and storage point of view, the overall objective of a waste form is to safely immobilize radioisotopes, in an efficient and economical way, to inhibit their migration into the environment and minimize their potential biological impact.

6.1. Waste Form Properties

In the case of salt disposal, the constituents of a waste form may include halides of alkali, alkaline earth, lanthanide, and actinide metals. Waste loading levels must be monitored to ensure that they do not present the possibility of nuclear criticality within a single waste form or between multiple waste forms during transportation or storage. Physical durability refers to the ability of the waste form to endure transport, long-term storage, and radiolysis while remaining mechanically intact and without producing excess fines. Chemical durability is assessed via its resistance to leaching when exposed to groundwater. Thermal durability refers to the ability to endure elevated temperatures due to decay heat without breaking down and dissipate that heat through having high thermal conductivity. There are several parameters and factors that affect the resulting properties of a waste form, including the amount of fission product loading, the matrix composition, treatment temperatures, process gas compositions and flow rates, pressures, durations, and cooling rates [119]. It is important that quality control is maintained between production batches to achieve consistency leading to waste forms with reliable performance.

The desired properties of a waste form largely depend on its ultimate disposition and disposal path. Without understanding the conditions under which the waste form will be stored or disposed of, it is challenging to tailor the waste form to the storage environment. Repositories and storage sites can have a wide variety of geological and spatial conditions that influence the desired properties of a waste form including the type of waste form desired (e.g., salt, ceramic, metal alloy), the physical and chemical durability of the waste, and the maximum heat loading. While standards such as “Savannah River EA-Glass” and the proposed requirements for the Yucca Mountain repository [120] are currently used as a general baseline and guide, new storage requirements could require further research and adjustments to the waste form designs to ensure compliance.

In terms of salt waste generation, the primary difference between the OR and ER processes are the compositions of the base salt. The OR base salt is lithium chloride (LiCl) with a nominal 1 wt% concentration of lithium oxide (Li₂O), and the ER base salt is lithium chloride-potassium chloride (LiCl-KCl) eutectic with a nominal 5 wt% concentration of uranium trichloride (UCl₃). The OR salt only accumulates fission products that are more electropositive than lithium. All other fission products (including actinides) will not be present in OR salt waste. By contrast, ER salt accumulates all fission products that are more electropositive than uranium, resulting in a wider spectrum of fission products present in ER salt waste. The OR salt can accumulate certain alkali and alkaline earth fission products,

while the ER salt can accumulate alkali, alkaline earth, lanthanide, and actinide fission products. Transition metal fission products do not accumulate in the salts because these metals are not oxidized to halides. There are several ceramic and glass waste form options in development for both OR and ER salts. The most notable and well-developed is the ceramic waste form (CWF), which can be applied to both OR and ER salts with a salt loading in the CWF of approximately 10 to 14 wt%.

6.2. Salt Partitioning Strategies

As described above, certain fission products accumulate in the OR and ER salts. To reduce the quantity of salt that must be disposed of as high-level waste, several partitioning strategies have been developed to concentrate the fission products into smaller volumes of salt waste. These strategies include fractional distillation, melt crystallization, and reactive precipitation [121].

Fractional distillation exploits difference in the vapor pressures of salt species to affect partitioning. The distillation furnace provides a high-temperature zone and a low-temperature zone. The contaminated process salt is held in the high-temperature zone, and salt vapors condense in the low-temperature zone. The salt distillate is purified relative to the salt bottoms. This has been done with both OR and ER salt wastes, including OR and ER salt wastes that have been dechlorinated by a phosphate-based process [121, 122].

Melt crystallization (a.k.a., zone refining) exploits the chemical phase behavior of the salt system to affect partitioning. Partitioning results from the liquidus/solidus phase behaviors of the salt as a solidification front is slowly advanced through molten salt. The fission product impurities are partitioned to, and concentrated in, the decreasing volume of liquid salt as the volume of solid salt increases. The solidified salt is purified relative to the liquid salt. A limit is reached at which point the remaining liquid salt is rejected as waste salt [121, 123]. This occurs when the liquid phase can no longer support partitioning, usually because the solubility limit of impurities in the liquid phase is reached, meaning that the liquidus temperature of the liquid phase is reached.

For example, one method involves inserting an argon-cooled steel plate into molten salt to allow the salt to solidify on the plate. The solidified salt produced in this manner is purified relative to the molten salt that remains. A limit is reached at which point the steel plate is removed from the liquid salt, bringing with it the purified solid salt. Melt crystallization techniques have achieved separation efficiencies up to approximately 90% [121]. The purified solid salt can be recycled back to the OR or ER, while the remaining liquid salt is processed further or becomes waste. This process has been demonstrated on OR salt containing radioactive fission products in the Idaho National Laboratory (INL) Hot Fuel Examination Facility (HFEF) hot cell as shown in Figure 17 and on non-radiological surrogate ER salt outside of a hot cell as shown in Figure 18. In these two photographs, the heat shields are approximately 100 mm in diameter.

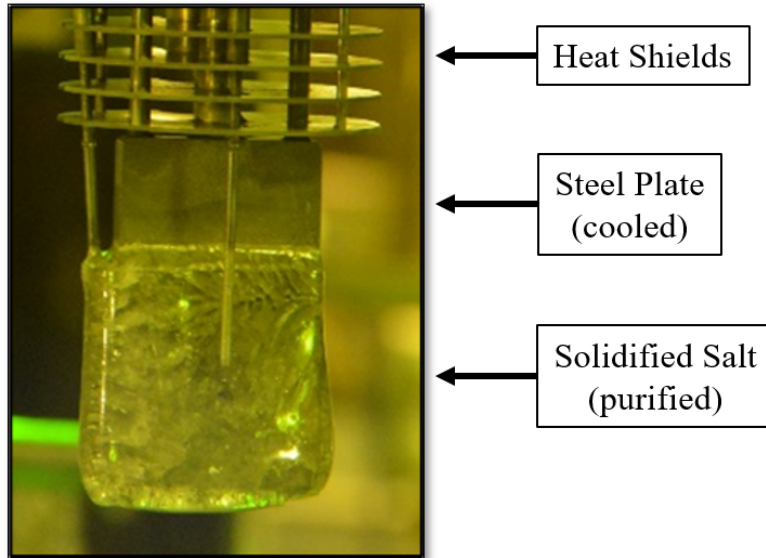


Figure 17. Photographs of purified (solidified LiCl) OR salt on a chilled steel plate. The salt is transparent and colorless.

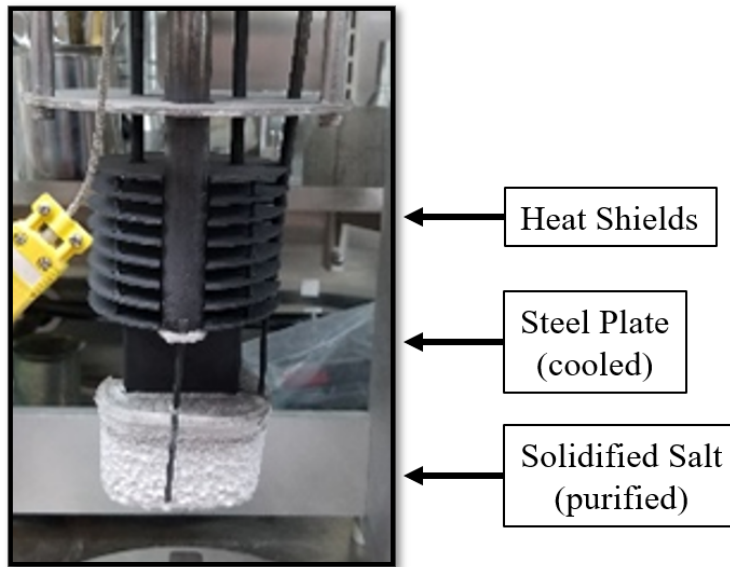


Figure 18. Photographs of purified (solidified LiCl-KCl) ER salt on a chilled steel plate. The salt is opaque and white.

Reactive precipitation exploits chemical reactions between the salt, and chemical additions made to the salt, to affect partitioning. The chemical additions to the salt convert the fission product halides in the salt into solids that precipitate from the salt. This process effectively purifies the salt. Examples include the additions of carbonate salts, phosphate salts, and metal hydroxides. Sparging with oxygen gas can be used to form oxides and oxyhalides that will precipitate from the salt. Filtration, decanting, and distillation can be used to separate the purified molten salt from the solid precipitates [121].

6.3. Ceramic Waste Form Development

Successful salt waste forms cannot be produced by directly incorporating halides into borosilicate glasses. This is due to both the low solubility of halide salts in the glasses and the high melting

temperature of the glasses, which causes salt to be lost due to vaporization during processing [121]. There are three approaches to overcome this challenge, as follows:

- Make a glass-bonded CWF
- Make a glass-bonded waste form using glass that has a low-melting temperature and high capacity for halide loading
- Make a halide-free waste form by entirely removing the halides from the salt via a dehalogenation process.

The most established method to dispose of halide salt waste is to occlude the salt into a glass-bonded CWF. In this waste form, the halides are incorporated into the ceramic grain structure, while most other components are immobilized in the intergranular glassy phase. Of the glass-bonded CWF technologies in development, glass-bonded sodalite is the most studied.

The original glass-bonded sodalite CWF process for ER salts was developed in the 1990s at ANL and INL [124]. A general schematic of the initial process is shown in Figure 19. This process involved occluding ER salt containing fission products into zeolite, encapsulating the zeolite in a glassy matrix, and thermally converting the zeolite into sodalite. The zeolite was ground and sized to 100% passing a 350- μm sieve and dried under vacuum at 500°C. Likewise, the ER salt was ground and sized to a similar sieve size. The zeolite and salt powders were then mixed in a V-mixer furnace at 500°C to allow the salt to adsorb into the zeolite structure while remaining a powder [125]. The salt-occluded zeolite (SOZ) was then combined with a borosilicate glass powder that acted as a binder for the final waste form. The mixture of SOZ and glass was loaded into a high-temperature furnace for sintering at 925°C [125]. During this high-temperature processing, the zeolite converts to sodalite. The result was a glass-bonded sodalite CWF that was loaded into a steel container that was sealed by welding. This process was demonstrated in the HFEEF hot cell using ER salt from EBR-II spent fuel treatment [126].

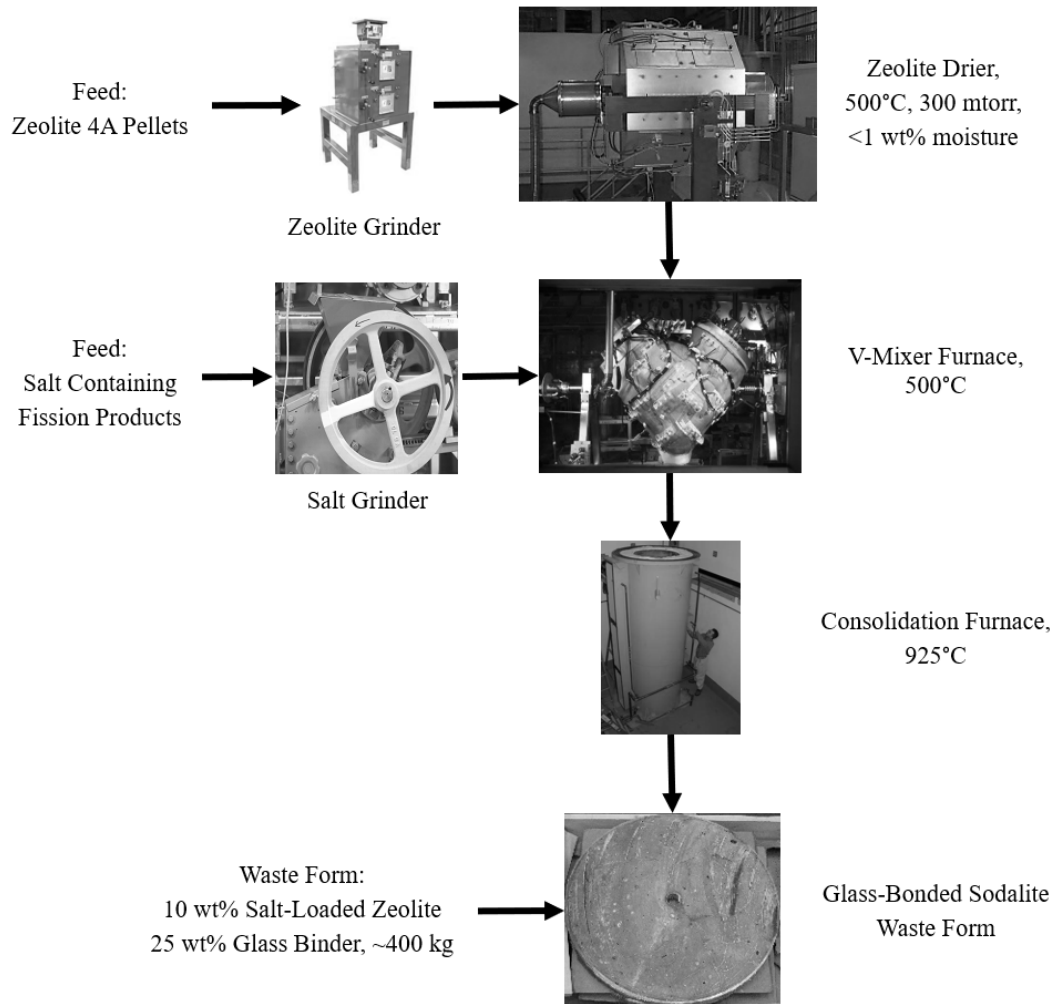


Figure 19. Schematic flowsheet of ceramic waste form processing.

To increase the loading, physical durability, and long-term chemical durability of the original CWF process, different glass binders have been evaluated as a replacement for borosilicate glass. Among the most promising is a mixture of sodium oxide, boron oxide, and silicon dioxide ($\text{Na}_2\text{O}-\text{B}_2\text{O}_3-\text{SiO}_2$) with an approximate concentration of 20 wt% Na_2O , designated “NBS-4 Glass,” although other concentrations have been tested [127]. Glass-bonded sodalite waste forms made with this binder are sometimes referred to as advanced ceramic waste forms (ACWF). An example of an ACWF is shown in Figure 20. The ACWF improves upon the original CWF by increasing the salt loading (from 10 to 14 wt%), the sodalite yield, the physical durability, and the corrosion resistance [127]. Efforts are underway to simplify processing of the ACWF to increase efficiency and viability of manufacture in a hot cell facility.

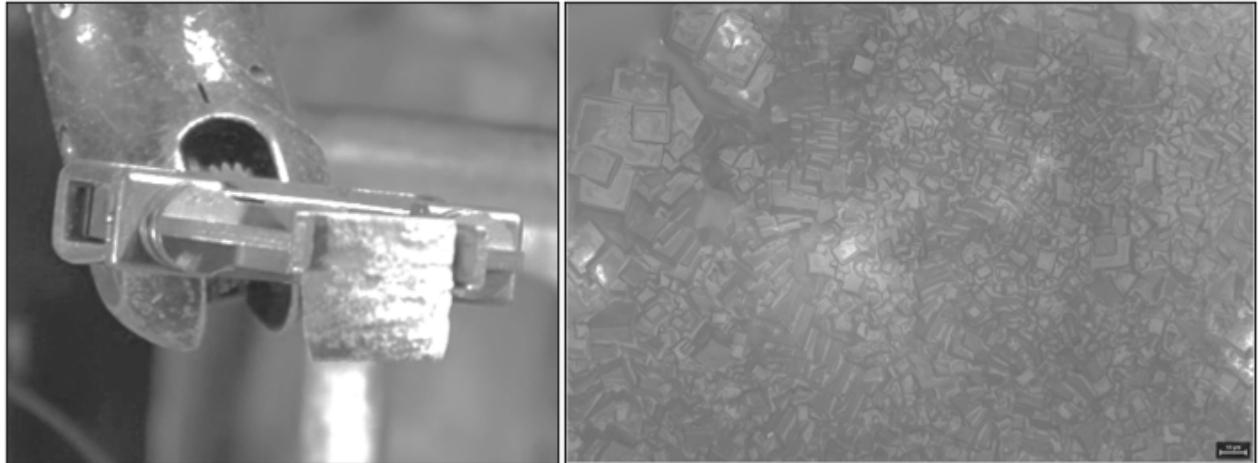


Figure 20. Photographs of an ACWF containing radioactive fission products (left) and an optical image of the microstructure (right). The photomicrograph is approximately 250 μm wide.

Researchers have identified a list of 12 performance criteria for ideal glass binders in a glass-bonded sodalite CWF [125, 127]. These criteria are as follows:

1. Glass softening temperature is less than 750°C so it can be processed in the ideal temperature range of $750\text{--}925^{\circ}\text{C}$.
2. Glass has a broad working temperature range so as not to drain through the zeolite/sodalite during heat treatment.
3. Glass wets the SOZ and the sodalite mixture.
4. Glass has a coefficient of thermal expansion compatible with SOZ and sodalite mixtures to minimize cracking during cooldown.
5. Glass as a powder must be free flowing.
6. Glass waste form achieves 40–45% of the theoretical density.
7. Glass undergoes uniform densification during the thermal cycle.
8. Glass waste form has a non-friable surface.
9. Glass composition provides additional Na_2O for incorporation into the sodalite structure, which helps immobilize long-lived halogen radionuclides such as I-129 and Cl-36.
10. Glass composition incorporates alkali, alkaline earth, transition metal, lanthanide fission products, and actinides.
11. Glass waste form is chemically durable upon ion exchange with the SOZ.
12. Glass waste form is volumetrically efficient as not to create excessive waste volume.

In addition to the traditional CWF process described above, researchers have studied hydrothermal, low-temperature solution-based, and sol-gel processing methods to make sodalite-based waste forms [128]. Titanate and zirconate ceramic waste forms have been studied for disposal of LWR spent fuels [129].

6.4. Tellurite Glass Waste Forms

Tellurite glasses are being considered for salt waste forms due to their greater capacity for halide loadings and their lower processing temperatures compared to borosilicate glasses [121]. Tellurite glasses are primarily composed of tellurium oxide (TeO_2) but may include other network modifying, vitrifying

agents, or binding agents such as aluminum oxide (Al_2O_3), boron oxide (B_2O_3), sodium oxide (Na_2O), calcium oxide (CaO), and lead oxide (PbO) [121, 130]. Tellurite glasses differ from borosilicate glasses in that they can accommodate halide loadings that are an order of magnitude higher than borosilicate glasses, have much lower melting points and glass transition temperatures, and exhibit higher bulk densities. Two tellurite glass waste forms of note are lead-tellurite glass ($\text{TeO}_2\text{-PbO}$) and alumina-tellurite glass ($\text{TeO}_2\text{-Al}_2\text{O}_3$). However, lead-tellurite glass has been shown to allow considerable leaching when exposed to groundwater, so it is a poor option for long-term storage and immobilization of fission products [121]. Alumina-tellurite glass has shown great success in immobilizing long-lived components, such as technetium-99 [130].

6.5. Dehalogenated Salt Waste Forms

Another approach to the challenge of immobilizing radionuclides in salt is to remove the halides through a dehalogenation process. The processing for this type of waste form is more complex but results in an overall lower waste volume for long-term storage, as the chloride or fluoride component is removed and potentially recycled.^f Dehalogenation can also produce acidic off-gases such as hydrogen fluoride (HF) and hydrogen chloride (HCl). The chemical form of the dehalogenated metal halide may be metal oxide. Metal oxides are generally less water-soluble than their halide counterparts. For example, lanthanide oxides are much less water-soluble than lanthanide chlorides. Some disadvantages of the dehalogenation processes include driving off some of the semi-volatile fission products such as iodine, which were previously trapped in the salt.

Several waste forms have been developed to dispose of dehalogenated salt, including iron phosphate glass, silica-alumina-phosphate (SAP), ultra-stable H-Y zeolite, lanthanide borosilicate (LaBS), lanthanide alumina borosilicate glass, and zinc-in-titania. Iron phosphate glass is made by reacting chloride salts with phosphate precursors such as phosphoric acid (H_3PO_4), ammonium phosphate ($\text{NH}_4\text{H}_2\text{PO}_4$), or ammonium biphosphate ($(\text{NH}_4)_2\text{HPO}_4$) at moderate temperatures ($\leq 600^\circ\text{C}$) to dehalogenate the salts [121]. The halogens leave as volatile byproducts such as ammonium chloride (NH_4Cl), hydrogen chloride (HCl), ammonium iodide (NH_4I), hydrogen iodide (HI), iodine (I_2), and water (H_2O) and are captured in a scrubber trap. The alkali metals and fission products react to form oxides and a glass compound with phosphorous pentoxide (P_2O_5) [121, 131]. Iron oxide (Fe_2O_3) is added to the mix at a ratio of approximately 2:3 ($\text{Fe}_2\text{O}_3\text{:P}_2\text{O}_5$) to enhance the chemical durability of the glass. The iron phosphate glass is an amorphous flowable liquid at high temperatures ($\geq 600^\circ\text{C}$). It is vitrified at its glass transition temperature into an amorphous solid, resulting in a stable and durable waste form. Cooling rates are controlled to prevent devitrification. An schematic overview of the fabrication process for iron phosphate glass waste forms is shown in Figure 21 [131]. This waste form has been demonstrated in the Fuel Conditioning Facility (FCF) at INL using used ER salt from EBR-II fuel processing. A photograph of a waste form made in the FCF hot cell is shown in Figure 22.

Possible advantages of the iron phosphate glass waste form are that it may reduce the loss of chlorine-37 to salt waste^g, it has high waste loading, it can be used for both chloride and fluoride salts, and the halide off-gas streams may be recycled to re-halogenate actinide metals that are needed for the application [119]. The disadvantages are that phosphate glasses chemically attack the refractory materials used in melting furnaces, their low viscosity makes vitrification challenging, and the chemical durability is more sensitive to changes in composition than in borosilicate glasses [119].

-
- f. What to do with the halides liberated from salt during dehalogenation is an open-ended question. If the application is pyrochemical reprocessing, the chlorine could be used to make UCl_3 oxidant that is consumed during uranium electrorefining. If the application is molten salt reactor fuel reprocessing, then the chlorine or fluorine could be used to make actinide chlorides or fluorides, respectively, for use in the reactor fuel salt. If there are no uses for the liberated halides, then these materials are themselves wastes.
- g. In the application of chloride molten salt reactors, there may be benefits to using chlorine enriched with respect to Cl-37 to minimize the formation of Cl-36 by the activation of Cl-35. In this case, Cl-37 enriched salts may have an intrinsic economic value. This is not unlike Li-7-enriched salts used in fluoride molten salt reactors.

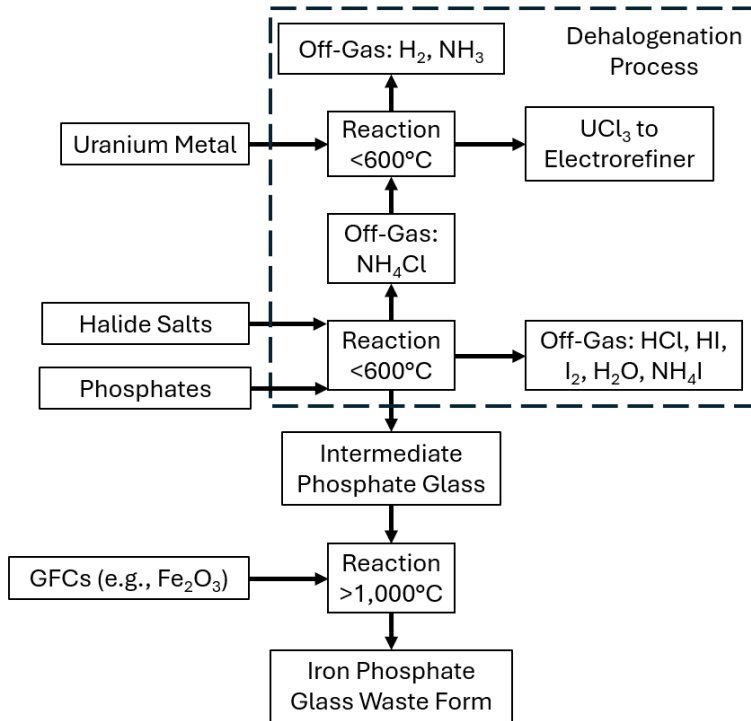


Figure 21. Schematic showing the process flow for fabricating an iron phosphate waste form.

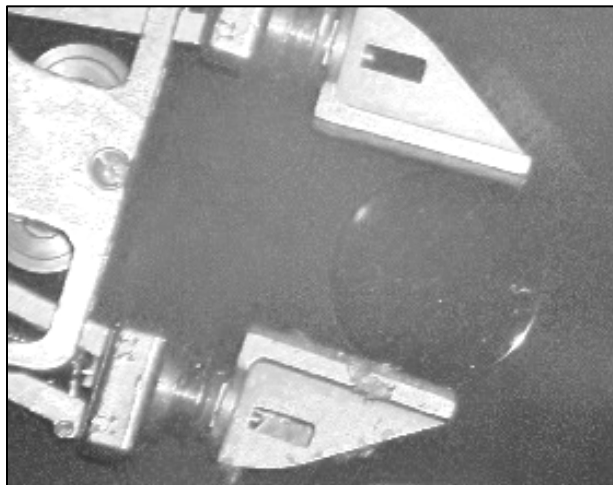


Figure 22. Photograph of iron phosphate glass waste form containing used ER salt.

SAP glass waste forms are similar to iron phosphate glasses in both their production and performance. SAP glass is formed by reacting pyrochemical reprocessing salt with a $\text{SiO}_2\text{-Al}_2\text{O}_3\text{-P}_2\text{O}_5$ stabilizer and then mixing in additional glass binders [121]. The resulting waste form has good corrosion resistance. Photographs of examples of SAP waste forms fabricated in the HFEF hot cell are shown in Figure 23.

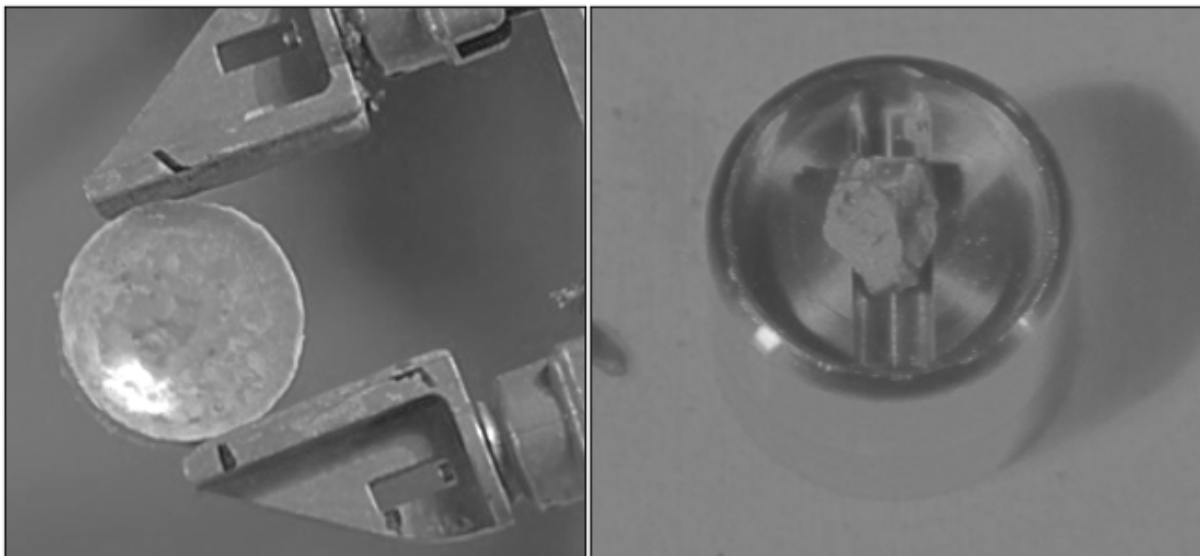


Figure 23. Photographs of SAP waste form containing pyrochemical reprocessing salt (left) and in the process of being mounted for imaging (right).

Ultra-stable H-Y zeolite waste forms are produced by reacting halide salts directly with dried, H-Y zeolite [121]. The halide ions react with hydrogen ions in the H-Y zeolite, forming hydrogen chloride (HCl) and HI, which leave the waste form as gases and can be captured using inline scrubber traps. The cations within the salt (including the fission products) are incorporated into the zeolite structure. The zeolite can then be consolidated using a low-temperature ($< 600^{\circ}\text{C}$) glass binder followed by cold pressing and heat treatment to form a monolith. Work has been done to optimize factors that affect this dehalogenation process, including stirring, argon purging, and temperature, resulting in reported dechlorination efficiencies of 95 to 99% [121].

LaBS glass, lanthanide alumina borosilicate glass, and ZIT waste forms require halide salts to first be dehalogenated. For example, alkali metal bicarbonate will react with lanthanide fission products to produce oxides that precipitate from the salt solution and can be separated by salt distillation leaving behind the oxides. Lanthanide glasses have extremely high loadings (up to 60% by mass) for lanthanide and actinide oxides [121]. They also have high liquidus temperatures, high glass transition temperatures, moderate bulk densities, and good chemical durability. A photograph of an example of a LaBS glass is shown in Figure 24. Zinc-in-titania can immobilize lanthanide oxides with 20 wt% loading with very low leach rates and up to 40 wt% loading with reduced chemical durability [121].



Figure 24. Photograph of LaBS glass containing 60 wt% surrogate ER fission products added as oxides.

6.6. Metal Waste Forms

Metal waste forms are designed to dispose of the transition metal fission products that are not oxidized into ER salt (i.e., anode residue). The transition metal fission products include zirconium (Zr), molybdenum (Mo), ruthenium (Ru), rhodium (Rh), technetium (Tc), palladium (Pd), tellurium (Te), iron (Fe), silver (Ag), and niobium (Nb) [132]. In addition to the anode residue, the metal waste form also accommodates fuel cladding and retired fuel assembly hardware. Figure 25 shows a photograph of a production-scale metal waste form produced in the HFEF hot cell as part of EBR-II spent fuel treatment [133]. The ingot is approximately 40 cm in diameter.



Figure 25. Photograph of ingot from the first production-scale metal waste form.

Spent fuel from an SFR will have stainless steel cladding, stainless steel assembly hardware, and metallic fuel alloy. Spent fuel from an LWR will have zirconium-alloy cladding, stainless steel assembly hardware, and uranium oxide fuel. Metal waste forms for an SFR application will be an SS-15 wt% Zr alloy, and metal waste forms for an LWR application will be an SS-8 wt% Zr alloy [132]. These waste forms have great physical and chemical durability and are easily produced by melting the metal components together. In addition to these established metal waste forms, cermet alloys that are specific to different waste streams are also being evaluated [134]. A disposal option for LWR metal waste incorporates zirconium-alloy cladding hulls, stainless steel assembly hardware, residual fuel (oxide and metal), and chromium (Cr) and molybdenum (Mo) trim metals to produce a durable zirconium-chromium-molybdenum (Zr-Cr-Mo) cermet alloy. Photographs of this waste form are shown in Figure 26. A disposal option for SFR metal waste incorporates stainless steel cladding hulls, stainless

steel assembly hardware, residual fuel (metal), and Cr and Mo trim pieces to produce a durable Cr-Mo cermet alloy. Photographs of this waste form are shown in Figure 27. The ingot is approximately 20 cm in diameter.

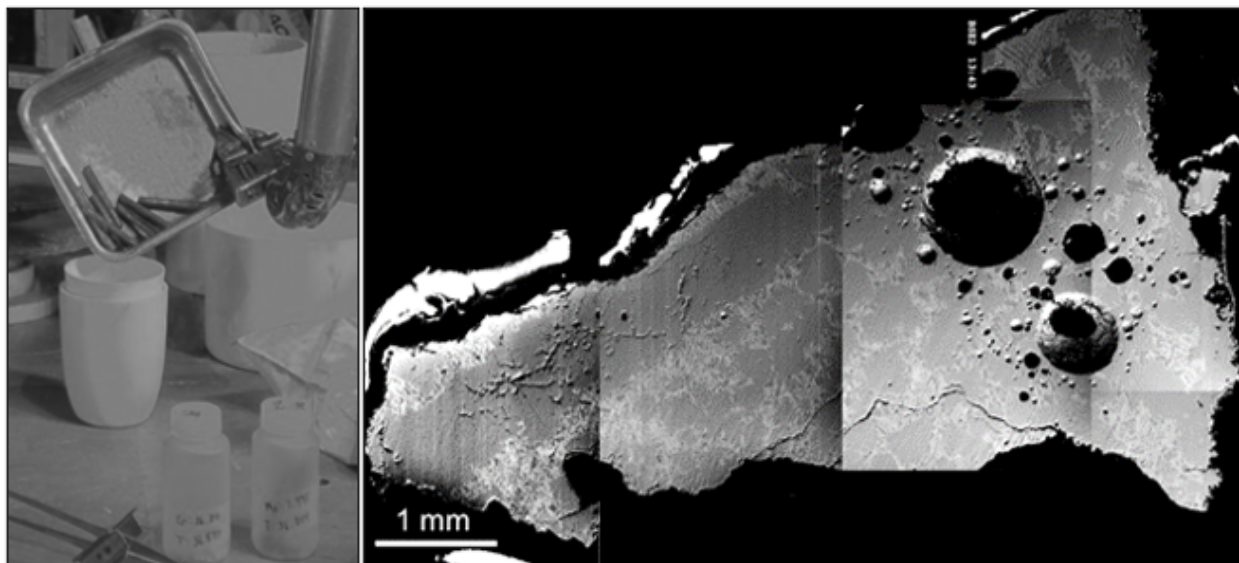


Figure 26. Photographs of zirconium-alloy cladding waste containing spent fuel residuals (left) and the resulting cermet waste form (right).

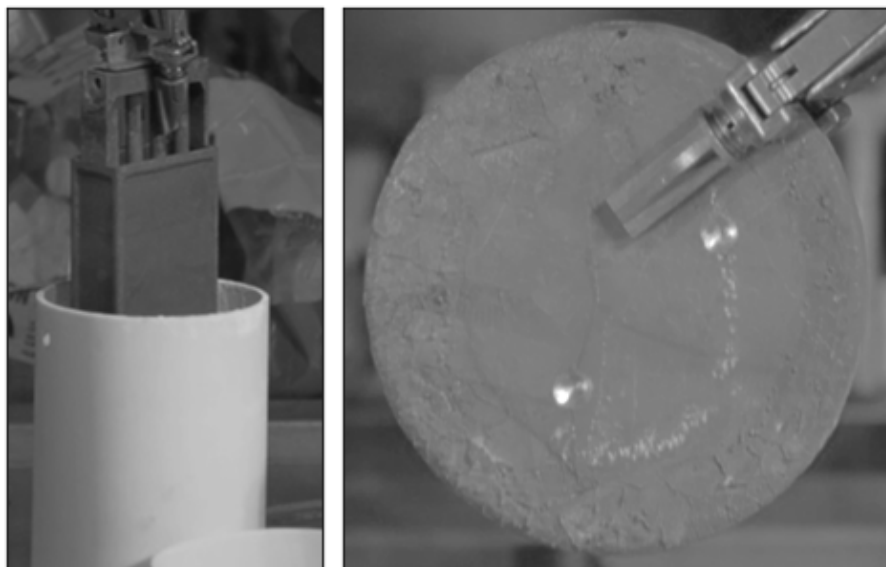


Figure 27. Photographs of used stainless steel hardware containing spent fuel residual (left) and the resulting cermet waste form (right).

6.7. Captured Volatile Fission Product Waste

During pyrochemical reprocessing, volatile fission products are released into the off-gas streams that must be captured and properly managed. Volatile fission products that need to be considered include tritium (H-3), ruthenium (Ru-106), krypton (Kr-85), and iodine (I-129). Most of the published research in this area has focused on the capture and sequestration of iodine or krypton generated during aqueous reprocessing. However, volatile fission product waste form technologies developed for aqueous

reprocessing can be applied to pyrochemical reprocessing. Similarly, although research to date has primarily focused on the disposition of iodine and krypton, the same general principles of capture and sequester may be applied to other volatile and semi-volatile fission product streams although the chemistry will be different.

Ideal waste forms for volatile fission products will be tailored to the capture technologies used to avoid excessive processing steps. The currently explored capture technologies for volatile fission products may be organized into the following categories: sorption, cryogenic distillation, and wet scrubbing. Because volatile radioisotopes are more difficult to retain within waste forms than their companion non-volatile radioisotopes, such waste forms are designed with the goal of maintaining safe release rates to the environment rather than retaining them for the entirety of their decay [135, 136].

Proposed waste forms for the disposal of iodine may be organized into the following three categories: consolidated sorbents, inorganic minerals and ceramics, and iodine-bearing salt waste forms. Since iodine is readily ionized to form iodide, waste forms for iodide are most often focused on disposing of it either in the form of iodide ions directly incorporated into a sorbent or as iodide or iodate salts, most commonly silver iodide (AgI). Because the large porosity of sorbents makes long-term retention of iodine difficult, sorbents do not perform well as waste forms unless they are first consolidated. Consolidation methods for iodine include hot pressing, sintering, vitrification, and cementation [129,137]. Inorganic mineral and ceramic iodine waste forms aim to convert iodine into forms that resemble naturally occurring and stable iodine-containing minerals. Examples of iodine-bearing minerals include silver iodide (AgI), lead iodide (PbI₂), copper iodide (CuI), mercury iodide (HgI₂), copper iodate (Cu(IO₃)₂), calcium iodate (Ca(IO₃)₂), and barium iodate (Ba(IO₃)₂). Ceramic media used to capture iodine include titanate, sodalite, cancrinite, perovskite, silver zeolite, calcium phosphate-apatite, lead vanadate-apatite, bismuth oxides, boracite, silver nitrate (AgNO₃)-impregnated alumina (Al₂O₃), silver nitrate (AgNO₃)-impregnated silica (SiO₂), and silicon carbide (SiC) [129, 131]. Iodine-bearing salt waste forms are based on the same principles as the other salt waste forms described above but are made to incorporate iodide and iodate salts rather than chloride salts. Examples of these waste forms include glasses, glass-bonded ceramics, glass composite materials, ceramic composites, and cement [129, 131].

Since krypton is a noble gas and cannot be converted to a salt form, waste form technologies for krypton take a different approach than for iodine. Proposed waste forms for krypton include the following [130]:

- Direct storage in compressed gas cylinders
- Immobilization in a solid sorbent or MOF followed by disposition in a canister
- Immobilization in a metal via vapor co-deposition (also referred to as ion implantation) followed by disposition in a canister.

If a solid sorbent is used to capture and dispose of krypton, it may optionally be consolidated further before disposal using the same techniques described above for iodine.

6.8. Sodium-Bonded Metal Fuel

SFR metallic fuels are clad in stainless steel and contain bond-sodium. Fuel alloys include binary alloys of uranium and zirconium and ternary alloys of uranium, plutonium, and zirconium. The purpose of the bond-sodium is to enhance the thermal conductivity between the fuel and the cladding. The bond-sodium is known to collect significant quantities of fission products such as cesium and iodine, among others [138]. Management of bond-sodium adds complexity to pyroprocessing operations.

Two options for managing bond-sodium are: 1) diverting some of the sodium away from the electrorefiner, and 2) processing all the sodium in the electrorefiner. The former is achieved by distilling a portion of the sodium out of the chopped fuel prior to electrorefining. A challenge associated with sodium distillation is that it produces a highly reactive metal waste form containing radioactive fission products. Additionally, processing all the sodium in the electrorefiner leads to a significant increase in the amount of salt waste.

7. REPROCESSING OF OTHER SPENT FUEL TYPES

Pyrochemical reprocessing technologies are still being investigated for TRISO fuels and aluminum-clad research reactor fuels. TRISO fuels are under development as highly refractory materials designed for high-temperature reactor environments. The fuel compositions are typically oxide or cermet. Reprocessing these fuels is of interest for the development of future fuel cycle applications. Aluminum-clad research reactor fuels exist in large quantities and come in a variety of designs and fuel alloy types including metallic, oxide, hydride, and cermet. Reprocessing these fuels is of interest as a source of high-assay low-enriched uranium (HALEU) for the near-term deployment of commercial demonstration reactors.

7.1. TRISO Fuel

TRISO fuel is an advanced type of nuclear fuel in which fissile material is coated by layers of pyrolytic carbon (PyC) and SiC. Figure 28 shows a magnified view of a typical TRISO fuel particle. These particles are approximately 1 mm in diameter and are made up of an inner fuel core or *kernel* that is about 350 to 500 μm in diameter consisting of uranium dioxide (UO_2), uranium carbide (UC), uranium oxycarbide (UCO), or uranium nitride (UN) followed by several layers of ceramic often referred to as the *hull*. The first coating layer is a *buffer* layer of low-density semiporous pyrolytic carbon that is approximately 100 μm thick. This buffer layer provides space for fission product gases to accumulate over the lifetime of the particle. The buffer layer is followed by a high-density pyrolytic carbon layer approximately 40 μm thick, sometimes referred to as the inner pyrolytic carbon layer (IPyC), that helps retain fission product gases and protects the particle surface from chlorine gas during the SiC deposition step. This IPyC layer is followed by a layer of SiC about 35 μm thick, which provides the primary mechanical strength of the particle and prevents the fission products from leaving the fuel particle. The SiC layer is followed by a final layer of high-density pyrolytic carbon approximately 40 μm thick, sometimes referred to as the outer pyrolytic carbon layer (OPyC), which protects the SiC and provides a surface for the particle to be bonded to the graphite compact matrix. On the order of tens of thousands of TRISO particles are encapsulated in a single graphite compact in the form of a spherical *pebble* or a cylinder.

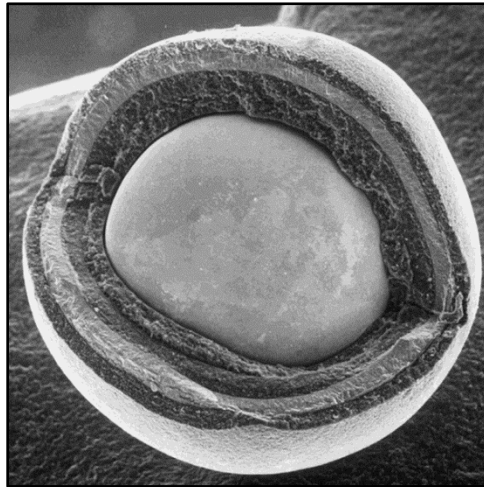


Figure 28. Magnified view of a TRISO fuel particle clearly showing each of the structural layers. Source: DOE photograph.

TRISO fuel has several advantages over traditional LWR fuel. This fuel was developed primarily for the purpose of achieving higher burnup than typical LWR fuel. Due to the layers of ceramic coatings acting as a form of cladding, TRISO fuel does not require traditional metal cladding. This allows TRISO-

fueled reactors to operate at higher temperatures, thus increasing the thermal-to-mechanical energy conversion efficiency [139]. TRISO particles are designed to be nearly indestructible. This helps with non-proliferation concerns but makes reprocessing TRISO fuel very challenging.

TRISO fuel particles dispersed in cylindrical graphite fuel compacts are shown in Figure 29. These compacts measure 12.5 mm diameter by 50 mm length. These were designed for a prismatic-core HTGR where they are loaded into hexagonal graphite elements fitted with channels for cooling gas flow and fuel compacts.

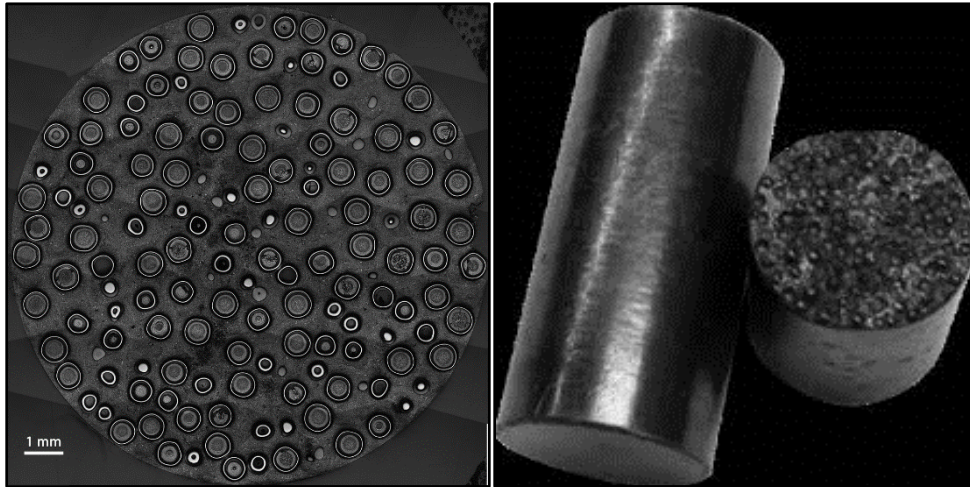


Figure 29. Photographs of graphite cylinder containing a dispersion of TRISO fuel particles. The image on the left is a cross section of the cylinder. Source: DOE photographs.

TRISO fuel particles dispersed in spherical graphite pebbles are shown in Figure 30. These spheres measure 60 mm diameter. The two-part design includes a 50 mm diameter inner spherical fuel zone surrounded by 5 mm thick fuel-free shell. These were designed for a pebble-bed HTGR.

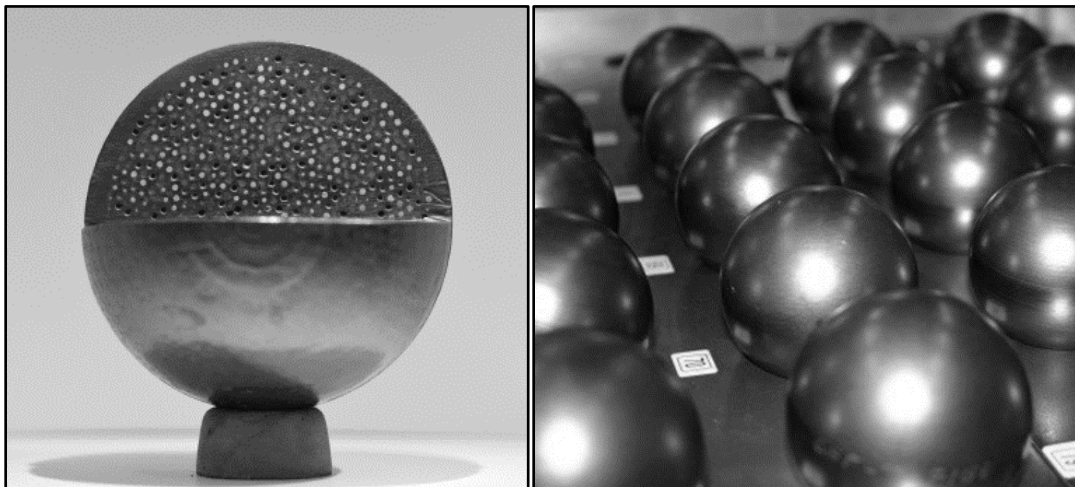


Figure 30. Photographs of a graphite sphere (pebble) containing a dispersion of TRISO fuel particles. The image on the left is a partial cross section of a graphite sphere. Source: DOE photographs.

The main challenge of reprocessing TRISO fuel is related to the graphite compacts and the PyC/SiC hulls surrounding the fuel kernels. If both the compacts and the hulls can be fully removed, the fuel kernels can then be reprocessed using existing reprocessing technologies like any other used nuclear fuel. Many different ideas have been proposed for head-end processes to remove TRISO hulls, with the goal of

either breaching the hulls to expose the fuel kernels or removing the hulls entirely. This process is further complicated by the fact that PyC and SiC are chemically inert by design and that breaching the hulls will inevitably release the volatile fission products trapped inside, which must then be managed appropriately.

The compact and hull materials themselves create additional reprocessing challenges. One major concern is the presence of ^{14}C in the irradiated PyC and SiC and to a lesser extent the graphite compacts. If the amount of ^{14}C in reprocessing waste streams is not mitigated, reprocessing TRISO fuel could potentially create much larger volumes of radioactive waste than if the compacts were disposed of whole. After head-end processes are complete, carbon-bearing contaminants in the spent fuel are expected to cause operational difficulties during pyrochemical reprocessing. The carbon contaminants will float on the surface of the salt in the OR cell and the electrorefining cell resulting in electrical bridging between the anode and cathode electrodes, thus reducing efficiency. This has been observed previously when trying to use graphite electrodes during OR [140]. To overcome this challenge, the amount of carbon fines left over from head-end processing of TRISO fuel must be minimized [141].

The benefits of reprocessing TRISO spent fuel are likely less than those of other spent fuels. The obvious motivation of recycling the fissile material in TRISO particles is diminished by their high-burnup design. With such little fissile material left over, it is only marginally economical to recover the material at all. The other primary motivator to TRISO fuel reprocessing is to reduce the amount of nuclear waste. In theory, if the graphite compacts can be sufficiently separated from the fuel particles, they may then be disposed of as low-level waste (LLW). Unfortunately, this would require near-perfect separation of all TRISO particles from the compacts without allowing for any contamination. Less than 10 out of the approximately 19,000 TRISO particles in a fuel compact may be allowed to remain for the waste to qualify as LLW [142].

7.1.1. Current Head-End Processing Options

7.1.1.1. Mechanical

Mechanical head-end processes involve crushing, cracking, or puncturing the TRISO fuel to remove the compacts and/or the hulls. The compacts and hulls may then be removed from the TRISO fuel kernels by means of physical solid-solid separations such as sifting, cyclonic separation, flotation, or by chemical separation techniques or combustion. The advantages of mechanical processing include that it is direct, cheap, and uses off-the-shelf equipment. The disadvantages include that mechanical equipment requires frequent maintenance and the graphite from the compacts is frequently contaminated with crushed or damaged TRISO particles.

7.1.1.2. Combustion

Combustion head-end processes make use of the combustibility (high-temperature oxidation) of the graphite compacts and the layers of PyC in the hulls to separate them from the fuel kernels. Combustion process designs can involve either burning the graphite and PyC together in an oxygen-rich environment or burning them sequentially with a mechanical processing step in-between. The advantages of combustion processes include their efficiency at removing carbon from the fuel. The primary disadvantage of combustion head-end processing is that it creates large amounts of carbon monoxide (CO) and carbon dioxide (CO₂) gases as nuclear waste contaminated with ^{14}C that then must be disposed of properly.

7.1.1.3. Thermal Shock

Thermal shock head-end processes involve subjecting the fuel to a large, abrupt change in temperature to cause it to fracture or split open. This has been attempted both by first heating the fuel in a furnace before subjecting it to liquid nitrogen and by first putting the fuel in liquid nitrogen before submerging it in room temperature water. Thermal shock processes are like mechanical head-end processes in that they must be followed by additional physical, chemical, or combustion separations. The

disadvantages of thermal shock processing include the following: (1) multiple thermal shock cycles may be required to sufficiently fracture the fuel, (2) subjecting the fuel to elevated temperatures tends to oxidize the graphite and PyC to form CO₂, and (3) it provides similar separation to mechanical head-end processes but with lower efficiency.

7.1.1.4. Chemical

Chemical head-end processes involve exposing the TRISO fuel to highly reactive chemicals to remove the compacts and hulls. This is commonly done with the assistance of high temperatures or microwave heating [143]. Examples of chemical head-end processes include hot chlorine gas treatment or acid intercalation using mixtures of sulfuric and nitric acids. The advantages of chemical head-end processing include reliability and high efficiency, its ability to be easily controlled and adapted to changes in TRISO feed, and the lack of moving parts that would require maintenance. The main disadvantage is that highly reactive chemicals, particularly in combination with radioactive materials and high temperatures, present serious hazards and additional waste disposal challenges.

7.1.1.5. Acoustic

Acoustic head-end processing involves submerging TRISO fuel in aqueous or molten salt solutions and subjecting it to ultrasonic waves to both cause the compact graphite to break apart and to breach the fuel hulls. This process has been shown to be successful in both breaking down graphite particles and breaching the PyC/SiC coatings in aqueous systems. Although it has been proposed, to date no attempt has been made to apply acoustic processing to molten salt systems. The advantages of these methods include low hazards and their adaptability. The disadvantages include that the hulls are merely breached, and the fuel must then be extracted from the hulls. While this should not be a problem for aqueous leaching, the presence of the PyC and SiC hull materials in pyrochemical reprocessing could severely reduce efficiency.

7.1.1.6. Pyrometallurgical

Pyrometallurgical head-end processes involve placing the fuel in molten salt and using a combination of both chemical and electrolytic reactions to dissolve or remove the hulls. Processes involving both halide and non-halide salts have been proposed, but little work has been done to develop them. The advantages of pyrochemical processing include few mechanical equipment needs, and its potential to integrate seamlessly into traditional pyrochemical technologies. The main disadvantage is that many of these methods have not been reliably validated, nor have means been developed to integrate them with further reprocessing technologies.

7.1.1.7. Electrolytic Dissolution

Electrolytic dissolution head-end processes involve applying an electrical current to the TRISO fuel to either dissolve away or fracture the compacts and hulls. Two primary types of methods have been proposed: constant current methods and pulsed current methods.

Constant current methods involve applying a relatively small oxidizing current to the TRISO compacts to slowly dissolve and break down the compact. The advantages to constant current methods include their consistency, ability to minimize the amount of CO₂ produced, and relatively small hazards. Disadvantages include that a way to contain the graphite particles as they break down has not been developed.

Pulsed current methods involve applying an instantaneous, massive current to TRISO compacts in water to create a high-temperature (~10,000 K), high-pressure (~10¹⁰ Pa) zone, which fractures the fuel [5]. The advantages to pulsed current methods include their efficiency at reducing the compacts to powders, thus fully exposing the fuel particles, and their ability to be easily tuned to changes in operating conditions. The main disadvantage is the hazard of applying high currents and voltages to radioactive material.

Although many head-end processes for reprocessing TRISO fuel have been proposed, there has not yet been enough work done to determine conclusively whether reprocessing is economically viable. Each of the proposed technologies for exposing fuel kernels are at very early stages of development and need many more tests before they can be considered for full-scale use with TRISO fuel.

To help evaluate which technologies are most promising for reprocessing TRISO fuel, Arm [143] created a list of seven criteria. They are as follows: technology robustness, technology adaptability, ability to integrate with established technologies for actinide recovery, hazard control, waste management, practicability of technology maturation for deployment, and capacity for remote operations. Based on the above evaluation criteria, the technologies most likely to be viable for reprocessing TRISO fuel are acoustic fracture, pyrochemical reprocessing, and constant current electrolytic dissolution.

7.2. Aluminum-Clad Research Reactor Fuel

The category “research reactor” encompasses a very wide variety of reactor types, sizes, and functions. Compared to commercial-scale electrical utility reactors, research reactors are much smaller and used for purposes other than electricity generation. Thermal power ratings range from less than 1 kWt to greater than 200 MWt.

The status and disposition of research reactors are important topics because they operate on enriched uranium fuels spanning the full spectrum from LEU to HEU, including so-called “weapons grade” uranium at 93 wt% ^{235}U . This means that the status of fresh and spent fuels from research reactors is of significant interest due to concerns of the proliferation risks and safeguard requirements of these materials. In response, the U.S. Department of Energy (DOE) began the Global Threat Reduction Initiative, which included the Reduced Enrichment for Research and Test Reactors (RERTR) Program, and the U.S. Foreign Research Reactor Spend Nuclear Fuel (FRR SNF) Acceptance Program. The primary purposes of these programs are to convert research reactors from HEU to LEU fuels, and to return HEU fuels to the countries of origin. To accommodate these changes much research has been carried out on new fuel designs with a focus on increasing the uranium density and volume fraction to offset the undesirable performance characteristics of LEU fuels.

By far, the most common fuel is aluminum-clad plate-type fuel. In this fuel design, a uranium compound is formed into a thin plate and clad between two aluminum plates forming a fuel plate. Fuel and plate thicknesses are on the order of 0.5 to 1.5 mm, respectively. Assemblies containing aluminum-clad fuel plates from the INL Advanced Test Reactor are shown schematically in Figure 31. The current fuel is an aluminum-uranium alloy clad in aluminum. Cooling is provided by air or water, and fuel temperatures remain low. There are many hundreds of fuel designs and configurations used in research reactors. Widely used uranium compounds include aluminides, silicides, hydrides, and molybdenites of uranium. The stoichiometries of these compounds vary according to application. Conversion of a reactor from HEU to LEU often accompanies changing the uranium aluminide fuel to the newer uranium silicide or uranium molybdenite fuels for their increased fuel densities.

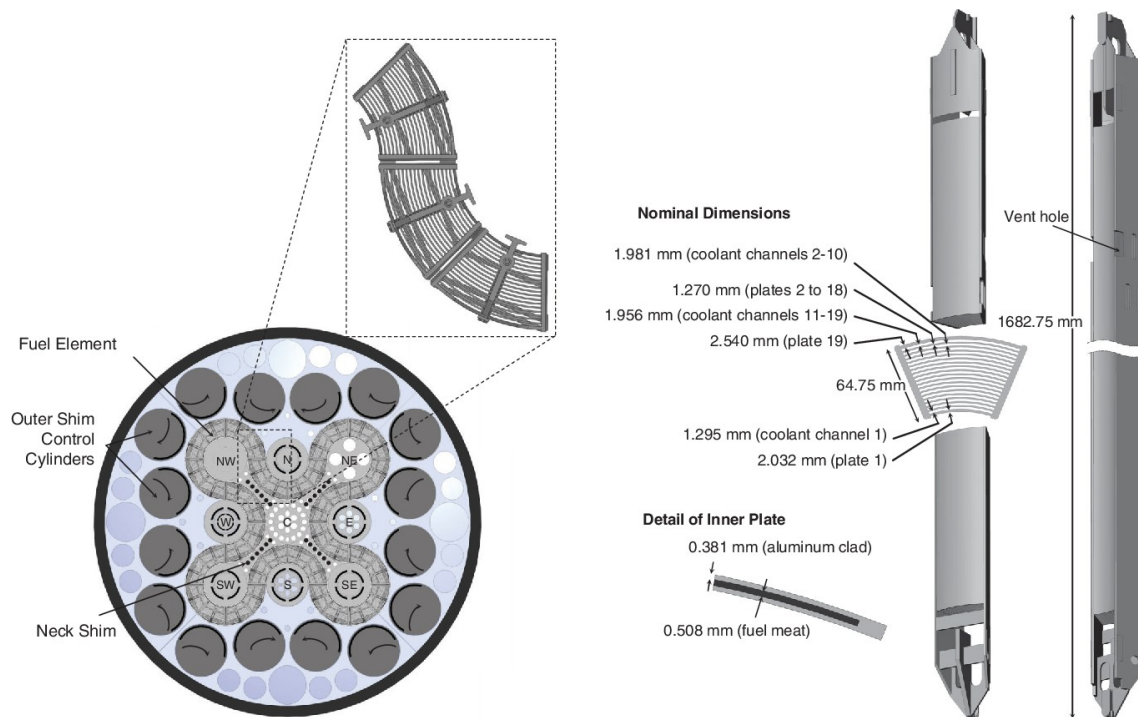


Figure 31. Schematic of INL Advanced Test Reactor fuel arrangement.

Aluminum- (Al)-clad fuel has traditionally been used in several U.S high-performance research reactors [144]. Al-clad fuels come in two major types: uranium aluminide (UAl_x) fuel and uranium-molybdenum (U-Mo) fuel. UAl_x fuel consists of a matrix of enriched uranium (U) mixed with Al, typically in the form of a mixture of 60 wt.% UAl_3 and 40 wt.% UAl_4 [145]. U-Mo fuel has more recently been proposed as a low-enriched alternative to UAl_x fuel and consists of a monolithic U-Mo alloy coated in a layer of zirconium (Zr). Both UAl_x and U-Mo fuels are enclosed in 6061 Al cladding.

The primary challenge of pyrochemical reprocessing Al-clad fuel is separating the Al and U. Mixtures of Al and U may not be directly electrorefined because Al and U form several stable intermetallic compounds. This results in requiring a higher applied potential to dissolve the U and Al anode in an electrorefiner (ER) and causes the Al and U to preferentially deposit together at the cathode, resulting in no separation. This is a major issue for UAl_x fuels but is less of an issue for U-Mo fuels. Due to the Zr layer in U-Mo fuel, the Al cladding does not normally make contact with the U in the U-Mo alloy. Because of this, U-Mo fuels may be reprocessed using conventional means once the cladding has been removed. Although U and Al may not be separated using conventional electrorefining, UAl_x fuel may still be electrorefined to recover a pure U-Al product free of fission products if that is desirable. A review of intermetallic fuel types is provided by Kim [146].

7.2.1. Reprocessing Options

7.2.1.1. Aqueous Reprocessing

Although pyrochemical reprocessing applied to mixtures of Al and U is challenging as stated above, aqueous reprocessing of aluminum-clad fuel does not change significantly from other types of used nuclear fuel, and the Plutonium Uranium Redox Extraction or PUREX process may still be used effectively. This has traditionally been done in the H-canyon at Savannah River National Laboratory.

7.2.1.2. Decladding Options

Removing the cladding may aid the reprocessing of both UAl_x and U-Mo fuels. Several options have been proposed to separate the fuel from the cladding in aluminum-clad fuels including a hybrid zirconium extraction (ZIRCEX) process, hydride/dihydride, caustic dissolution, and molten metal dissolution.

The ZIRCEX process was originally developed for zirconium-clad fuels. It involves exposing the fuel to hydrogen chloride (HCl) gas at elevated temperatures to chlorinate both the cladding and the inner fuel, turning them into chloride salts. Since zirconium chloride ($ZrCl_4$) is much more volatile than uranium chlorides, it sublimates away from the inner fuel. Although the ZIRCEX process is developed for zirconium-clad fuel, the same process can be used for aluminum-clad fuels due to the similar high volatility of aluminum chloride ($AlCl_3$). A hybrid ZIRCEX method specifically for aluminum-clad fuels has been developed at INL, but no results have yet been published externally [147].

The hydride/dehydride method involves separating the fuel and the aluminum cladding by reducing the fuel to a powder using hydrogen (H_2) gas. By exposing the fuel to H_2 gas at elevated temperatures (200°C), the uranium metal will react to form uranium hydride (UH_x), a fine powder, while the aluminum remains intact. The hydrogen is then removed from the UH_x by heating the fuel under vacuum. This process is repeated until the fuel has completely been reduced to a powder and removed from the aluminum cladding [148].

Caustic soda (sodium hydroxide) solutions have been shown to be very effective at dissolving aluminum. By immersing aluminum-clad fuels in caustic solution, the aluminum can be dissolved while leaving the inner fuel intact. This has been demonstrated with U-Mo fuel [149]. Although tests with non-irradiated U-Mo fuel had success removing the cladding and subsequently electrorefining the U metal, tests with irradiated U-Mo fuel were only able to remove the cladding. Irradiated U-Mo fuel reacts with the caustic solution and becomes oxidized, causing it to no longer be able to be electrorefined using conventional means.

Molten metal dissolution is similar to caustic dissolution and involves immersing the fuel in a molten metal to dissolve away the aluminum cladding. This method relies on picking a molten metal that has a high solubility for aluminum and almost no solubility for the other fuel components (U, Mo, and Zr). Molten magnesium (Mg) has been tested as a metal solvent with great success [150]. Due to the difficulties of separating the Mg and the Al after molten metal dissolution, molten lithium (Li) has been proposed as an alternative. Li and Al have been shown to be easily separable using vacuum distillation.

7.2.1.3. Options to Separate U and Al

Since UAl_x may not be electrorefined using conventional means, as explained above, several alternative reprocessing methods have been proposed to separate U from Al. These methods include silicon (Si)-aided electrorefining in molten fluoride salts, in situ anodic precipitation, and halogenation.

Si-aided electrorefining is a method proposed by workers at ANL [151, 152, 153]. This process involves first melting the fuel completely and adding Si. The Si helps stabilize the U in the alloy, which separates the oxidative dissolution potentials of U and Al. The choice of molten fluoride salts instead of the traditional chloride salts separates the two potentials further, allowing Al to be successfully electrorefined, leaving behind a U-Si alloy. The U can then be electrorefined out of the U-Si alloy in a subsequent step. This method has been proven to be successful at producing Al metal deposits with < 0.05 wt.% U.

The in situ anodic precipitation method involves electrorefining the Al in UAl_x in molten $NaAlCl_4$ at 180°C. Like with other chloride-based electrorefining of UAl_x , the U and the Al both oxidize to form uranium chloride (UCl_x) and aluminum chloride ($AlCl_3$). The UCl_x has a very low solubility in this salt system so it precipitates out while the $AlCl_3$ is transported to the cathode to deposit as pure Al. This process has shown recovery rates of 99.4% for Al and 94.6% for U [154].

Halogenation involves reacting the fuel with halogen-bearing substances at high temperatures to turn it into halide salts and then separating those salts based on their volatilities. This method uses the same principles as ZIRCEX but is applied to the UAl_x fuel as a whole instead of just the cladding. This method has been demonstrated using chlorine (Cl_2) gas [155], HCl gas [156], ammonium chloride (NH_4Cl) powder [145], and ammonium bromide (NH_4Br) powder [145].

8. SPENT FUEL AGE

Two consequences regarding spent fuel age that impact reprocessing are radioactive decay (decay heat) and fuel integrity (corrosion). Spent fuel age is measured starting from the time the fuel is removed from the reactor core. Decay heat is the heat generated from the radioactive decay process as the fuel ages. Corrosion can occur during periods of storage and alter the chemistry of the spent fuel.

8.1. Decay Heat

Decay heat of spent fuel is often reported in engineering units of Watts per quantity (i.e., energy per time per quantity). Commonly cited units include Watts per fuel assembly, Watts per kilogram of heavy metal, and Watts per metric ton of uranium oxide. Decay heat as a function of time for EBR-II driver fuel assemblies is shown in Figure 32. An EBR-II driver fuel assembly contained approximately 3 kg of enriched uranium. The figure shows that the decay heat was in the vicinity of 1,000 W (or more depending on the degree of burnup) when the assemblies were first removed from the reactor. The figure also shows that the rate at which decay heat diminishes slows over time, which is a form of exponential decay. This decay behavior is approximately the same for both LWR oxide and SFR metallic spent fuels.

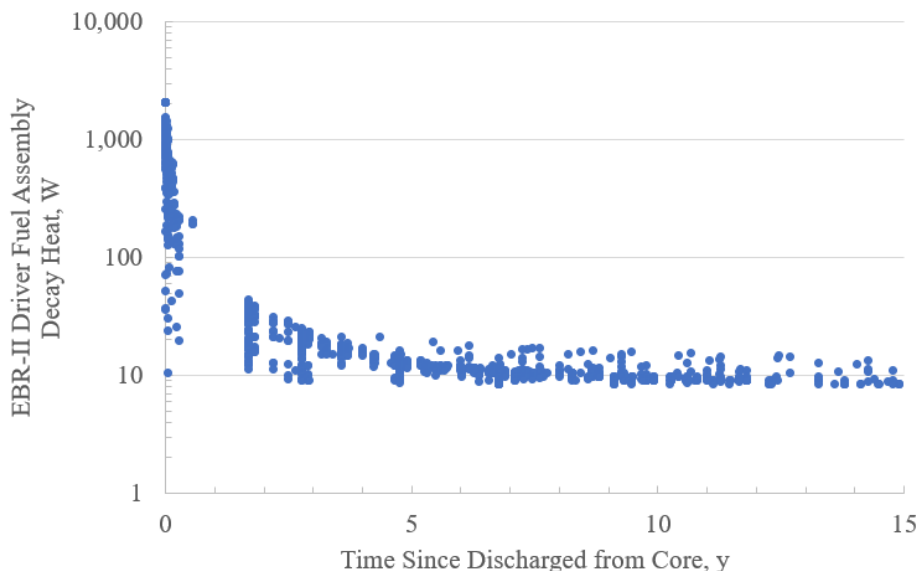


Figure 32. EBR-II driver fuel assembly decay heat as a function of time.

In preparation for aqueous reprocessing, spent fuel may be allowed to cool for 5 to 7 years, which makes the fuel more manageable with respect to decay heat, radiation shielding, radiolysis of process chemicals, waste disposal, etc. Keep in mind that an aqueous reprocessing flowsheet does not accumulate fission products. The fission products pass through the flowsheet and report to a waste raffinate stream, which continues to waste storage and processing for final disposition.

In comparison to aqueous reprocessing, pyrochemical reprocessing has two different considerations with respect to decay heat. First, the process chemicals used in pyrochemical reprocessing are not subject to degradation by radiolysis, which, taken by itself, implies that pyrochemical reprocessing can accept younger spent fuel than aqueous reprocessing. Second, unlike aqueous reprocessing, fission products do accumulate in the pyrochemical reprocessing flowsheet, mostly in the OR salt (if that operation is utilized) and the electrorefiner salt.

In other words, aqueous reprocessing of young fuel is challenged (among other things) by radiolytic degradation of the process chemicals. Whereas pyrochemical reprocessing of young fuel is challenged (among other things) by the accumulation in the salts of fission products that are generating the decay

heat. It may be true that less cooling time is required for pyrochemical reprocessing than for aqueous reprocessing, but the amount of cooling time required for either will be application specific.

8.2. Spent Fuel Storage

Spent LWR oxide fuels are commonly stored in water pools for decay heat management and radiation shielding. After a sufficient length of time, the spent fuels can be transferred from the water pools to dry cask storage. In contrast, there is much less experience with the storage of spent SFR metallic fuels. These fuels are not candidates for water pool storage because sodium-coolant, bond-sodium, and metallic fuel are highly reactive with water. Instead, these fuels may need to be stored in pools of molten sodium for decay heat management.

There is a notable exception that bears consideration. The EBR-II experience with spent fuels was atypical of what would be anticipated in a commercial-scale SFR reprocessing scenario. During early operations, EBR-II was located next to a reprocessing facility (consisting of air-atmosphere and argon atmosphere hot cells). There was a basket within the pool of primary sodium for holding fuel assemblies that were going into the core or coming out of the core. Fuel assemblies coming out went through the sodium wash station and then into the air-atmosphere hot cell. From there, the spent fuel had four paths for disposition, as follows:

- Between 1963 and 1967 only, fuel was reprocessed by the melt refining process (MRP) in the argon atmosphere hot cell. The MRP was very different from, and predates by over 20 years, the present concept of pyrochemical reprocessing.
- Fuel was packaged into stainless steel bottles and transferred to the Idaho Chemical Processing Plant (ICPP)^h where the fuel was stored in water pools prior to aqueous processing to recover the uranium. The fuel and bottles were dissolved together in nitric acid.
- Fuel was packaged into stainless steel cans and transferred to the Radioactive Scrap and Waste Facility (RSWF) for storage in below ground silos. This is a form of dry cask storage.
- Fuel specimens were sent to post-irradiation examination facilities for analyses and characterization.

Both EBR-II and ICPP were closed in 1994. All EBR-II fuels remaining at ICPP after the closure have since been returned to the Materials and Fuels Complex (MFC) and placed in the FCF or RSWF. Since 1996, EBR-II fuels have been processed in FCF under the DOE Spent Fuel Treatment Program, which is expected to be completed in 2028. All fuels processed are first inspected for corrosion because oxidized metal fuels are not candidates for treatment by the pyrochemical process in FCF.

8.3. Corrosion

Fuel cladding failure is when the fuel cladding is compromised and no longer serves as a barrier to protect the fuel from the outside environment. Fuel failure can occur inside and outside of the reactor core. This type of failure can lead to the release of fission products from the fuel into the outside environment. Fuel failure is caused by several mechanisms that include metallurgical, mechanical, radiological, and chemical effects.

Fuel corrosion is when the fuel chemically reacts with the outside environment. Fuel corrosion often follows fuel cladding failure. LWR oxide fuels are not particularly prone to corrosion because the fuel is already in an oxide form. In this respect, SFR metallic fuels are in stark contrast to LWR oxide fuels. SFR metallic fuels are highly reactive with the outside environment as the bond-sodium and uranium metal will react with oxygen and water in the atmosphere. Oxidation of SFR metallic fuels will generate heat and hydrogen gas. Once oxidation begins, the entire fuel element will ultimately corrode because the

h. The ICPP is now called the Nuclear Technology and Engineering Center (INTEC).

corrosion products cause the fuel volume to swell and split the stainless steel cladding, which exposes more of the fuel.

Oxide or metallic fuels that have failed and/or corroded are not an impediment to aqueous reprocessing because the fuels are dissolved in nitric acid solutions. The condition of the fuel may be important with respect to storage and materials handling but not with respect to chemical processing when the fuel is going to be dissolved in its entirety. The same is not true for pyrochemical reprocessing where the corrosion product will significantly interfere with the process chemistry. Thus, where metallic spent fuels are involved, significant amounts of corrosion would prevent direct pyrochemical reprocessing; pre-treatment would be needed since electrorefining can only be conducted using metals.

8.4. Molten Salt Reactor Fuel Salts

Some concepts for managing MSR fuel salt chemistry rely on diverting a slip stream of the fuel salt away from the reactor and into a chemical processing plant for treatment. In this scenario, there is no cooldown period. Treatment may be the recovery and purification of fissile metals to make fresh fuel salts, or treatment may be the recovery and disposal of fission products to increase the operational life of the fuel salt. In either case, the slip stream that was diverted away from the reactor is returned to the reactor in a purified form to keep the reactor operating. In these scenarios, fuel salts are extremely young when being discharged from the reactor for processing. Therefore, the impact of short-lived isotopes may need to be considered during the treatment of MSR fuel salts. Alternatively, treatment of the fuel salt may be deferred until the end-of-life of the reactor. However, these scenarios are speculative as the treatment of MSR fuel salts has yet to be demonstrated.

Fuel salts are subject to chemical degradation (what can be considered a form of corrosion) when exposed to air. Some salts are very hygroscopic and will attract significant amounts of water. Hydrolysis reactions of chloride salts can release hydrogen gas (H_2) and hydrogen chloride gas (HCl). Hydrolysis reactions of fluoride salts can release hydrogen gas and HF gas. Hydrogen chloride and HF are very corrosive to metals and hydrogen can present an explosion hazard. The potential for these reactions would likely need to be considered when managing spent fuel salts from MSRs.

9. SUMMARY

Several of the reprocessing strategies described in this report rely on the use of high-temperature highly reactive process gases for oxidation (e.g., voloxidation of oxide fuel using oxygen), chlorination (e.g., decladding aluminum-clad fuels via chloride volatility using chlorinating gaseous reagents), and fluorination (e.g., actinide separations via fluoride volatility using fluorinating gaseous reagents). In these operations, reactive gases (i.e., powerful oxidizers) that are not consumed in the process will be sent to the off-gas ventilation system as excess. In some cases, the excess may be recovered, purified, and reused. In other cases, the excess may be managed as a waste stream. Reactive gases are corrosive gases and suitable materials of construction must be used that suppress the degree of corrosion to manageable levels. In some instances, corrosion and combustion from reactive gases (e.g., oxygen and chlorine) share similar chemistries, the main difference being a matter of the rate at which the chemical reactions occur. Corrosion occurs more slowly than combustion. However, under the right conditions, halogen or halogen-containing oxidizers can support combustion in much the same way as oxygen can support combustion [157]. These are factors that should likely be considered in the safety analysis of the proposed designs for a reprocessing facility.

Waste processing is an integral requirement of any reprocessing facility. During aqueous reprocessing, fission products do not accumulate in the process flowsheet and are instead partitioned to a waste stream called “raffinate.” In contrast, during pyrochemical reprocessing, certain fission products do accumulate in the process flowsheet. Generally, fission products that are more electropositive than lithium accumulate in the OR salt (if OR is used) and fission products that are more electropositive than uranium accumulate in the electrorefiner salt. Eventually, these chloride salts must be managed and converted to waste forms that are suitable for storage, transportation, and geologic disposition. Some of the chemical processes proposed for making salt waste forms (e.g., dehalogenation) liberate the chlorine as chlorine gas or hydrogen chloride gas.

The age of the spent fuel entering a reprocessing facility is important with respect to the fission product composition, radiation levels, decay heat load, and potential corrosion of the spent fuel that may have occurred during storage and changed the chemical composition of the spent fuel. The aqueous and organic chemistries of aqueous reprocessing are susceptible to radiation damage, while the molten salt chemistries of pyrochemical reprocessing are immune to radiation damage. This implies that pyrochemical reprocessing can accept younger spent fuels (i.e., those more recently removed from the reactor) than aqueous reprocessing. However, pyrochemical reprocessing must manage the accumulation of the fission products, which are responsible for the decay heat load, in the process salts. Furthermore, fuel dissolution into acidic solutions means that aqueous reprocessing is more tolerant of direct reprocessing of corroded spent fuel than pyrochemical reprocessing. For example, a pyrochemical reprocessing facility designed for only metallic fuels would not be able to process oxidized metallic fuels, unless pre-treatment is applied.

There are many process options available for both aqueous and pyrochemical reprocessing. Some of these processes have been demonstrated, while others have not and are only speculated. Detailed design requires detailed design requirements. For a specific closed fuel cycle, it is possible to downselect from the many process options available to create a tailored flowsheet that meets the objectives of that fuel cycle.

10. REFERENCES

1. D. E. Shropshire, K. A. Williams, J. D. Smith, B. W. Dixon, M. Dunzik-Gougar, R. D. Adams, D. Gombert, J. T. Carter, E. Schneider, F. Hebditch, "Advanced Fuel Cycle Cost Basis," Idaho National Laboratory, INL/EXT-07-12107, December 2009
2. G. L. Fredrickson, T. S. Yoo, "Review – Nuclear Fuels and Reprocessing Technologies: A U.S. Perspective", Idaho National Laboratory, INL/EXT-20-59106, March 2021
3. J. E. Bodine, et al., "Oxidative decladding of uranium dioxide fuels," Nuclear Science and Engineering, 19.1 (1964) 1-7
4. G. E. Brand, E. W. Murbach, "Pyrochemical Reprocessing of UO₂ By AIROX: Summary Report," North American Aviation, Inc., Canoga Park, CA, Atomics International Div., NAA-SR-11389, 1965
5. M. Iwasaki, et al. "Oxidation of UO₂ Pellets in Air: Effect of Heat-Treatment of Pellet on Particle Size Distribution of Powders Produced," Journal of Nuclear Science and Technology 5.12 (1968) 652-653
6. J. H. Goode, "Voloxidation: Removal of Volatile Fission Products from Spent LMFBR Fuels," Oak Ridge National Laboratory, ORNL-TM-3723, 1973
7. J. C. Bresee, A. R. Griffith, E. D. Collins, R. T. Jubin, G. D. DelCul," Chemical Pre-Treatment of Used Fuel for Long-Term Storage," Procedia Chemistry, 7 (2012) 66-71
8. T. S. Yoo, et al., "Analysis and Modeling of Oxide Reduction Processes for Uranium Oxides," Journal of Nuclear Materials, 545 (2021) 152625
9. J. W. Kim, et al., "Smoothed Particle Hydrodynamics Modeling and Analysis of Oxide Reduction Process for Uranium Oxides," Chemical Engineering Science, 261 (2022) 117974
10. J. W. Kim, et al., "Modelling and Analysis of Salt-Convection Effect on Oxide Reduction Process for Uranium Oxides using Smoothed Particle Hydrodynamics," International Journal of Heat and Mass Transfer, 206 (2023) 123965
11. Y. Kosaka, et al., "A Study on the Dry Pyrochemical Technique for the Oxide Fuel Decladding," Journal of Nuclear Science and Technology 39, Supplement 3 (2002) 902-905
12. Z. Liu, et al. "Particle Size Distributions of U₃O₈ Produced by Oxidation in Air at 300-900°C," The 13th Annual Conference of the Canadian Nuclear Society, Saint John, New Brunswick, Canada, June 1992
13. F. Mernache, et al., "Recycling Process of Defective Aged Uranium Dioxide Pellets," Journal of Nuclear Science and Technology, 53.6 (2016) 790-796
14. B. R. Westphal, et al., "Effect of Process Variables During the Head-End Treatment of Spent Oxide Fuel," Nuclear technology, 162.2 (2008) 153-157
15. G. Rousseau, et al., "A detailed study of UO₂ to U₃O₈ Oxidation Phases and the Associated Rate-Limiting Steps," Journal of Nuclear Materials, 355.1-3 (2006) 10-20
16. G. I. Park, et al., "Evaluation of Decladding Efficiency Using High Burn-Up Spent Nuclear Fuels," American Nuclear Society Transactions, 98 (2008) 105-106
17. M. E. Whatley, et al., "Engineering Development of the MSBR Fuel Recycle." Nuclear Applications and Technology, 8.2 (1970) 170-178

18. J. A. Stone, D. R. Johnson, "Measurement of Radioactive Gaseous Effluents from Voloxidation and Dissolution of Spent Nuclear Fuel," Savannah River Laboratory, DP-MS-78-7, 1978
19. K. C. Song, et al., "Fractional Release Behavior of Volatile and Semivolatile Fission Products During a Voloxidation and OREOX Treatment of Spent PWR Fuel," Nuclear Technology, 162.2 (2008) 158-168
20. N. S. Shcherbina, N. Kivel, I. Günther-Leopold, "Effect of Redox Conditions on the Fission Products Release from Irradiated Oxide Fuel," Procedia Chemistry, 7 (2012) 104-109
21. B. R. Westphal, et al., "Selective Trapping of Volatile Fission Products with an Off-Gas Treatment System," Separation Science and Technology, 43.9-10 (2008) 2695-2708
22. R. T. Jubin, et al., "AFCI Fuel Reprocessing R and D: Performance of the Coupled End-to-End: Integrated Voloxidation and Dissolver Off-gas Treatment Systems," Global 2009, Paris, France, 2009
23. J. M. Shin, J. Myeong, et al., "Design of an Engineering Scale Off-Gas Trapping System at KAERI," Korean Atomic Energy Research Institute, KAERI/TR-4193/2010, 2011
24. O. A. Ustinov, et al., "Local Gas Purification System in Spent Nitride Fuel Oxidation," Atomic Energy, 123.4 (2018) 244-247
25. N. R. Soelberg, et al., "Radioactive Iodine and Krypton Control for Nuclear Fuel Reprocessing Facilities," Science and Technology of Nuclear Installations, 2013.1 (2013) 702496
26. S. Frank, et al., "The Fate of Radiogenic Iodine During the Electrochemical Treatment of Spent EBR-II Fuel," MRS Online Proceedings Library (OPL), 1265 (2010) 1265-AA09
27. Y. H. Kim, et al., "Engineering Design of a Mechanical Decladder for Spent Nuclear Rod-Cuts," Science and Technology of Nuclear Installations, 2019.1 (2019) 9273503
28. Y. H. Kim, Y. Z. Cho, J. M. Hur, "Experimental Approaches for Manufacturing of Simulated Cladding and Simulated Fuel Rod for Mechanical Decladder," Science and Technology of Nuclear Installations, 2020.1 (2020) 1905019
29. J. W. Lee, et al., "Estimation on Feeding Portions of Slitting Decladded Fuel Fragments to Electrolytic Reduction Process," Nuclear Technology, 204.1 (2018) 101-109
30. M. Reverdy, V. Potocnik, "History of Inventions and Innovations for Aluminum Production," Supplemental Proceedings of TMS 149th Annual Meeting & Exhibition, 2020
31. G. Z. Chen, D. J. Fray, T. W. Farthing, "Direct Electrochemical Reduction of Titanium Dioxide to Titanium in Molten Calcium Chloride," Nature, 407 (2000) 361-364
32. E. J. Krell, R. D. Pierce, T. P. Mulcahey, "Treatment of Oxide Spent Fuel Using the Lithium Reduction Process," Conference Proceedings of the Annual Meeting of the American Nuclear Society, Reno, NV, 1996
33. H. Ohta, et al., "Pyroprocessing of Light Water Reactor Spent Fuels Based on an Electrochemical Reduction Technology," Nuclear Technology, 150.2 (2005) 153-161
34. E. Y. Choi, S. M. Jeong, "Electrochemical Processing of Spent Nuclear Fuels: An Overview of Oxide Reduction in Pyroprocessing Technology," Progress in Natural Science: Materials International, 25.6 (2015) 572-582
35. S. W. Kim, et al., "Carbon Anode with Repeatable Use of LiCl Molten Salt for Electrolytic Reduction in Pyroprocessing," Journal of Radioanalytical and Nuclear Chemistry, 310 (2016) 463-467

36. J. M. Hur, J. S. Cha, E. Y. Choi, "Can Carbon be an Anode for Electrochemical Reduction in a LiCl-Li₂O Molten Salt?," *ECS Electrochemistry Letters*, 3.10 (2014) E5
37. A. Merwin, et al., "A Parametric Study of Operating Carbon Anodes in the Oxide Reduction Process," *Journal of Nuclear Materials*, 511 (2018) 297-303
38. Y. Sakamura, M. Iizuka, "Applicability of Nickel Ferrite Anode to Electrolytic Reduction of Metal Oxides in LiCl-Li₂O Melt at 923K," *Electrochimica Acta*, 189 (2016) 74-82
39. M. K. Jeon, S. W. Kim, E. Y. Choi, "Corrosion Behavior of Stainless Steel 316 for Carbon Anode Oxide Reduction Application," *Journal of Nuclear Fuel Cycle and Waste Technology*, 18.2 (2020) 169-177
40. S. D. Herrmann, et al., "Electrolytic reduction of spent nuclear oxide fuel as part of an integral process to separate and recover actinides from fission products," *Separation Science and Technology* 41.10 (2006) 1965-1983
41. S. Herrmann, S. Li, and M. Simpson, "Electrolytic reduction of spent light water reactor fuel bench-scale experiment results," *Journal of Nuclear Science and Technology*, 44.3 (2007) 361-367
42. S. Herrmann, S. Li, B. Serrano-Rodriguez, "Observations of Oxygen Ion Behavior in the Lithium-Based Electrolytic Reduction of Uranium Oxide," *Global 2009*, American Nuclear Society, 2009
43. D. Gabe, "Electrodeposition: Historically Old, Technologically Advanced," *Surface Engineering*, 27.9 (2011) 639-641
44. P. F. Mentone, "Pulse vs. DC Plating: Knowing How and When to Use Each System is Critical for Producing Plated Metals," *Metal Finishing*, 103.6 (2005) 14-18
45. S. D. Herrmann, et al., "Comparative Study of Monolithic Platinum and Iridium as Oxygen-Evolving Anodes During the Electrolytic Reduction of Uranium Oxide in a Molten LiCl-Li₂O Electrolyte," *Journal of Applied Electrochemistry*, 49 (2019) 379-388
46. Y. Sakamura, "Solubility of Li₂O in molten LiCl-MCl_x (M= Na, K, Cs, Ca, Sr, or Ba) Binary Systems," *Journal of The Electrochemical Society*, 157.9 (2010) E135
47. Y. Kado, Yuya, G. Takuya, R. Hagiwara, "Dissolution Behavior of Lithium Oxide in Molten LiCl-KCl Systems," *Journal of Chemical & Engineering Data*, 53.12 (2008) 2816-2819
48. M. K. Jeon, K. Min, S. W. Kim, E. Y. Choi, "Preliminary Study on Chlorination Reaction of Lithium Carbonate for Carbon-Anode-Based Oxide Reduction Applications," *Journal of Nuclear Fuel Cycle and Waste Technology*, 19.2 (2021) 225-231
49. H. Y. Ryu, et al., "Electrochemical Carbon Formation from a Graphite Anode in Li₂O-LiCl Molten Salt," *Asian Journal of Chemistry*, 25.12 (2013) 7019-7022
50. D. C. Horvath, et al., "Experimental Observations for Anode Optimization of Oxide Reduction Equipment," *Journal of Nuclear Fuel Cycle and Waste Technology*, 20.4 (2022) 383-398
51. M. K. Jeon, S. W. Kim, E. Y. Choi, "Corrosion Behavior of Stainless Steel 316 for Carbon Anode Oxide Reduction Application," *Journal of Nuclear Fuel Cycle and Waste Technology*, 18.2 (2020) 169-177
52. R. S. Fielding, D. L. Porter, "Volatile Species Retention During Metallic Fuel Casting," *Journal of Nuclear Materials*, 441.1-3 (2013) 530-534

53. C. L. Trybus, J. E. Sanecki, S. P. Henslee, "Casting of Metallic Fuel Containing Minor Actinide Additions," *Journal of Nuclear Materials*, 204 (1993) 50-55
54. M. P. Murchie, S. J. Reid, "Uranium Conversion and Enrichment," *Advances in Nuclear Fuel Chemistry*, (2020), DOI: <https://doi.org/10.1016/B978-0-08-102571-0.00010-0>
55. W. H. Reas, "The Aquafluor Process," Kjeller Report, Reprocessing of Fuel from Present and Future Power Reactors, Advanced Course Organized by the Netherland's – Norwegian Reactor School, Institutt for Atomenergi, KR-126, (September 1967) 361-384
56. W. D. Bond, J. C. Mallen, G. E. Michaels, "Evaluation of Methods for Decladding LWR Fuel for a Pyroprocessing-Based Reprocessing Plant," Oak Ridge National Laboratory, ORNL-TM-12104, October 1992
57. J. J. Barghusen, "Volatility Processes," *Reactor and Fuel-Processing Technology*, 11, 1 (1967-1698) 54-59
58. M. Kamoshida, F. Kawamura, A. Sasahira, T. Fukusawa, T. Sawa, J. Yamashita, "A New Concept for the Nuclear Fuel Recycle System: Application of the Fluoride Volatility Reprocessing," *Progress in Nuclear Energy*, 37, 1-4 (2000) 145-150
59. O. Amano, K. Yasui, A. Sasahira, Y. Kani, M. Takahashi, T. Fukasawa, Y. Shibata, F. Kawamura, "FLUOREX Reprocessing Technology with Uranium Removal from Spent Fuel by Fluorination – Volatilization Reaction of Uranium," *Journal of Nuclear Science and Technology*, Sup. 3 (2002) 890-893
60. H. Kobayashi, O. Amano, F. Kawamura, M. Aoi, K. Hoshino, A. Sasahira, Y. Kani, "FLUOREX Reprocessing System for the Thermal Reactors Cycle and Future Thermal/Fast Reactors (Coexistence) Cycle," *Progress in Nuclear Energy*, 47, 1-4 (2005) 380-388
61. K. Kani, A. Sasahira, K. Hoshino, F. Kawamura, "New Reprocessing System for Spent Nuclear Reactor Fuel Using Fluoride Volatility Method," *Journal of Fluorine Chemistry*, 130 (2009) 74-82
62. T. Fukasawa, K. Hoshino, D. Watanabe, A. Sasahira, "Application of Fluoride Volatility Method to the Spent Fuel Reprocessing," *Journal of Nuclear Science and Technology*, 57, 1 (2020) 49-56
63. G. Strickland, F. L. Horn, R. Johnson, "The Nitrofluor Process for Reactor Fuel", Symposium on Volatility Reprocessing of Nuclear Reactor Fuels: Part 1, Fifty-Fourth Annual Meeting, American Institute of Chemical Engineers, New York, New York, December 2-7, 1961
64. G. Strickland, F. L. Horn, "Nitrofluor Process – A Non-Aqueous Fluoride-Volatility Method for Recovering Uranium and Plutonium from Various Reactor Fuels", *Progress in Nuclear Energy, Series III, Process Chemistry*, 4 (1970) 399-425
65. "Research and Development on Nonaqueous Processing," *Reactor Fuel Processing*, 5, 1, (1962): 22-40.
66. G. Fredrickson, G. Cao, R. Gukhar, T. S. Yoo, "Molten Salt Reactor Salt Processing – Technology Status," Idaho National Laboratory, INL/EXT-18-51033
67. M. J. Bell, "Calculated Radioactivity of MSRE Fuel Salt," Oak Ridge National Laboratory, ORNL-TM-2970, May 1970
68. R. P. Milford, "Engineering Design of Oak Ridge Fluoride Volatility Pilot Plant," *Industrial and Engineering Chemistry*, 50, 2 (1958) 187-191

69. R. E. Thoma, B. J. Strum, E. H. Guinn, "Molten-Salt Solvents for Fluoride Volatility Processing of Aluminum-Matrix Nuclear Fuel Elements," Oak Ridge National Laboratory, ORNL-3594, August 1964
70. M. R. Bennett, G. I. Cathers, R. P. Milford, W. W. Pitt, J. W. Ullmann, "Fused-Salt Fluoride-Volatility Process for Recovering Uranium from Spent Aluminum-Based Fuel Elements," *Industrial and Engineering Chemistry, Process Design and Development*, 4, 4 (1965) 387-394
71. M. J. Szulinski, "Fluoride Volatility Processing of Reactor Fuels," Isochem Inc, Richland, Washington, ISO-627, December 1966
72. J. J. Reilly, S. J. Wachel, R. Johnson, E. Wirsing, L. P. Hatch, "Fluidized Bed Reprocessing of Graphite Matrix Nuclear Fuel," *Industrial and Engineering Chemistry, Process Design and Development*, 5, 1 (1966): 51-59
73. D. L. Breton, R. B. Schappel, J. R. Merriman, J. H. Pashley, C. C. Littlefield, K. E. Habiger, "A Conceptual Study of a Fluoride Volatility Plant for Reprocessing Light Water Reactor Fuels," Union Carbide Corporation, K-1759, December 1968
74. J. Uhlir, M. Marecek, M. Precek, "Progress in Development of Fluoride Volatility Reprocessing Technology," *ATALANTE* 2008, P1-21
75. J. Uhlir, M. Marecek, "Fluoride Volatility Method for Reprocessing of LWR and FR Fuels," *Journal of Fluorine Chemistry*, 130 (2009) 89-93
76. J. Uhlir, M. Marecek, J. Skarohlid, "Current Progress in R&D of Fluoride Volatility Method," *Procedia Chemistry*, 7 (2012) 110-115
77. B. K. McNamara, M. J. O'Hara, S. Morrison, C. Z. Soderquist, A. M. Casella, R. A. Clark, R. Carter, "Separations of U/Pu and Np/Pu Using Fluoride Volatility," *Journal of Fluorine Chemistry*, 257-258 (2022) 109952
78. L. B. Asprey, P. G. Eller, S. A. Kinkead, "Formation of Actinide Hexafluorides at Ambient Temperatures with Krypton Difluoride," *Inorganic Chemistry*, 25-5 (1986) 670-672
79. HSC Chemistry 10, Software Version 10.4.2.2
80. K. Seppelt, "Molecular Hexafluorides," *Chemical Review*, 115 (2015) 1296-1306
81. A. Perez-Villa, J. David, P. Fuentealba, A. Restrepo, "Octahedral Complexes of the Series of Actinides Hexafluorides AnF₆," *Chemical Physics Letters*, 507 (2011) 57-62
82. D. Ramaswami, N. M. Levitz, J. T. Holmes, A. A. Jonke, "Part 1: Bench-scale Investigation of a Process for Zirconium-Uranium Alloy Fuel," Argonne National Laboratory, ANL-6829, 1963
83. D. Ramaswami, N. M. Levitz, A. A. Jonke, "Part 2: Bench-scale Investigation of a Process for Aluminum-Uranium Alloy and Stainless Steel-Cermet Fuels," Argonne National Laboratory, ANL-6830, 1963
84. L. J. Anastasia, J. D. Gabor, W. J. Meclid, "Part 3: Fluid-bed Fluorination of Uranium Dioxide Fuel Pellets," Argonne National Laboratory, ANL-6898, 1963
85. J. D. Gabor, W. J. Mecham, "Part 4: Fluidized-packed Beds: Studies of Heat Transfer, Solids-Gas Mixing, and Elutriation," Argonne National Laboratory, ANL-6859, 1963

86. G. J. Vogel, E. L. Carls, W. J. Mecham, "Part 5: Description of a Pilot-Scale Facility for Uranium Dioxide-Plutonium Dioxide Fuel Processing Studies," Argonne National Laboratory, ANL-6901, 1963
87. I. E. Knudsen, N. M. Levitz, A. A. Jonke, "Part 6: Preparation of Dense Uranium Dioxide Particles from Uranium Hexafluoride in a Fluidized Bed," Argonne National Laboratory, ANL-6902, 1963
88. A. A. Chilenskas, G. E. Gunderson, "Part 7: The Corrosion of Nickel in Process Environments," Argonne National Laboratory, ANL-6979, 1963
89. J. T. Holmes, H. L. Stethers, J. J. Barghusen, "Part 8: Pilot-plant Development of a Process for Uranium Alloy Fuels," Argonne National Laboratory, ANL-6973, 1963
90. J. T. Holmes, D. Ramaswami, "Part 9: Computer Programs for Alloy-fuel Process Calculations," Argonne National Laboratory, ANL-6992, 1963
91. A. A. Chilenskas, K. S. Turner, J. E. Kincinas, G. L. Potts, "Part 10: Bench-scale Studies on Irradiated Highly Enriched Uranium Alloy Fuels," Argonne National Laboratory, ANL-6994, 1963
92. D. Ramaswami, L. J. Anastasia, N. M. Levitz, W. J. Mecham, A. A. Jonke, "Part 11: Off-gas Analysis," Argonne National Laboratory, ANL-7339, 1963
93. J. D. Gabor, D. Ramaswami, "Part 12: Exploratory Tests on Fluorination of Uranium Oxide with BrF₅ in a Bench-scale Fluid-bed Reactor System," Argonne National Laboratory, ANL-7362, 1963
94. J. T. Holmes, L. B. Koppel, N. Saratchandran, J. B. Strand, D. Ramaswami, "Part 13. Pilot-Plant Studies of the Fluorination of Uranium Oxide with Bromine Pentafluoride," Argonne National Laboratory, ANL-7370, 1963
95. R. L. Jarry, L. J. Anastasia, J. Fischer, L. E. Trevorow, T. D. Baker, J. J. Stockbar, "Laboratory Investigations in Support of Fluid-Bed Fluoride Volatility Process, Part I. The Fluorination of Uranium Dioxide-Plutonium Dioxide Solid Solutions," Argonne National Laboratory, ANL-6742, 1963
96. M. J. Steindler, "Laboratory Investigations in Support of Fluid-Bed Fluoride Volatility Process, Part II. The Properties of Plutonium Hexafluoride," Argonne National Laboratory, ANL-6753, 1963
97. L. E. Trevorow, J. Fischer, J. Riha, "Laboratory Investigations in Support of Fluid-Bed Fluoride Volatility Process, Part III. Separation of Gaseous Mixtures of Uranium Hexafluoride and Plutonium Hexafluoride by Thermal Decomposition," Argonne National Laboratory, ANL-6762, 1963
98. R. L. Jarry, A. V. Hariharan, G. Manevy, J. Fischer, J. J. Stockbar, J. G. Riha, T. D. Baker, G. W. Redding, "Laboratory Investigations in Support of Fluid-Bed Fluoride Volatility Process, Part IV. The Fluid Bed Fluorination of U₃O₈" Argonne National Laboratory, ANL-6763, 1963
99. M. J. Steindler, D. V. Steidl, J. Fischer, "Laboratory Investigations in Support of Fluid-Bed Fluoride Volatility Process. Part V. The Radiation Chemistry of Plutonium Hexafluoride," Argonne National Laboratory, ANL-6812, 1963
100. M. J. Steindler, W. H. Gunther, "Laboratory Investigations in Support of Fluid-Bed Fluoride Volatility Process. Part VI. A. The Absorption Spectrum of Plutonium Hexafluoride. B. Analysis of Mixtures of Plutonium Hexafluoride and Uranium Hexafluoride by Absorption Spectrometry," Argonne National Laboratory, ANL-6817, 1964

101. R. P. Wagner, W. A. Shinn, J. Fischer, M. J. Steindler, "Laboratory Investigations in Support of Fluid-Bed Fluoride Volatility Process. Part VII. The Decomposition of Gaseous Plutonium Hexafluoride by Alpha Radiation," Argonne National Laboratory, ANL-7013, 1965
102. L. E. Trevorow, R. W. Kessie, M. J. Steindler, "Laboratory Investigations in Support of Fluid-Bed Fluoride Volatility Process. Part VIII. Analysis of an Accidental Multigram Release of Plutonium Hexafluoride in a Glovebox," Argonne National Laboratory, ANL-7068, 1965
103. R. L. Larry, A. V. Hariharan, J. Fischer, M. J. Steindler, J. J. Stockbar, T. D. Baker, W. H. Gunther, G. W. Redding, "Laboratory Investigations in Support of Fluid-Bed Fluoride Volatility Process. Part IX. The Fluid-bed Fluorination of Plutonium-containing Simulated Oxidic Nuclear Fuel in a 1.25-inch-diameter Reactor," Argonne National Laboratory, ANL-7077, 1965
104. D. R. Vissers, M. J. Steindler, "Laboratory Investigations in Support of Fluid-Bed Fluoride Volatility Process. Part X. A Literature Survey on the Properties of Tellurium, Its Oxygen and Fluorine Compounds," Argonne National Laboratory, ANL-7142, 1966
105. "Laboratory Investigations in Support of Fluid-Bed Fluoride Volatility Process. Part XI. Vapor-Liquid Equilibria in the System Uranium Hexafluoride Plutonium Hexafluoride," Argonne National Laboratory, ANL-7186, 1966
106. L. E. Trevorow, M. J. Steindler, D. V. Steidl, J. T. Savage, "Laboratory Investigations in Support of Fluid-Bed Fluoride Volatility Process. Part XII. The Melting-point Diagram for the System Uranium Hexafluoride-Plutonium Hexafluoride," Argonne National Laboratory, ANL-7234, 1966
107. L. E. Trevorow, M. J. Steindler, D. V. Steidl, J. T. Savage, "Laboratory Investigations in Support of Fluid-Bed Fluoride Volatility Process. Part XIII. Condensed-phase Equilibria in the System Molybdenum Hexafluoride-Uranium Hexafluoride," Argonne National Laboratory, ANL-7240, 1966
108. W. H. Gunther, M. J. Steindler, "Laboratory Investigations in Support of Fluid-Bed Fluoride Volatility Process. Part XIV. The Corrosion of Nickel and Nickel Alloys by Fluorine, Uranium Hexafluoride, and Selected Volatile Fission Product Fluorides at 500°C," Argonne National Laboratory, ANL-7241, 1966
109. L. E. Trevorow, M. J. Steindler, "Laboratory Investigations in Support of Fluid-Bed Fluoride Volatility Process. Part XV. Estimation of Rates of Thermal Decomposition of Plutonium Hexafluoride in Process Streams," Argonne National Laboratory, ANL-7347, 1967
110. L. J. Anastasia, P. G. Alfredson, M. J. Steindler, G. W. Redding, J. G. Riha, M. Haas, "Laboratory Investigations in Support of Fluid-Bed Fluoride Volatility Process. Part XVI. The Fluorination of UO₂-PuO₂-Fission-product Oxide Pellets with Fluorine in a 2-inch-diameter Fluid-bed Reactor," Argonne National Laboratory, ANL-7372, 1967
111. L. E. Trevorow, T. J. Gerding, M. J. Steindler, "Laboratory Investigations in Support of Fluid-Bed Fluoride Volatility Process. Part XVII. Fluorination of Neptunium (IV) Fluoride and Neptunium (IV) Oxide," Argonne National Laboratory, ANL-7385, 1968
112. W. A. Shinn, M. J. Steindler, "Laboratory Investigations in Support of Fluid-Bed Fluoride Volatility Process. Part XVIII. Neutron Counting as an Analytical Method for Plutonium Fluorides," Argonne National Laboratory, ANL-7402, 1968
113. R. L. Jarry, J. J. Stockbar, M. J. Steindler, "Laboratory Investigations in Support of Fluid-Bed Fluoride Volatility Process. Part XIX. Reaction of Bromine Pentafluoride with Selected Compounds of Uranium and Plutonium," Argonne National Laboratory, ANL-7412, 1968

114. D. R. Vissers, M. J. Steindler, "Laboratory Investigations in Support of Fluid-Bed Fluoride Volatility Process. Part XX. Fission-Product Tellurium Off-Gas Disposal in the Fluid-Bed Fluoride Volatility Process," Argonne National Laboratory, ANL-7464, 1968
115. L. J. Anastasia, P. G. Alfredson, J. M. Steindler, "Fluidized-Bed Fluorination of UO₂-PuO₂-Fission Product Pellets with BrF₅ and Fluorine. Part I: The Fluorination of Uranium, Neptunium, and Plutonium," *Nuclear Applications and Technology*, 7 (1969) 425-432
116. L. J. Anastasia, P. G. Alfredson, J. M. Steindler, "Fluidized-Bed Fluorination of UO₂-PuO₂-Fission Product Pellets with BrF₅ and Fluorine. Part II: Process Considerations," *Nuclear Applications and Technology*, 7 (1969) 433-442
117. J. J. Schmets, "Reprocessing of Spent Nuclear Fuels by Fluoride Volatility Processes," *Atomic Energy Review*, 8(1) (1970) 3-126
118. R. Scheele, A. Casella, "Assessment of the Use of Nitrogen Trifluoride for Purifying Coolant and Heat Transfer Salts in the Fluoride Salt-Cooled High-Temperature Reactor," PNNL-19793, September 2010
119. B. J. Riley, J. D. Vienna, W. L. Ebert, "Road Map for Developing Iron Phosphate Waste Forms for Salt Wastes," Pacific Northwest National Laboratory, PNNL-30998, 2021
120. "Yucca Mountain Repository License Application, Safety Analysis Report," U.S. Department of Energy, DOE/RW-0573, Rev. 0, June 2008
121. B. J. Riley, "Electrochemical Salt Wasteform Development: A Review of Salt Treatment and Immobilization Options," *Industrial & Engineering Chemistry Research*, 59 (2020) 9760-9774
122. P. Murray, H. Werth, S. Sullivan, B. J. Riley, M. Simpson, C. Lonergan, K. Carlson, "Phosphate-Based Dechlorination of Electrorefiner Salt Waste using a Phosphoric Acid Precursor," *ACS Omega*, 9 (2024) 19395-19400
123. M. R. Rodriguez-Laguna, K. R. Tolman, M. T. Kropp, J. A. Yingling, S. C. Baldivieso, T. S. Yoo, "Separation of Fission Products from High-Level Waste Salt Systems by Partial Crystallization: CsCl-NaCl-LiCl-KCl Study," *Separation and Purification Technology*, 332 (2024) 125602
124. G. L. Fredrickson, M. N. Patterson, D. Vaden, G. G. Galbreth, T. S. Yoo, J. C. Price, E. J. Flynn, R. N. Searle, "History and Status of Spent Fuel Treatment at the INL Fuel Conditioning Facility", *Progress in Nuclear Energy*, 143 (2022) 104037
125. S. Priebe, K. Bateman, "The Ceramic Waste Form Process at Idaho National Laboratory," *Nuclear Technology*, 162-2 (2008) 199-207
126. W. L. Ebert, C. T. Snyder, B. J. Riley, S. M. Frank, "Designing Advanced Ceramic Waste Forms for Electrometallurgical Processing Salt Waste," Argonne National Laboratory, FCRD-MRWF-2016-000038, March 2016
127. B. J. Riley, J. D. Vienna, S. M. Frank, J. O. Kroll, J. A. Peterson, N. L. Canfield, Z. Zhu, J. Zhang, K. Kruska, D. K. Schreiber, "Glass Binder Development for a Glass-Bonded Sodalite Ceramic Waste Form," *Journal of Nuclear Materials*, 489 (2017) 42-63
128. B. J. Riley, D. A. Pierce, S. M. Frank, J. Matyáš, C. A. Burns, "Efficacy of a Solution-Based Approach for Making Sodalite Waste Forms for an Oxide Reduction Salt Utilized in the Reprocessing of Used Uranium Oxide Fuel," *Journal of Nuclear Materials*, 459 (2015) 313-322
129. J. T. Reiser, K. R. Tolman, M. T. Kropp, R. M. Kissinger, S. A. Saslow, D. A. Cutforth, J. V. Crum, B. N. Seiner, G. L. Smith, J. D. Vienna, "Fabrication of Radioactive and Non-Radioactive

- Titanate and Zirconate Ceramics for Immobilization of Used Nuclear Fuel,” *Journal of Nuclear Materials*, 572 (2022) 154033
130. J.-Y. Pyo, C. W. Lee, H.-S. Park, J. H. Yang, W. Um, J. Heo, "Tellurite Glasses for Vitrification of Technetium-99 from Pyrochemical Processing," *Journal of Nuclear Materials*, 493 (2017) 1-5
 131. B. J. Riley, J. A. Peterson, J. D. Vienna, W. L. Ebert, S. M. Frank, "Dehalogenation of Electrochemical Processing Salt Simulants with Ammonium Phosphates and Immobilization of Salt Cations in an Iron Phosphate Glass Waste Form," *Journal of Nuclear Materials*, 529 (2020) 151949
 132. S. M. McDeavitt, D. P. Abraham, J. Y. Park, "Evaluation of Stainless Steel-Zirconium Alloys as High-Level Nuclear Waste Forms," *Journal of Nuclear Materials*, 257 (1998) 21-34
 133. B. Westphal, S. Frank, W. McCartin, D. Cummings, J. Giglio, T. O'Holleran, P. Hahn, T. Yoo, K. Marsden, K. Bateman, M. Patterson, "Characterization of Irradiated Metal Waste from the Pyrometallurgical Treatment of Used EBR-II Fuel," *Metallurgical and Materials Transactions*, 46 (2013) 83-92
 134. V. K. Gattu, W. L. Ebert, J. E. Indacochea, S. M. Frank, "Electrochemical Corrosion of a Multiphase Alloy/Oxide Composite Nuclear Waste Form," *Corrosion Science*, 184 (2021) 109358
 135. R. M. Asmussen, J. Turner, S. Chong and B. J. Riley, "Review of Recent Developments in Iodine Waste Form Production," *Frontiers in Chemistry*, 10 (2022) 1-24
 136. R. T. Jubin, S. H. Bruffey, B. B. Spencer and D. M. Strachan, "The Effect of Kr-85 Decay to Rb-85 on Waste Forms – 17105," *Proceedings of Waste Management 2017*, Phoenix, AZ, 2017
 137. B. J. Riley, J. D. Vienna, D. M. Strachan, J. S. McCloy and J. L. Jerden Jr., "Materials and processes for the effective capture and immobilization of radioiodine: A review," *Journal of Nuclear Materials*, 470 (2016) 307-326
 138. G. W. Keilholtz, G. C. Battles, "Fission Product Release and Transport in Liquid Metal Fast Breeder Reactors," Oak Ridge National Laboratory, ORNL-NSIC-37, March 1969
 139. G. L. Fredrickson, T. S. Yoo, "Review - Nuclear Fuels and Reprocessing Technologies: A U.S. Perspective," Idaho National Laboratory, INL/EXT-20-59106, March 2021
 140. P. Motsegood, J. Willit, M. A. Williamson, "Graphite Anodes for Electroreduction of Uranium Oxide," *ECS Meeting Abstracts*, MA2015-01 (2015) 1225-1225
 141. M. A. Rose, W. C. Phillips, R. O. Hoover, M. E. Woods, "An Assessment of Applying Pyroprocessing Technology to Advanced Pebble-Type Fuels," Argonne National Laboratory, ANL/CFCT-23/6 Rev. 1, September 2023
 142. E. J. Mulder, W. A. Boyes, "Neutronics characteristics of a 165 MWth Xe-100 Reactor," *Nuclear Engineering and Design*, 357 (2020) 110415.
 143. S. T. Arm, G. B. Hall, G. J. Lumetta, B. E. Wells, "Plan for Developing TRISO Fuel Processing Technologies," Pacific Northwest National Laboratory, PNNL-32969, June 2022
 144. J. Marra, S. Frank, S. Herrmann, T. Rudisill, R. Sindelar, Greg Vandergrift, M. Williamson, "Options Analyses for Back-End of the Fuel cycle for USHPRR U-Mo Fuel," Savannah River National Laboratory, SRNL-2013-00009, 20114
 145. S. D. Herrmann, H. Zhao, M. Shi, M. M. Jones, M. N. Patterson, "Halogenation of used aluminum matrix test reactor fuel – a bench-scale," *Journal of Nuclear Science and Technology*, 59 (2022) 395-406

146. Y. S. Kim, "Uranium Intermetallic Fuels (U-Al, U-Si, U-Mo)," *Comprehensive Nuclear Materials*, Vol. 3 (2012) 391-422, Elsevier
147. S. Gallier, "Looking high and low for HALEU," *Nuclear News*, pp. 26-29, September 2019
148. M. I. Solonin, A. V. Vatulin, Y. A. Stetsky, Y. I. Trifonov, B. D. Rogozkin, "Development of the method of high density fuel comminution by hydride-dehydride processing," 23rd International Meeting on Reduced Enrichment for Research and Test Reactors (RERTR), Las Vegas, 2000
- 149vS. Herrmann, K. Norbash, D. Wachs, "Separation and Recovery of Uranium from Next Generation Research Reactor Fuel via Molten Salt Electrorefining," *Fray International Symposium*, 2011
150. S. Herrmann, K. Norbash, "Method of Separating and Recovering Uranium from Aluminum-Clad Metallic Nuclear Fuel," U.S. Patent US10418138B1, 22 October 2018
151. S. A. Slater, A. G. Raraz, J. L. Willit, E. C. Gay, "Electrochemical Separation of Aluminum from Uranium for Research Reactor Spent Nuclear Fuel Applications," *Separation and Purification Technology*, 15 (1999) 197-205
152. J. L. Willit, E. C. Gay, W. E. Miller, C. C. McPheeters, J. J. Laidler, "Electrometallurgical Treatment of Aluminum-Matrix Fuels," DOE Spent Nuclear Fuel and Fissile Material Management, Reno, Nevada, June 16-20, 1996
153. J. L. Willit, A. Slater, A. Raraz, E. C. Gay, "Electrometallurgical Treatment of Aluminum-based Fuels," DOE Spent Nuclear Fuel and Fissile Material Management, Charleston, South Carolina, September 8-11, 1998
154. Y.-K. Zhong, Y.-L. Liu, K. Liu, L. Wang, L. Mei, J. K. Gibson, J.-Z. Chen, S.-L. Jiang, Y.-C. Liu, L.-Y. Yuan, Z.-F. Chai, W.-Q. Shi, "In-situ Anodic Precipitation Process for Highly Efficient Separation of Aluminum Alloys," *Nature Communications*, 12 (2021) 5777
155. P. Souček, R. Malmbeck, C. Nourry, J.-P. Glatz, "Pyrochemical Reprocessing of Spent Fuel by Electrochemical Techniques Using Solid Aluminium Cathodes," *Energy Procedia*, 7 (2011) 396-404
156. R. Meier, P. Souček, R. Malmbeck, T. Fanghänel, "Recycling of Uranium from Uranium-Aluminium alloys by Chlorination with HCl(g)," *Procedia Chemistry*, 7 (2012) 785-790
157. T. Dokter, "Fire and Explosion Hazards of Chlorine-Containing Systems," *Journal of Hazardous Materials*, 10 (1985) 73-87